

Event-based complexity in atmospheric turbulence

Paolo Paradisi^{1,*} and Rita Cesari²

¹ Istituto di Scienza e Tecnologie dell'Informazione (ISTI-CNR),
Via G. Moruzzi 1, 56124 Pisa, Italy

² Istituto di Scienze dell'Atmosfera e del Clima (ISAC-CNR),
Strada Prov.le Lecce-Monteroni Km 1,200 73100 Lecce, Italy

Abstract. Since the studies of Kolmogorov and Oboukhov in 1941, the problem of intermittent large velocity excursions was recognized to be one of the most intriguing and elusive aspects of turbulent flows. While many efforts were devoted since 1960s to the magnitude intermittency, related to the statistics of the large increments in the turbulent signals, the attention towards the so-called clustering intermittency has started to increase only in the last two decades, even if some pioneering studies were carried in previous years. The low attention towards the clustering intermittency is somewhat surprising, as intermittency itself is essentially defined as an alternance of extended quiescent periods/regions and short/small high activity periods/zones. It is then natural to characterize intermittency by means of events marked along the dependent variable axes, whatever time or space. Conversely, the concept of crucial events and of temporal complexity, related to non-trivial clustering properties of these same events, has been proposed as a general interpretative framework for the investigation of complex systems with metastable self-organizing dynamics.

Without any claim to being complete, in this chapter we give a review of event-based complexity approaches used in literature for the description of turbulence in the planetary boundary layer. The main goal is to put a first bridge between turbulence studies exploiting event-based complexity approaches, such as clustering exponents and classical Oboukhov intermittency exponents, and studies about intermittent complex systems, where concepts and ideas developed in the fields of non-equilibrium statistical physics, probability theory and dynamical system theory are jointly exploited.

Keywords: Intermittency, complexity, self-organization, event detection, turbulence, renewal, signal processing

[*] Corresponding author; Email: paolo.paradisi@cnr.it

This is a pre-print version. Please cite as:

Paradisi, P. and Cesari, R., Event-based complexity in turbulence, in “Paolo Grigolini and 50 Years of Statistical Physics” (edited by Bruce J. West and Simone Bianco), Cambridge Scholar Publishing, pp. 199-277 (2023). ISBN: 1-5275-0222-8

Table of Contents

Event-based complexity in atmospheric turbulence	1
<i>Paolo Paradisi^{1,*} and Rita Cesari²</i>	
1 Introduction	2
2 A very short introduction to intermittent complex systems	6
2.1 Crucial events and complex intermittency	7
2.2 Renewal processes	11
3 A brief history of intermittency in turbulence	16
3.1 Small-scale intermittency in ideal homogeneous and isotropic turbulence	16
3.2 Magnitude Intermittency vs. Clustering Intermittency	21
4 A few words about Planetary Boundary Layer meteorology	22
5 Self-organized structures and crucial events in turbulence	28
6 Event detection techniques in turbulent signals	32
7 Event-based complexity measures: intermittency, clustering and friends	39
8 Some relations between complexity exponents: SOC and EDDiS method	45
9 Intermittency, clustering and complexity in the PBL	49
10 Concluding remarks	58
10.1 A personal memento by Paolo Paradisi	59

1 Introduction

The term *fluid or hydrodynamical turbulence* denotes a dynamical condition of a fluid flow characterized by “certain complex and unpredictable motion” [40] and, in particular, by the emergence of vortex structures. More generally, turbulence is associated with the emergence of self-organized structures that can have different statistical and geometrical features, depending also on the range of considered space/time scales and on the boundary conditions. The main reference hydrodynamical model for fluid turbulence is given by the so-called *Newtonian fluid*, where a linear stress-strain relationship is assumed. This led to introduce a viscosity matrix and, under the isotropy assumption, which is a natural one in many applications, a dynamic viscosity coefficient μ_f . By also adding an incompressibility hypothesis, the following Navier-Stokes motion equation can be derived for the velocity field $\mathbf{u}(\mathbf{x}, t)$ [239,256] of a isotropic, incompressibile Newtonian fluid¹:

$$\frac{\partial \mathbf{u}}{\partial t} + \mathbf{u} \cdot \nabla \mathbf{u} = -\frac{1}{\rho_f} \nabla P(\mathbf{x}, t) + \nu \nabla^2 \mathbf{u} + \mathbf{F}(\mathbf{x}, t) \quad (1)$$

where $P(\mathbf{x}, t)$ is the pressure, $\mathbf{F}(\mathbf{x}, t)$ a generic term encoding an external forcing such as, e.g., gravity and buoyancy, ρ_f the fluid density (constant for incompressible fluids) and $\nu = \mu_f / \rho_f$ the kinematic viscosity. The Navier-Stokes equation is ubiquitously applied to many viscous fluids, including water and atmosphere. For these same Newtonian fluids, a huge number of experimental studies prove that turbulence emerges when the nonlinear advective term $\mathbf{u} \cdot \nabla \mathbf{u}$ becomes dominant

¹ It is worth noting that here the fluid is isotropic, in the sense that the stress-strain relationship is isotropic, but the *fluid flow*, i.e., the velocity field, can be anisotropic depending on the boundary and initial conditions.

with respect to the viscous term $\nu \nabla^2 \mathbf{u}$, where the first term encodes momentum transport by the velocity field and the second one momentum diffusion by molecular viscosity. This condition is parameterized by means of the adimensional Reynolds number:

$$Re = \frac{U L}{\nu} \Leftrightarrow \frac{\text{advection or inertia}}{\text{viscous dissipation}}, \quad (2)$$

being U and L a velocity and length scale coming out from the geometrical and dynamical boundary conditions. Being the Reynolds number a reference value for the ratio between advective and viscous terms, thus the onset of turbulence corresponds to the limit $Re \rightarrow \infty$ and, thus, to vanishing viscosity. This interplay or competition among inertia forces, given by the nonlinear advective term, and viscous dissipation is the most interesting aspect of Navier-Stokes hydrodynamics, as it hides the still elusive mechanism triggering the onset of turbulence [87]. The most problematic point lies in the so-called *dissipative anomaly* [40]. In fact, the dissipation goes to zero with the viscosity ν when the fluid flow is laminar, but this does not occur in the turbulent case. *Atmospheric turbulence*

Atmospheric turbulence is a very intriguing phenomenon that characterizes the so-called Planetary Boundary Layer (PBL) and that has attracted the interest of many researchers since decades. Oboukhov himself got a fundamental result from the analysis of atmospheric measurements [181], that is, the confirmation of the Kolmogorov-Oboukhov $-5/3$ spectral exponent [127,128,182] and, at the same time, the failure of the assumed universality of the pre-factor in the Power Spectral Density (PSD).

PBL turbulence is, in fact, the turbulent fluid flow reaching the higher Reynolds numbers and, thus, going very near to the ideal case $Re \rightarrow \infty$.

The interest towards PBL turbulence is also related to the problem of pollution, as turbulence near the ground highly affect the transport properties of contaminants and, thus, their diffusivity near the surface, thus a better understanding of PBL turbulence can give an effort in the improvement of local, regional and global forecasting, thus impacting on pollution management policies at both local and global levels.

However, the turbulent PBL is clearly not a controlled laboratory experiment and, thus, the analysis and modeling of turbulent motions can be quite dependent on the particular atmospheric condition and, especially, on the particular site. For this reason, after the pioneering era of turbulence studies in the PBL over flat terrain, the interest of the scientific community has moved towards the so-called *complex terrain* problem, i.e., fluid flow over and inside vegetated and urban canopies, and/or in the region very near to the ground ($< 1 \text{ m}$). In both cases, the effect of surface geometry and of roughness is directly felt by the turbulent flow, so that it becomes much more difficult to discriminate the direct effect of both geometry and local sources over the ground from the internal dynamics of the fluid flow.

A further complication is the modulation of “local” PBL turbulence dynamics, especially by mesoscale dynamics, classically referring to scales of $10 - 1000 \text{ km}$ and $1 - 10 \text{ hours}^2$, but also by synoptic-scale atmospheric dynamics, involving spatial scales of thousands km and temporal scales of days.

² This reference spatial and temporal scales are the classical ones and represent a quite rough classification that is nowadays almost overwhelmed by finer classifications. We do not go into these details here, but the reader can refer to recent literature (see, e.g., [149,255]).

Richardson's energy cascade and K41 model

The finite non-zero limit of the mean dissipation rate of Turbulent Kinetic Energy (TKE), usually denoted as $\langle \epsilon \rangle$ or $\bar{\epsilon}$, is one of the assumptions exploited by Kolmogorov and Oboukhov to derive the famous 2/3 and 5/3 laws, [127,128,182], that we will briefly introduce later and are named *K41 model* or *K41 theory* in the literature³. Another concept exploited in the K41 model is the concept of turbulent energy cascade, conjectured for the first time by Richardson in 1920 [225]. This concept is described in a famous sentence by Richardson itself that can be found at page 66 of his book “Weather Prediction by Numerical Processes” [226] and that sounds very much like a poem:

“Big whirls have little whirls
that feed on their velocity,
And little whirls have lesser whirls
and so on to viscosity -
in the molecular sense.”

Thus, energy flows from the largest scales of *energy-containing eddies*⁴, which are directly fed by some source of energy through an external forcing, to smallest scales, where TKE is directly dissipated into heat as a consequence of viscosity. In the Richardson picture, the passage of energy is among near scales.

In K41 model, Kolmogorov assumed that the energy flowing across scales was constant across scales themselves, which corresponds to assume a *quasi-equilibrium* picture between energy fluxes from the largest scales down to the smallest scales, namely the scales where viscous dissipation equals production of kinetic energy. This quasi-equilibrium condition defines the *inertial subrange*, i.e., the set of scales where the TKE coming from the large scales of motion is in equilibrium with the TKE that is dissipated into heat at the smallest scales due to viscosity. Thus, according to this Richardson-Kolmogorov view of an inertial subrange at equilibrium, the energy is transferred from larger to contiguous smaller scales of motion without loss of TKE at intermediate scales, until the dissipation scale is reached. By definition, the scales in the inertial subrange do not feel neither the large-scale forcing nor the viscous dissipation at small scales. This range of scales is usually delimited by the scales L and λ_K .

The so-called integral scale L is defined as the mean correlation length of the energy-containing eddies. The dissipation scale λ_K , also named Kolmogorov microscale, is the smallest scale with some kind of flow structure, i.e., the scale of the smallest eddies beyond which the viscous forces dissipate the TKE into heating [35].

Intermittency and events

The K41 model is still a milestone in turbulence studies, both experimental and theoretical, and the 5/3 law a reference to which compare new models and analyses are compared. However, as we will see in Section 3, a few years later it was already clear that K41 model needed an improvement due to the non-negligible presence of intermittency in the velocity increments and, thus, in the dissipation rates [36].

³ Considering the important contribution to this model by Oboukhov, this should better denoted as the Kolmogorov-Oboukhov, i.e., KO41 model.

⁴ The term *energy-containing* is related to the maximum of the turbulent energy (power) spectrum, whose location is taken as an approximate estimate of the length scale of energy-containing eddies themselves.

Interestingly, most studies on turbulence intermittency are devoted to the so-called Magnitude Intermittency (MI), while a more recent interest was focused on the so-called Clustering Intermittency (CI), that was almost neglected in the *first era* of turbulence studies [42,121,251].

As the name says, MI is related to the amplitude variations, i.e., to the increments of turbulent signals, and investigates the distribution of, and correlations among, such increments. This allowed to characterize not only the non-Gaussianity of signal increment distribution, but also its multiscaling features [183], being multiscaling a synonym of intermittency in turbulence studies. In fact, as known, a non-Gaussian distribution is the signature of large excursions in the signal that are less rare than in the Gaussian case, a condition possibly related to the emergence of anomalous diffusion [162] while the multiscaling in the moment of signal increments, also denoted as *structure functions*, is a signature of so-called *strong anomalous diffusion* [20,54].

Conversely, CI looks at the temporal (or spatial) order, that is, at the distances between the time instants or the space points at which large excursions occur. As large excursions occur in a short time and are relatively rare, this clearly reminds the concept of *event*, more precisely, of large excursion event, and the system's dynamical or geometrical properties can often be reduced to a set of point in time and/or space. The distribution of (time or space) distances among events and the inter-event correlations are important examples of CI measures. When the distribution is found to display a decaying stretched exponential or, more importantly, a slow power-law decay, the large excursion events become *crucial events* [281]. In fact, the power-law decay is a signature of self-similarity and, thus, of some kind of (self)-organization in the turbulent flow.

Even if less studies were devoted to a event-based approach, the interest towards the time/space ordering of large excursion events is increasing in the last decade or so. Further, the event-based approaches are somewhat associated with the concurrent research activity on turbulent flow structures, e.g., hairpin vortices in wall flows [141,257,263]. The availability of more accurate turbulence data could trigger in the next future a rapid increase in the interest of the scientific community.

Interestingly, similar approaches based on the concept of crucial events were recently proposed as a general theoretical picture of complex systems with metastable self-organizing dynamics [281].

Thus, the main goal is here to put a first bridge between turbulence studies exploiting event-based complexity approaches and studies about intermittent complex systems, where the focus is on the paradigm of cooperation and emergence of metastable self-organization.

Far from being complete, in this chapter we give a brief review of the most recent research in turbulence, with particular attention to PBL turbulence, in the perspective of intermittency and focusing on approaches in the framework of so-called *event-based complexity*, where the detection of single crucial events, and of associated turbulent structures, is a central component of the analysis and modeling of turbulence data. We will carry out a survey of methods and results in event-based approaches and, thus, on its different definitions and associated detection algorithms. In particular, we will discuss some of the most used statistical indices, or event-based complexity measures. In summary, in this review chapter

we are interested in the CI more than in the MI. However, due to its importance we will also briefly review fundamental results of turbulence MI.

The chapter is organized as follows.

In Section 2 a short introduction to intermittent complex systems and to the concept of crucial event is given, also including a brief survey of the dynamical foundations of renewal point processes. In Section 3 a brief outline of the main results about magnitude intermittency in turbulence is sketched, including a discussion on the differences between magnitude and clustering intermittency. To the sake of completeness, Section 4 is devoted to a short introduction of the planetary boundary layer, where turbulence emerges. In Section 5 the interplay between self-organized turbulent structures and crucial events is discussed and a convention about terminology is given. Sections 6 and 7 are devoted to a short survey of the most used event detection algorithms and event-based complexity measures/exponents, respectively. Section 8 discusses significant relations between some event-based complexity exponents and the applications of these same relations to data analysis. Section 9 reports an outline of some applications of event-based complexity analysis to PBL turbulence data that, in our opinion, can be considered as the most interesting ones in the recent literature. Finally, in Section 10 we sketch a brief discussion of the conclusions reached.

2 A very short introduction to intermittent complex systems

A great interest has rapidly increased in the last two decades towards systems, also including social dynamics, with many units that cooperate having the goal of maximizing self-regulation capacity and flexibility under the effect of rapidly changing environmental conditions. Essentially, there is a change in the paradigm, where the focus is on the *emerging self-organizing* dynamics of cooperative nonlinear systems. This paradigm is usually referred to as *complexity science*, a field of research that combines the experiences and expertise of many different scientific and technological fields. This paradigm nowadays involves not only the scientific community, but also policy makers, private companies and other socio-economic actors, and follows from the capability of nowadays observation systems to collect and store huge amounts of data. In fact, the present temporal accuracy of data acquisition is accompanied by the collection of countless aspects from a single system component that can be simultaneously observed on very large numbers of these same components without resorting to bulk measurements. These single components are representative of working units, particles, agents, fluid regions or other depending on the specific research field. Thus, the “mining” on these large datasets is nowadays requiring increasingly refined and powerful algorithms involving so-called feature extraction. Artificial Intelligence (AI), big data mining and complex network analysis [47,229,260,284] are examples of hot topics ubiquitously exploited in nowadays research that involve feature extraction algorithms. In a nutshell, we can say that complexity science investigates *how self-organization emerges from cooperative dynamical systems and what functionality of the entire complex system the above self-organizing behavior is optimizing*.

Even if complexity is a somewhat elusive concept and a universally accepted definition does not exist, we here refer to Ref. [193], where a cooperative system is defined to be *complex* if some kind of self-organized structures can be recognized

by means of statistical indices displaying self-similarity (mono- or multi-scaling) and there is not a master directly driving the great majority of the system's components, if not all, i.e., almost all the internal degrees of freedom are not slave variables of an external forcing.

The complexity paradigm has yet a long history, starting from very different scientific disciplines, such as sociology, psychology, cybernetics [37], physics and chemistry [178,219], and biology [158].

More recently, the network science introduced new perspectives in the way complex systems are modeled and analyzed, e.g., introducing concept such as connectivity measures derived from the topological structure of the complex network [47,284].

Nowadays the complexity paradigm as emergence of self-organizing states is exploited in many different research fields and applications, such as: brain cortex organization in neurosciences [52,53,259]; graph theory with application to social networks, e.g., the detection of communities [84,189,231]; detection of competing clusters in economy [217]; resilience of social networks and activities [81,144], a concept that has come nowadays to the forefront in the recent period in view of a response to the pandemic effects of Covid-19 on socio-economic activities [206]; all the -omics, e.g., genomics [163], proteomics and transcriptomics [31], metabolomics [115].

From the emerging self-organization paradigm follows the development, and application to large datasets ("Big Data"), of algorithms for the recognition of emerging structures and calculation of related emerging properties. This term refers to the evaluation of statistical indices related to the identification of some form of structure within the data. Depending on the scientific field and on the ultimate goal of the specific research, the identification of data structures takes on particular facets, assumes particular terminologies (sometimes indicating similar properties in different contexts) and uses different approaches derived through mathematical tools, in particular statistical tools derived from probability theory, stochastic processes, nonlinear dynamical system theory, network science, topological data analysis, deep learning.

2.1 Crucial events and complex intermittency

In complex systems where the self-organizing behavior dynamically evolve in time, the role of emerging self-organized states is tightly bound with that of *crucial events* marking the transitions between two ordered, i.e., self-organized states or between a ordered and a disordered state. The term "event" comes from the ubiquitous observation, both experimental and theoretical, that the transitions *Order* \Rightarrow *Order* or *Order* \Leftrightarrow *Disorder* occur in a time interval much shorter than all other characteristic time scales in the system, thus also including the so-called *life-times* of the self-organized states.⁵ Thus, the general picture is that of an alternance of self-organized states, with some kind of internal structure, and of

⁵ In the following, the self-organized states will also be named *self-organized structures*. In many papers on turbulence, the large scale self-organized structures, which are essentially given by the so-called energy-containing eddies, are denoted as *coherent structures*, e.g., eddies, vortices and so on. In our opinion, the small scale vortex structures that, as will be explained later, are triggered by the dynamical instabilities at the sharp edges of the large scale energy-containing eddies, could be also considered as self-organized states of the flow, but at temporal and spatial scales that are smaller with respect to the large scale eddies. As it will be explained below, in order to avoid ambiguities, we

totally disordered states of an alternance between two different self-organized states, in both cases being the passage marked by a transition occurring very quickly and with an abrupt change in the observed variables.

These large excursions are also associated with a fast memory drop in the system, which often reflects a drastic change in some topological features of the system itself. In complex networks, the transition can be given by a fast change in the connectivity; in turbulence or other continuum mechanical systems, it can be given by a fast passage from short-range to long-range synchronous/correlated motion of fluid particles. In any case, the memory drop recalls of a transition event occurring in a somewhat “random” fashion and the assumption of a time shorter than all the time scales of interest can be well approximated by just a time point. This opens the way to a modeling of Rapid Transition Events (RTEs) as point stochastic processes [77] and, in particular, as renewal point processes [76], that will be briefly introduced below. Conversely, the coherence of self-organized states is mirrored in the emergence of a inverse power-law decay in the Probability Density Function (PDF) of Inter-Event Times (IETs):

$$\psi(\tau) \sim \frac{1}{\tau^\mu}, \quad (3)$$

which thus becomes a signature of self-organization. In particular, the system is considered to have higher complexity for lower values of the exponent μ .

To our knowledge, the first studies proposing a event-based modeling approach were carried out by Montroll and co-workers in the 1960s. The milestone papers were a series of four papers: “Random Walk on Lattices I-IV” [167,168,169,170], where the Continuous Time Random Walk (CTRW) model was firstly introduced (see also [275] for a review). The CTRW is a random walk where the time step is not constant like in the Markovian random walk, but it is randomly distributed. The underlying microscopic dynamics are those of a particle motion in the presence of potential wells, where particles are trapped, with the superposition of a random force. Thus, the trapping time has a strong dependence on the position and velocity of the particle before falling inside the well itself and the exit time becomes essentially a random variable. These exit times corresponds to the above introduced IETs, also denoted as Waiting Time (WTs) in the framework of point stochastic processes [76,77]. The first applications of the CTRW model were in the context of charge mobility in disordered solids [168,237,238,265] and it is nowadays still applied as a basic modeling approach for *anomalous diffusion* [125,161,162], which is defined by a non-Gaussian distribution of a diffusing stochastic process $X(t)$ and a nonlinear time dependence of the variance⁶:

$$\langle X^2 \rangle \sim t^{2H}; \quad (4)$$

where H is the second moment scaling, which is the same as the Hurst exponent of rescalig analysis [111]. CTRW-based modeling attracted, and is still attracting, the interest of many research group, both regarding applications to experimental data analysis and theoretical/mathematical studies. The relations between CTRW and Fractional Diffusion Equations (FDEs) has attracted the attention

will denote both small scale and large scale structures as *self-organized turbulent structures*, leaving the term *coherent* only for the large-scale eddies.

⁶ An exception that was recently investigated is given by the Brownian yet non-Gaussian motion, where the variance is linear in time but the distribution is non-Gaussian [248].

of many research groups since more than three decades: Hilfer and Anton [104], Compte [72] Barkai, Klafter, Metzler and co-workers [34,160,161,162], Mainardi, Pagnini, Paradisi and co-workers [190,191,236,249]. The mathematical properties and solutions of FDEs were extensively investigated by Mainardi and co-workers [152,153,154,185,202,203] and others [234], while Grigolini, West and co-workers focused more on the physical aspects of FDEs [102,180,276,277,278,279,280,282]. It is worth noting that Mainardi, Pagnini, Paradisi and co-workers investigated the relationships of fractional diffusion in the framework of other modeling perspectives, e.g., subordination [95], generalized grey Brownian Motion (ggBM) [164,171,187,188], fractional random walks [92,93,94] and heterogeneous ensemble of Brownian particles [79,80,188,186,246,249,271].

CTRW, event detection methods, anomalous and fractional diffusion were and are still widely applied in many different contexts: turbulence and turbulent transport [78,197,199,200], human mobility [247], heterogeneous media [177,79,249], network science [105,106,156], transport in biological cells [51,85,112,160], foraging [270], porous media [233], pollution studies [32,62].

Starting from the CTRW Model, Grigolini and co-workers recognized the central role of crucial events and gave a fundamental contribution in understanding that crucial events underlie fundamental dynamics that lead to self-organization [6,8,10,11,12,49,96,100,143,192,193,213,235,268,281]. In fact, they found that anomalous diffusion is only one of the important mechanisms triggered by the presence of crucial events. Thus, the following definition can be given:

Definition (Crucial events):

A sequence of events is defined by a birth/death point process of self-organization and they are considered “crucial events” if:

- (i) the *renewal* condition [76], apparent or hidden, is satisfied;
- (ii) an inverse power-law decay is seen in the IET-PDF, given in Eq. (3) with $1 < \mu \leq 3$.

Following Refs. [38,96,192,193,205,268], the above conditions (i-ii) are denoted as *Fractal Intermittency* or *Complex Intermittency* and identifies the emergence of *Temporal Complexity* (TC) or *Intermittency-Driven Complexity* (IDC). The range $1 < \mu < 3$ is related to an infinite variance of the fluctuating IETs. In the case $1 < \mu \leq 2$, also the mean IET is infinite and the complex system is also non-ergodic due to strong aging.

The presence of crucial events is then the signature of cooperative dynamics where the emergence of self-organization is given not by a static but by a dynamically evolving structure and is one-by-one associated with a kind of instability that starts slowly and then has a rapid acceleration, i.e., the RTE occurrence, that destroys the self-organized structure, but only to trigger a new one.

This behavior reminds the concept of *metastability* and metastable states. This concept was discussed by Afraimovich and Rabinovich, who proposed and discussed a model for brain cognitive dynamics and information flow [2,222,223,224]. The dynamical laws have a set of equilibrium saddle points that, as known, also involve stable and unstable separatrices and manifolds and that are combined into a single structure called *stable heteroclinic channel*. This is defined by the set of trajectories moving in the neighborhood of the separatrices, moving from one saddle point to the other. When the system reaches a region around a given saddle point, there is a slow motion along the stable separatrix and towards the point

itself. During this long residence time interval, the system displays long-term memory and spatial/topological coherence, i.e., falls into a self-organized state⁷. After a relatively long *life-time*, the dynamical instabilities start to increase, the system moves towards the unstable separatrix until a sudden acceleration (the event) determines a fast motion of the system along the unstable separatrix that then becomes the stable one of the next saddle point, where the same temporal pattern is repeated.

Another example is given by the Manneville-Pomeau (MP) map [155,216], which is a prototype of so-called Type-I intermittency and will be briefly discussed below. Interestingly, the MP model was proposed as a toy model for a fluid particle motion experiencing an alternance of long time intervals with laminar, or quiescent, motion and of short-time *turbulent bursting* events. Thus, the MP map could be thought as a model for the intermediate regime of turbulence, that is, when a Richardson's energy cascade is still not fully developed⁸. In the MP model, a marginally stable point determines the slow "laminar" motion towards the chaotic region, where a turbulent bursting occurs. Shortly, the particle position comes back to the laminar region and the low predictability of the chaotic region acts as a random back injection to the laminar region⁹. The RTEs are here given by the passages from the laminar to the chaotic/turbulent region and *vice versa* and the IETs are given by the inter-burst times¹⁰.

There is an interesting link between intermittent complex systems and critical phenomena. In fact, it is well-known that second-order phase transitions are associated with long-range, i.e., power-law decaying, correlation functions. It was proven that these correlations follow as a consequence of serial MP intermittent dynamics driving the fluctuations of the "order parameters". This crucial result was derived both analytically [73,74] and numerically [268,269] and was found to have important consequences on the critical brain dynamics [14,18,19,68,86,196].

The concept of crucial event is recently entering also in the so-called *big data* or *data science*, where data mining, machine and deep learning and, in general, artificial intelligence tools are used. Complex network analysis came to the forefront about two decades ago and it still a widely used tool for big data mining (see, e.g., [47,284]). Complex network measures, e.g., centrality, degree distribution, clustering, shortest path, are basically static and are still widely exploited in network analysis, even when applied to time-varying networks, where time is just used to build up the statistical ensemble. However, for some time-varying networks, these static measures, or metrics, can cause some misinterpretation of

⁷ When carrying out the statistical analysis of the signal derived from the complex system, which is based on time or ensemble averages, long-range correlations and some kind of synchronization can be observed.

⁸ We recall that the mechanisms triggering the fully developed energy cascade of turbulence are associated with instabilities at the sharp edges of the main, energy-containing eddies. In this sense, the meaning of transition event could be applied to the formation of smaller vortex structures from the instabilities of the larger ones. This concept is at the basis of random cascade models (see, e.g., [87]).

⁹ Grigolini, West and co-workers have extensively studied a continuous-time version of the MP time-discrete model [6,7,8,10]. Paolo Grigolini often used to denote this model as "cheerful equation" as, in Italian, *cheerful* translates in "allegra", which sounds like Allegrini, one of the colleagues who contributed the most to the study of this continuous-time version of the MP model. For this reason, in the following we will denote this model as Allegrini's model.

¹⁰ In the MP time-discrete model, the burst duration is not always negligible, but this does not change the essential results. Alternatively, it is almost equivalent to consider the differences between the times at which two successive bursts begin.

the results. A central point is the rough approximation that considers all links, or edges, among nodes always the same, active or not active, thus without any change over time. On the contrary, links can have their own dynamics possibly triggering an alternance of active periods and non-active periods. In recent years, the concept of *temporal networks* was introduced and widely investigated [107,108]. The temporal network is represented not by a single adjacency matrix, but by a temporal sequence of adjacency matrices. According to Ref. [108], “The fundamental building blocks of temporal networks are *events* (or contacts, links, or dynamic links). These represent units of interaction between a pair of nodes at specified times.”

However, it is worth noting that, with respect to the concept of event as a local transition in the link/edge activity, the above introduced RTEs have to be thought as a transition in the self-organizing behavior of the network, both at the local and global level. Thus, the self-organizing RTE and the single link activity transition event are somewhat different concepts, but they are surely inter-related and this aspect should deserve further investigations.

2.2 Renewal processes

In the following, we sketch the main definition and results of Cox’s renewal theory and its dynamical foundations on the basis of both Manneville-Pomeau [155,216] and Allegrini models [6,7,8,10].

The MP map and its continuous-time version given by the Allegrini’s stochastic model represent basic prototypical toy models of TC/IDC complex systems. In fact, as said above, these models satisfy the renewal condition and reproduce the inverse power-law behavior in the Probability Density Function (PDF) of IETs, in the following denoted as IET-PDF. The MP time-discrete deterministic model for turbulent bursting is given by the following iterated map [155,216]:

$$\begin{cases} X_{n+1} = X_n + k|X_n|^z & \text{if } X_n < r \\ X_{n+1} = (X_n - r)/(1 - r) & \text{if } X_n > r \end{cases} \quad (5)$$

being $z > 1$ and r is defined by the relation: $r + k|r|^z = 1$. The basic function of the MP iteration map is plotted in Fig. 1, where the laminar and chaotic zones are reported.

Fig. 1 sketches the general behavior of the MP map and Fig. 2 report an example of a typical trajectory with turbulent bursting. Considering that $X = 0$ is a marginally unstable fixed point, it can be seen that trajectories starting near this point will spend a large amount of time near it, remaining in the laminar zone for a relatively extended time interval. Comparing Figs. 1 and 2, it is easy to see that in the laminar region the motion is smooth and highly predictable. On the contrary, when passing through the threshold r , the motion becomes chaotic and unpredictable until a return to the laminar region occurs that marks the end of the burst. This is mirrored in the inverse power-law IET-PDF given in Eq. (3).

Now, let us rescale the discrete time $1 \rightarrow \Delta t$ with $k = \alpha_0 \Delta t$ and $y(t_n) = y(n\Delta t) = X_n$. Thus, carrying out the continuous-time limit $\Delta t \rightarrow 0$ in Eq. (5), we clearly get the following equation:

$$\begin{cases} \dot{y} = \alpha_0 y^z ; & y \in [0, 1] \\ y(t_n^-) = 1 \Rightarrow y(t_n^+) = u(0, 1) , \end{cases} \quad (6)$$

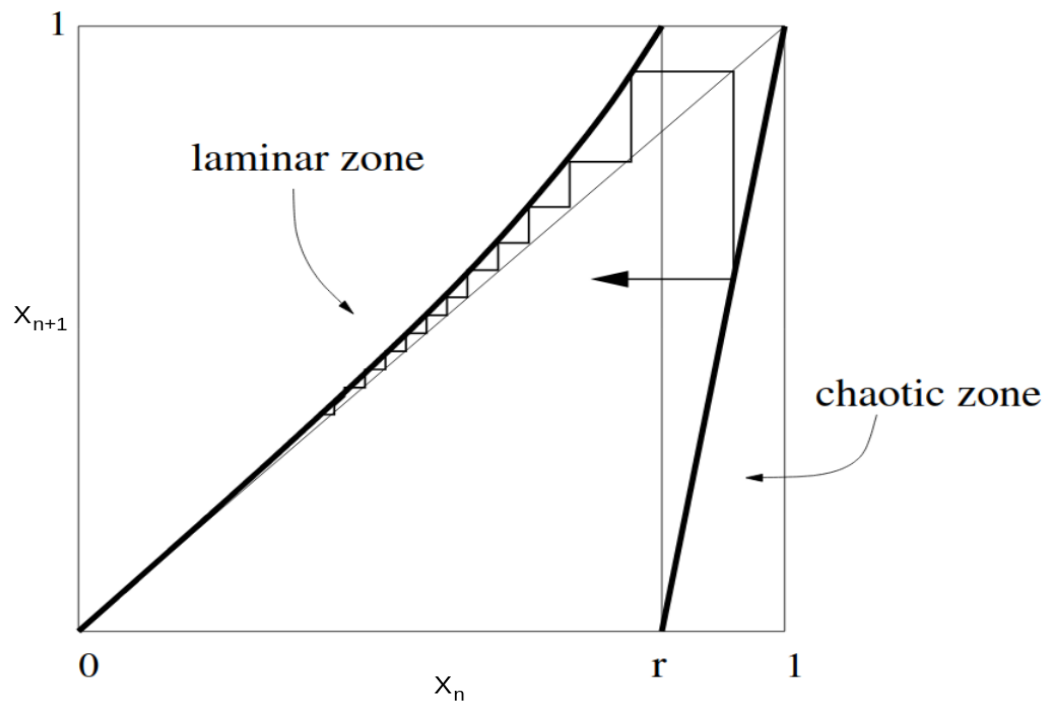


Fig. 1. Plot of the basic function x_{n+1} vs. x_n of the iterated map.

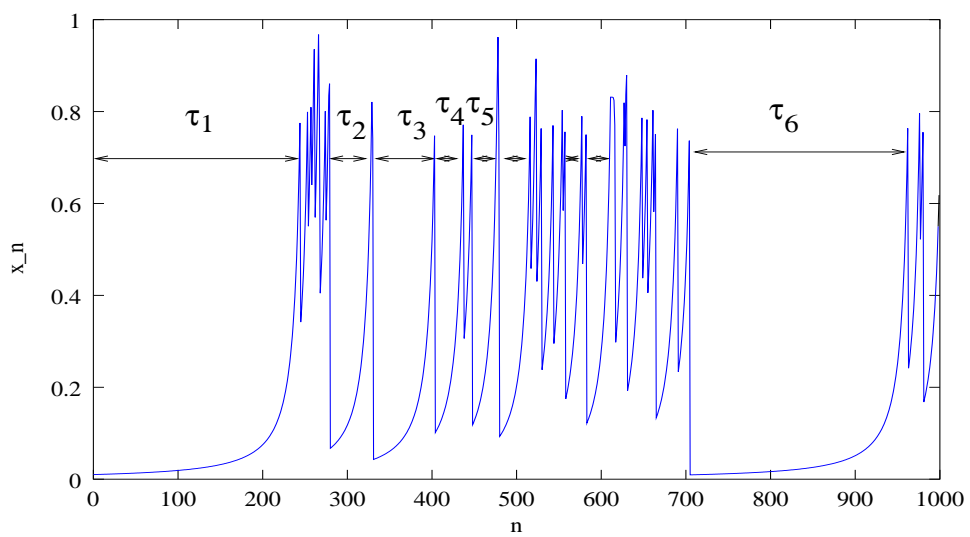


Fig. 2. A typical trajectory of the Manneville-Pomeau time-discrete map.

where $u(0, 1]$ is a uniform random variable in the interval $(0, 1]$. The initial condition is given by: $y(t = 0^+) = u(0, 1]$ ¹¹. The limit $\Delta t \rightarrow 0$ implies $r \rightarrow 1$ by

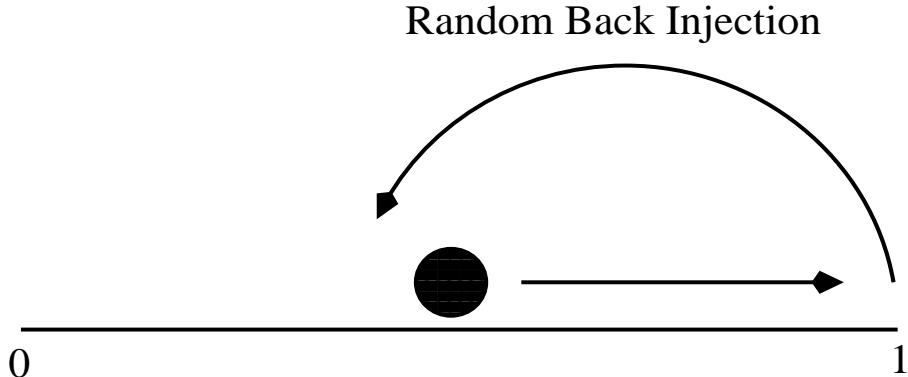


Fig. 3. Sketch of the Allegrini's stochastic model and of the random back injection.

definition, thus the chaotic region collapse into the boundary point $y = 1$. The random back injection, sketched in Fig. 2.2, mimics the effect of the bursting activities, whose duration are reduced to the time occurrences t_n of a stochastic point process. Thus, the sequence of event occurrence times:

$$\{t_n\}_{n \in \mathcal{N}} ; \quad t_{n+1} > t_n , \quad (7)$$

being $\mathcal{N} = \{0, 1, 2, \dots\}$ the set of positive integer numbers, is a *point process* that is also represented as a stochastic counting process $N(t)$:

$$N(t) = \int_0^t Z(t') dt' ; \quad Z(t) = \sum_n \delta(t - t_n) \quad (8)$$

where $\delta(\cdot)$ is the Dirac function. The IETs are given by:

$$\tau_n = t_n - t_{n-1} ; \quad t_0 = 0 ; \quad n \geq 1 . \quad (9)$$

A *renewal process* is defined as a point process whose IETs are mutually independent random variables [76]:

$Pr(\tau_i | \tau_j) = Pr(\tau_i)$, or, equivalently, $Pr(\tau_i, \tau_j) = Pr(\tau_i | \tau_j)Pr(\tau_j) = Pr(\tau_i)Pr(\tau_j)$, for whatever couple (i, j) , $i > j$.

A renewal process is also time-homogeneous, i.e., stationary, if the IETs are not only statistically independent, but also identically distributed. In this case, the renewal process is uniquely defined by the IET distribution:

$$\begin{cases} \Psi(\tau) = Pr \{ \text{IET} > \tau \} ; & \text{(Survival Probability Function)} \\ \psi(\tau) = -d\Psi/d\tau ; & \text{(Probability Density Function)} \end{cases} \quad (10)$$

being $\psi(\tau)d\tau = Pr \{ \tau < \text{IET} < \tau + d\tau \} = \Psi(\tau) - \Psi(\tau + d\tau)$. Clearly, it results:

$$\Psi(\tau) = \int_{\tau}^{\infty} \psi(s) ds = 1 - \int_0^{\tau} \psi(s) ds .$$

¹¹ In this formulation we avoid both the initial condition and the return to $y = 0$, because this would give an infinite time to reach the border $y = 1$, thus giving an infinite exit time. This does not change the computation of probabilities as $y = 0$ is a subset with zero Lebesgue measure. In other words, for any given τ_* , there will exist a time t_n such that $t_n - t_{n-1} > \tau_*$.

Equivalently, the renewal process can be described by the *local rate of event production* $r_c(t)$, also denoted as the *Cox's event rate*, which is the expected number of events per time unit in a neighborhood of the time t [76] (see also [4,199,201] for more details). More rigorously, $r_c(t)$ is defined as the conditional probability density that an event occurs in an infinitesimal time interval $[t, t+dt]$, given that no events occurred in the time interval $[t_n, t](t > t_n)$:

$$r(t) = \lim_{dt \rightarrow 0} \frac{1}{dt} \Pr \{ t < t_{n+1} \leq t + dt \mid t_{n+1} > t \} . \quad (11)$$

Limiting for simplicity to the case $t_0 = 0$, we have:

$$r(t) = \frac{\psi(t)}{\Psi(t)} = -\frac{1}{\Psi(t)} \frac{d\Psi(t)}{dt} . \quad (12)$$

This is exactly the definition that Cox gave starting from the concept of a statistical ensemble of independent trajectories that have a unique event. In the context of intermittent complex signals, Eq. (12) is generalized by means of time shift $t \rightarrow t - t_n$ and the Cox's rate becomes trajectory dependent¹² [4,201]. Thus, always limiting for simplicity to the first IET, so that $t_0 = 0$, we have the following relationship between the event rate and the Survival Probability Function (SPF):

$$\Psi(\tau) = \exp \left(- \int_0^\tau r(\tau') d\tau' \right) . \quad (13)$$

where $\Psi(0) = \Pr\{IET > 0\} = 1$ was the trivial initial condition. The time-homogeneous Poisson process is a particular case of a renewal process that is associated with intermittent system that do not display self-organizing behavior. The IET-SPF of a Poisson process is an exponential function: $\Psi(\tau) = \exp(-r_0\tau)$ and the rate does not change in time: $r(t) = r_0$. At variance with Poisson processes, a renewal Non-Poisson process is characterized by a Non-Poisson distribution of the events, a non-exponential WT distribution and a changing in time event rate $r(t)$. This condition is a necessary, but not sufficient condition that a intermittent complex system should satisfy.

Coming back to the Allegrini's model, Eq. (6), it is possible to derive the following exact expressions for the IET-PDF and the IET-SPF:

$$\psi(\tau) = \frac{\mu - 1}{T_0} \left(\frac{T_0}{T_0 + \tau} \right)^\mu ; \quad \Psi(\tau) = \left(\frac{T_0}{T_0 + \tau} \right)^{\mu-1} , \quad (14)$$

where

$$\mu = \frac{z}{z-1} ; \quad T_0 = \frac{1}{\alpha_0(z-1)} . \quad (15)$$

A crucial aspect is that both $\psi(\tau)$ and $\Psi(\tau)$ display an inverse power-law decay in the long-time regime $t \gg T_0$, thus satisfying scale invariance and self-similarity. Similarly, it is possible to derive the following expression for the event rate:

$$r(\tau) = \frac{r_0}{1 + r_1 \tau} , \quad (16)$$

being

$$T_0 = \frac{1}{r_1} ; \quad \mu = 1 + \frac{r_0}{r_1} , \quad (17)$$

¹² This also allows for a perturbation theory of event-driven processes [3,12,26,33]

The Non-Poisson renewal process reduces to a Poisson one when $r_1 \rightarrow 0$, which is equivalent to the the limit $T_0, \mu \rightarrow \infty$ in Eq. (14), with the constrain $(\mu-1)/T_0 \rightarrow r_0$. Thus, $\Psi(\tau)$ reduces to the exponential function $\exp(-r_0\tau)$.

Renewal Aging

The CTRW was recognized to have aging, i.e., a not negligible dependence on the initial condition even at very long times, even reaching the ideal case of infinite time in the subdiffusive case, i.e., $\langle X^2 \rangle \sim t^{2H}$ with $H < 0.5$, a condition determined by a very slow power-law decay in the IET-PDF ($\mu < 2$) [264,265,267]. Grigolini and co-workers recognized the central role of aging in intermittent complex systems even outside the CTRW model, that is, only referring to the sequence of crucial events, and developed a statistical tool, called *Renewal Aging* (RA) analysis [8,44,194], that can be exploited to give some clue about the validity of renewal condition¹³.

RA analysis can estimate the level of modulation, random or deterministic, of a complex system that displays a non-exponential IET-PDF and, in particular, a power-law decay $1/\tau^\mu$, usually with $\mu < 3$. Given a sequence of IETs $\{\tau_n\}$ and the associated event occurrence times $t_n = t_{n-1} + \tau_n$, the RA algorithm is given by the following steps [198]:

- (i) Given the aging time t_a and the event sequence $\{t_n\}$, let us consider the set of sliding windows:

$$\mathcal{T} = \{t_n \leq t < t_n + t_a; n = 0, 1, 2, \dots\}.$$

Then, the starting time of sliding windows are shifted from one occurrence time to the next one. This is equivalent to build up a set of trajectories that mimics a statistical ensemble of trajectories, even if the single realizations are not really independent each other.

- (ii) Given the n -th window, whose starting time is given by t_n , the first event k ($k > n$) occurring after the end of the time window is considered:

$$\text{Find } k : t_{k-1} < t_n + t_a < t_k$$

- (iii) The n -th truncated or aged IET is computed as: $\tau_n(t_a) = t_k - (t_n + t_a)$, and added to the sequence of aged IETs: $\{\tau_n(t_a)\}$, $n = 1, 2, \dots$

- (iv) A random shuffling is applied to the experimental sequence of IETs in order to get a *renewal* sequence $\{\tau_n^S\}$, where the prime S stands for “Shuffled”. In this way, a sequence with exactly the same IET-PDF of the experimental sequence, but without correlations among IETs, is obtained.

- (v) The steps (i-iii) are repeated on the shuffled sequence with the same t_a to get the sequence $\{\tau_n^S(t_a)\}$.

- (vi) The IET-PDFs and IET-SPFs for the three different IET sequences are computed:

- Brand-new distribution: $\psi_0(\tau)$ and $\Psi_0(\tau)$ from original sequence $\{\tau_n\}$.
- Aged experimental distributions: $\psi_{\text{exp}}(\tau, t_a)$ and $\Psi_{\text{exp}}(\tau, t_a)$ from the aged experimental sequence $\{\tau_n(t_a)\}$.
- Aged renewal distributions: $\psi_R(\tau, t_a)$ and $\Psi_R(\tau, t_a)$ from the aged shuffled sequence $\{\tau_n^S(t_a)\}$.

- (vii) The steps (i-vi) are carried out for several values of t_a .

¹³ In the application of the Renewal Aging analysis some care is needed and some aspect have to be considered, such as the presence of noise and modulating external forcings that can affect the results of the analysis (see, for example, [4,201,204])

In the following, Ψ_{exp} and Ψ_R will be denoted as *Experimental Aging* and *Renewal Aging*, respectively¹⁴. The three IET-PDFs can be graphically compared to get a clue about the amount of memory in the IET experimental sequence. The Renewal Aging acts as a reference curve for the aging time t_a . The comparison between Ψ_0 and Ψ_R gives an estimation of how far the IET distribution is from an exponential one, while the comparison between $\Psi_{\text{exp}}(\tau, t_a)$ and $\Psi_R(\tau, t_a)$ gives a measure of the departure from the renewal condition and, thus, on the memory of the event sequence. A quantitative evaluation of the *renewal content* can be carried out by introducing the Aging Intensity Function (AIF) [44,194]:

$$I_a(\tau, t_a) = \frac{\Psi_{\text{exp}}(\tau, t_a) - \Psi_0(\tau)}{\Psi_R(\tau, t_a) - \Psi_0(\tau)}. \quad (18)$$

In the purely renewal Non-Poisson case, $I_a(\tau, t_a) = 1 \forall \tau, t_a$. This property was verified comparing renewal Non-Poisson and slowly modulated Poisson models. The Non-Poisson model was a renewal process with the same IET-PDF of the Allegrini's model, given in Eq. (14). The slowly modulated model was derived in such a way to get the same IET-PDF. Clearly, the modulation introduces memory in the time ordering of the events. Thus, Renewal Aging was proven to detect this kind of memory in event sequences. In fact, the AIF showed a well-defined behavior with an asymptotic constant that was used as a measure of the renewal content of the artificial event sequences. The theoretical analysis gave the following general results [8,9,44,194]:

- For time-homogeneous Poisson processes there's no aging: $\psi_0(\tau) = \psi_{\text{exp}}(\tau, t_a) = \psi_R(\tau, t_a) \forall t_a$.
- For time-homogeneous renewal Non-Poisson processes: $\Psi_0(\tau, t_a) < \Psi_{\text{exp}}(\tau, t_a) = \Psi_R(\tau, t_a)$. This is the condition identifying a renewal process, but only if it is satisfied for any aging time $t_a > 0$.
- For Non-Homogeneous Poisson Processes with a random rate modulation generating Non-Poisson events, the Experimental Aging $\Psi_{\text{exp}}(\tau, t_a)$ decreases from the Renewal Aging $\Psi_R(\tau, t_a)$ to $\Psi_0(\tau, t_a)$ as the modulation becomes slower and slower. In other words, the Renewal Aging decreases as the ratio between Non-Poisson and Poisson events decreases.
- Very slow modulation has zero Renewal Aging, which means $\Psi_0(\tau, t_a) = \Psi_{\text{exp}}(\tau, t_a) \neq \Psi_R(\tau, t_a)$, even if the brand new WT distribution is not an exponential function but an inverse power-law.

RA analysis was successfully applied to the fluorescence intermittency of Blinking Quantum Dots [44,194]. In this application to real data, the AIF was not really constant, but it was found to reach an asymptotic behavior, even if with some fluctuations¹⁵ [45].

3 A brief history of intermittency in turbulence

3.1 Small-scale intermittency in ideal homogeneous and isotropic turbulence

The theoretical picture given by the K41 model, which still represents a guideline for all the turbulence theoretical research, is limited to the ideal case of *homoge-*

¹⁴ Slightly different conventions were sometimes used, such as Real instead of Experimental Aging, and Ψ_S instead of Ψ_R .

¹⁵ It is worth noting that AIF has to be treated with some care due to the possible small differences in the denominator of Eq. (18) that can cause large variations in the AIF.

neous and isotropic turbulence [166,287], also named *fully developed turbulence*. As said above, the basic assumptions are:

- (i) the dissipation rate remain finite and different from zero in the limit $Re \rightarrow \infty$ and
- (ii) a quasi-equilibrium condition across the scales of the inertial subrange, which naturally follows from the global energy conservation:

mean dissipation rate at small scales ($\langle \epsilon \rangle$) = energy flux at large scales

The K41 model and almost all turbulence studies are developed in the random field formalism, thus characterizing the statistics of the velocity increments:

$$\Delta \mathbf{u}(d\mathbf{x}, dt) = \mathbf{u}(\mathbf{x} + \Delta \mathbf{x}, t + \Delta t) - \mathbf{u}(\mathbf{x}, t) \quad (19)$$

Thus, multi-dimensional probability distributions are evaluated. The *p-th order structure functions* and, in particular, the *longitudinal p-th order structure functions*, are of particular interest:

$$S_p(\Delta x, \Delta t) = \left\langle \left| (\mathbf{u}(\mathbf{x} + \Delta \mathbf{x}, t + \Delta t) - \mathbf{u}(\mathbf{x}, t)) \cdot \frac{\Delta \mathbf{x}}{\Delta x} \right|^p \right\rangle \quad (20)$$

being $\Delta x = |\Delta \mathbf{x}|$ the distance between the two points at which velocity is measured¹⁶. In addition to the above assumptions, Kolmogorov made two basic similarity hypotheses that were assumed to be valid in the limit $Re \rightarrow \infty$ and $\Delta x \ll L$, where L is the integral scale of the energy-containing eddies introduced above:

First similarity hypothesis:

In isotropic conditions, the multi-dimensional distribution of the velocity increments are uniquely defined by mean dissipation rate $\langle \epsilon \rangle$ and the kinematic viscosity ν .

From this hypothesis follows that the length, velocity and time scales (Kolmogorov microscales) are defined as:

$$\lambda_K = \left(\frac{\nu^3}{\langle \epsilon \rangle} \right)^{1/4} ; \quad v_K = (\nu \langle \epsilon \rangle)^{1/4} ; \quad \tau_K = \left(\frac{\nu}{\langle \epsilon \rangle} \right)^{1/2} . \quad (21)$$

Then, we have the

Second similarity hypothesis:

The multi-dimensional distribution $P(\Delta \mathbf{u}_1, \dots, \Delta \mathbf{u}_N)$ at small scales, i.e., in the inertial subrange¹⁷:

$$\lambda_K \ll \Delta x_n \ll L ; \quad \tau_K \ll \Delta t_n \ll L/U ; \quad \forall n , \quad (22)$$

and satisfying the conditions:

$$\Delta x_n \gg \lambda_K ; \quad |\Delta \mathbf{x}_n - \Delta \mathbf{x}_m| \gg \lambda_K ; \quad n \neq m , \quad (23)$$

$$\Delta t_n \gg \tau_K ; \quad |\Delta t_n - \Delta t_m| \gg \tau_K ; \quad n \neq m , \quad (24)$$

are uniquely determined by mean dissipation rate $\langle \epsilon \rangle$ and are independent of ν .

¹⁶ Notice that homogeneous and steady conditions are implicit in the notation $S_p(\Delta x, \Delta t)$.

¹⁷ U is the mean large-scale velocity.

From the above assumptions and the two Kolmogorov similarity hypotheses follows the well-known scaling relationships of homogeneous and isotropic turbulence:

$$S_p(\Delta x, 0) \sim (\langle \epsilon \rangle \Delta x)^{p/3} ; \quad (25)$$

$$S_2(\Delta x, 0) = C_1 (\langle \epsilon \rangle \Delta x)^{2/3} ; \quad (26)$$

$$E(k) = C_2 \langle \epsilon \rangle^{2/3} k^{-5/3} ; \quad (27)$$

$$S_2(0, \Delta t) = C_0 \langle \epsilon \rangle \Delta t , \quad (28)$$

being $E(k)$ the spatial PSD in the wave number $k = 1/\Delta x$, whose $5/3$ scaling is valid in the range $1/L \ll k \ll 1/\lambda_K$. The K41 model was experimentally verified in his essential aspects in many experimental studies, but, even if the basic approach is still valid, some of the assumptions were questioned, both experimentally and theoretically.

In fact, Landau reported his objection on the universality assumption in the 1944 Russian edition of the book “Fluid mechanics”[132]:

“ ... averaging these expressions is dependent on the variation of ϵ over times of large-scale motions (scale L), and this variation is different for different specific flows. Therefore, the result of the averaging cannot be universal. ”

which means that the “universal” constants C_0 , C_1 and C_2 in Eqs. (26-28) are not really constant, but functions of space and time. This objection was confirmed by Oboukhov’s findings in atmospheric turbulence [181]. Analysis of different experimental samples confirmed the K41 $5/3$ and $2/3$ scaling exponents given in Eqs. (26-27), but found that the pre-factor has significant changes depending on the large scale dynamics and, thus, on the external forcing. This confirmed Landau’s objection and proves that the fluctuations in the energy dissipation rate are not negligible. Another similar objection came from the finding of intermittent behavior of velocity increments and dissipation rates at small scales, which results in the failure of the quasi-equilibrium assumption¹⁸. In fact, in 1949 Batchelor and Townsend [36] carried out experiments that revealed the intermittent nature of the instantaneous dissipation¹⁹. By analyzing the velocity derivatives, they found that energy dissipation at small scales (i.e., large wave-numbers) is very heterogeneous in space, with active regions displaying large excursions in the turbulent signals alternating with quiescent regions. Further, the fluctuations tend to an on-off intermittent discontinuous process, a behavior that becomes more relevant as the Reynolds number increases. This spatial intermittency determines the emergence of non-Gaussian shapes in the distributions of dissipation rates and velocity increments.

The finding of intermittency led to the *refined similarity hypothesis* proposed by Kolmogorov and Oboukhov [129,181], where the fluctuations of the dissipation rate are taken into account and, further, a direct local relationship between velocity increments and dissipation rates is assumed. As a consequence, multidimensional probability distributions of velocity increments and associated structure functions are directly related to the probability distribution of the local

¹⁸ The neglect of small scale intermittency was later remarked also by Landau himself, and it seems that Kolmogorov, trying to overcome this K41 limitation, interpreted Landau’s objection as mainly referred to the lack of intermittency in the K41 model.

¹⁹ According to Ref. [40], “the fact that small-scale activity in high-Reynold number turbulence becomes increasingly clumpy and that self-similarity is broken is generally referred to as *intermittency*”. However, it is worth noting that different definitions of turbulence intermittency can be found in the literature.

dissipation rate ϵ . In more detail, the refined similarity model assumes that the dissipation rate ϵ remains constant inside regions of the inertial subrange with size $r \gg \lambda_K$, and change passing from one region to another. Following this approach, Kolmogorov and Oboukhov introduced a local spatial average of the dissipation rate:

$$\epsilon_r(\mathbf{x}, t) = \langle \epsilon \rangle_r(\mathbf{x}, t) = \frac{1}{V_r} \int_{|\mathbf{z}| < r} \epsilon(\mathbf{x} + \mathbf{z}, t) d\mathbf{x}, \quad (29)$$

being $V_r = 4\pi r^3/3$ the volume of the sphere of radius r . Given the distance Δx , it follows that Eq. (26) is still valid on the local scale $r = \Delta x$, so that it can be mediated to provide the following expression:

$$S_p(\Delta x, 0) = C'_p \langle \epsilon_r^{p/3} | r = \Delta x \rangle \Delta x^{p/3} \quad (30)$$

In this formulation, the averaged dissipation rate $\epsilon_r(\mathbf{x}, t)$ depends on the large scales, i.e., on the structure of large-containing eddies, thus partially addressing the Landau's objection²⁰. In particular, Kolmogorov exploited this dependence to address the intermittency problem and, to this goal, he considered the Oboukhov's proposal of a log-normal distribution for ϵ_r , which is often referred to as the *third similarity hypothesis*²¹. In fact, in this approach, a proper model for the distribution of ϵ_r is sufficient to describe the velocity increment statistics. The third similarity hypothesis includes also an *ad hoc* assumption for the dependence of variance on distance $r = \Delta x$:

$$\sigma_r = \langle \log(\epsilon_r(\mathbf{x}, t)) \rangle = A(\mathbf{x}, t) + \mu^* \log \left(\frac{L}{r} \right), \quad (31)$$

where μ^* is assumed to be a universal constant. Applying the third hypothesis, it follows:

$$S_p(\Delta x, t) = D_p(\mathbf{x}, t) \langle \epsilon \rangle^{p/3} \Delta x^{\zeta_p}, \quad (32)$$

where

$$D_p(\mathbf{x}, t) = C_p(\mathbf{x}, t) L^{\mu^* p(p-3)/18} \quad (33)$$

depends on the large scale structure of the energy-containing eddies and

$$\zeta_p = \left[\frac{1}{3} + \frac{\mu^*}{6} \right] p - \frac{\mu^*}{18} p^2. \quad (34)$$

The nonlinear dependence of ζ_p on p is a signature of multiscaling²², i.e., the system's self-similarity is not described only by one exponent, but by a set of exponents that often depend on one or two adimensional parameters, such as μ^* in Eq. (34). The parameter μ^* is related to the autocorrelation function of the dissipation rate:

$$\langle \epsilon(x+r) \epsilon(x) \rangle \sim \left(\frac{L}{r} \right)^{\mu^*} \quad (35)$$

²⁰ The derivation of Eq. (30) follows from two modified similarity hypotheses involving conditional probabilities instead of total probabilities.

²¹ A log-normal distribution of a random variable X is defined as a Gaussian distribution of the random variable $Y = \log(X)$. Reading the original 1962 paper, Kolmogorov write explicitly that "...Oboukhov has now discovered how to refine our previous results in a way which takes Landau's comments into consideration" before introducing the basic modifications of the new model, that is, the local spatial average defining the random variable $\langle \epsilon \rangle_r(\mathbf{x})$ and the assumption of the associated log-normal distribution. Thus, Kolmogorov seems to have basically followed the ideas proposed by Oboukhov.

²² The case of a linear ζ_p with a constant (affine function) also falls into the multiscaling case.

and it can be also evaluated by the 6th-order velocity structure function [89].

The K62 model is probably the first model derived to reproduce intermittency of turbulent fluctuations by means of multiscaling exponents in the structure functions S_p . Since then, a very large number of studies faced the problem of turbulent intermittency and multiscaling carrying out Direct Numerical Simulations (DNS) of the Navier-Stokes equations or proposing different modeling approaches, mainly focused on local statistical features of the dissipation rate or on the energy cascade. This is the focus of so-called random cascade modeling approaches. In fact, an extended research line was, and is still, focused on the phenomenological modeling of intermittency in the framework of random cascade models mimicking the Richardson's turbulent energy cascade (see, e.g., [41] and, for a brief review, [82,241,250]). An example is given by the β -model [87,89], where the multiscaling exponent is given by:

$$\zeta_p = \frac{\mu^* + 1}{3}p - \mu^* \quad (36)$$

Alselmet et al. (1984) [22] carried out a famous experiment and an accurate evaluation of high-order velocity structure functions and they found that:

- (i) the linear and affine (linear+constant) behavior of K41 and β models, respectively, do not reproduce the experimental behavior of structure functions;
- (ii) k41 departs from the data starting from $p = 4$, while the β -model performs slightly better (up to $p \approx 6 - 7$);
- (iii) the K62 log-normal model reproduces the structure functions up to the 12-th order²³;
- (iv) the parameter μ^* was evaluated and given by: $\mu^* = 0.2 \pm 0.05$.

She and Leveque (1994) [242] proposed a stochastic model where the log-normal assumption is substituted with a log-Poisson one, thus getting:

$$\zeta_p = \frac{p}{3} - \frac{2p}{9} + 2 \left(1 - (2/3)^{p/3} \right) \quad (37)$$

These intermittency corrections much improved the agreement with both Navier-Stokes simulations and experiments [243,250], e.g., the multiscaling exponents given in Ref. [22] were much better reproduced by the She-Leveque log-Poisson model than by the K62 log-normal model.

In summary, many authors went on addressing the problem of intermittent fluctuations in turbulence, as it is at the heart of the main theoretical and mathematical issue of turbulence, namely, the existence of a solution of the Navier-Stokes equation in the limit $Re \rightarrow \infty$, i.e., for vanishing viscosity.

Regarding the investigation of intermittency by DNS of Navier-Stokes equations, interesting advancements were achieved about two decades ago by means of theoretical and numerical studies in the transport of passive scalars [61,88]. These results are considered to be a milestone in the study of intermittency in homogeneous and locally isotropic turbulence as they found some probably conclusive results on the universal character of the multiscaling spectrum in scalar intermittency [40]. Remarkably, these numerical investigations on passive scalar transport in Navier-Stokes turbulence started from the conjecture that Kraichnan developed in 1994 with a random field model mimicking the spatial Kolmogorov

²³ The orders greater than 12 have less accuracy, but the scaling relationship is preserved, so that the departure of K62 from the data for $p > 12$ is considered genuine and definitive.

spectrum [130], but with short-time correlation, thus suggesting that intermittency is mainly related to the spatial correlations of the turbulent velocity field. In summary, the discovery of intermittency in small-scale turbulence triggered a bunch of studies, both experimental and theoretical. It is interesting to notice that intermittency refers to *large excursion events* that occur randomly in the fluid flow. Thus, it seems natural to jointly investigate the statistics of large excursion statistics (Magnitude Intermittency) with that of the event spatial and/or temporal ordering (Clustering Intermittency).

3.2 Magnitude Intermittency vs. Clustering Intermittency

As anticipated in the Introduction, since Kolmogorov and Oboukhov papers in 1941 the great majority of the studies about intermittency in small-scale turbulence refer to the p -th order structure functions that characterize the Magnitude Intermittency (MI) without any link to the Clustering Intermittency (CI).

This gap is probably related to the intrinsic difficulties in defining events unambiguously and detecting them in experimental time series. In fact, the MI approach is a purely statistical approach that only needs the values of measured turbulent signals after a proper pre-processing, e.g., noise removal/reduction, of raw data. Conversely, the detection of single structures and related single transition events in the data needs some evaluation of the local geometrical shape of random signals and fields [5,184,220,257,286]. This is often a challenging task as it depends on recipes of signal processing that, even if starting from quite general concepts, involve *ad hoc* choices [198,200]. The reasoning leading to many of these choices follows from the specific problem, as they depend on the specific geometry of the structure to be detected within the signal or field. To give an intuitive idea, given the two-dimensional graphic of a signal with time/space on the horizontal axis and the signal intensity on the vertical one, MI (CI) is referred to the vertical (horizontal) axis. Being the horizontal (time or space) axis uniformly sampled, both the statistical distributions of this variable and of its increments are trivial. It is then clear that, at variance with MI, that only needs the signal values to derive statistical distributions, the CI approach need to refer to some definition of event and to the related algorithm of event detection, so that some assumptions must be made on the shapes that we want to detect in the light of their meaning linked to the underlying dynamical counterpart. In this sense, the CI approach is more difficult than the MI one. To our knowledge, the focus on the distinction between MI and CI was firstly introduced and investigated in Bershadskii et al. [42]. This involved the direct detection of episodes/events in the turbulent flow in order to evaluate the CI structure. In fact, the CI is directly linked to a viewpoint about turbulence that gives a primary relevance to the concept of *crucial event*. As far as we know, the application of *event-based* approaches to turbulence was first introduced or, at least, brought into the attention of the scientific community, by Narasimha and co-workers [116,173,174,175,176], who discussed this aspect and questioned about the need of an alternative “episodic” view of turbulence with respect to classical approaches based on concepts such as the eddy diffusivity²⁴.

²⁴ Eddy diffusivity modeling is an approach based on so-called Reynolds averaging of Navier-Stokes equations where, due to nonlinearities, the averaged dynamical equations must be closed with some assumptions about mean transport properties of eddies, i.e., of turbulent fluctuations. Estimation of local eddy diffusivity through a modeled relationship between fluxes (momentum, mass, heat) and gradients of mean fields (velocity, concentration, temperature) is the first-order development of

In particular, Narasimha recalls and extends a statement by Jeffrey (1926) [113] for which events “are not to be thought of as perturbations on the background general circulation but as essential to maintaining it” [175], where Jeffrey has in mind a background modeled as a superposition of harmonic random waves, according to the spectral approach to turbulence. Narasimha grounded his reasoning on experimental studies that highlight the episodic structure of turbulence (see, e.g., [75,126]).

Since 2004, many studies applied event-based approaches to turbulence studies in order to investigate the role of CI with respect to the more studied MI [42,251]. Nowadays, this is especially a hot topic in the context of experimental and modeling studies of atmospheric turbulence near the ground, i.e., in the so-called Planetary Boundary Layer (PBL), where turbulence is known to emerge. In particular, the case of turbulent flows over complex terrain [117,83] is taking momentum in the scientific community [57,58,109,110,121,214,215].

Being both linked to the occurrence of large excursions in the signal, CI and MI are two strictly interconnected aspects of the same intermittency phenomenon. However, they give somewhat different information about the complex system, in this case the turbulent flow, and it is not yet clear if the parameters, i.e., the scaling exponents, derived from both approaches are strictly related to each other by a unique relationship only related to the dynamical flow equations or if, on the contrary, their relationship changes according to the particular geometrical and dynamical conditions.

4 A few words about Planetary Boundary Layer meteorology

The Planetary (or Atmospheric) Boundary Layer (PBL or ABL) is an important part of natural environment where humans live. The role of turbulence is central in PBL dynamics. Thus, before passing to discuss the application of complexity concept to PBL turbulence, in this section we present a brief survey of the main PBL features and related terminology.

Basic concepts: The PBL concept is related to the more general one of boundary layer in fluid flows. This term was introduced in the literature by Prandtl in 1904 [218] for a flow of a fluid of low viscosity close to a solid boundary. As regard atmospheric flows, a precise definition of boundary layer is not so easy. It is useful to define the boundary layer as “that part of the troposphere that is directly influenced by the presence of the earth’s surface, and responds to surface forcing with a time scale of about an hour or less” [253]. The simplest and more *idealized* boundary layer is over an infinite flat surface. It is equivalent to a flow horizontally homogeneous [117]. In addition to horizontal homogeneity, for most applications the flow is assumed to be stationary. The PBL can be roughly divided in two region, in analogy to the two-dimensional boundary layer generated in a wind tunnel:

this approach. The evaluation of eddy diffusivity comes from two approaches: (i) scaling arguments, following the prescription of the Buckingham π theorem of dimensional analysis; (ii) spectral approaches, where eddy diffusivity is related to the correlation features of the turbulent fluctuations (Taylor’s theorem [258]).

1. The *inner region*, called *atmospheric surface layer* (ASL) where the interaction between the atmospheric flow and the ground surface is very strong. The wind structure is mainly affected by surface friction and by the vertical exchanges of heat and moisture, and the flow is little affected by the earth's rotation. This region extend above the roughness obstacle, on average, up to $10 \div 100$ m. In this region the effect of viscosity and of the structure of the roughness elements are negligible, the flow is fully turbulent and the vertical turbulent fluxes are mainly constant (their magnitude vary less than 10%) .
2. The *outer region*, sometimes referred as *Ekman layer* where the effect of the Coriolis force due to the Earth's rotation and of the pressure gradient are dominant. In this layer the surface fluxes decrease with height, that can reach $500 - 2000$ m.

An overlap region is present between the two layers. Above the PBL is the free atmosphere, the flow is nearly geostrophic and no longer influenced by the surface. An *interfacial sublayer* (or *microlayer*) between the earth surface and the bottom of the ASL extends up to about three or four times the height of the roughness obstacles. This layer may be *viscous* in the case of smooth ground surface, or a *canopy sublayer* over rough surface. In the interfacial sublayer the flow is very inhomogeneous and three-dimensional.

PBL turbulence depends on the atmospheric large-scale dynamics and on the momentum and heat exchanges at the surface, strictly related to the radiation balance and to the heat flux at the ground. In addition, moisture effects can be taken into account [256]. Turbulent motion can be described by a superposition of vortexes of different size, ranging from few millimeters to the depth of the boundary layers. Time series of meteorological variables can be used to represent spatial evolution of the variable under investigation, if the Taylor hypothesis of frozen turbulence is verified. This is true when the time life of a vortex is longer than the time the vortex needs to overpass the measurement instrument, that is the mean wind speed is large compared to turbulent intensity.

Stability of the Planetary Boundary Layer: The features of the PBL and its turbulent characteristics depend on the relative balance between the different process that generate turbulence, mainly due to buoyancy and mechanical forces. Mechanical turbulence production is generate from wind shear, while the buoyancy force are a consequence of the variation of air density with the altitude. This variation is produced by the thermal stratification due to heating of the ground by solar radiation during clear days, and its radiative cooling during the night. In an adiabatic atmosphere the potential temperature is constant. The potential temperature is the temperature that a fluid parcel, with absolute temperature T (in K degrees) and air pressure P at a height z , takes if it moves adiabatically to a reference height z_0 with pressure $P_0(z_0)$ and is given by:

$$\Theta = T \left(\frac{P}{P_0} \right)^{-R/c_p} \quad (38)$$

P_0 is a reference pressure, usually set to 100 kPa or to the surface pressure, R is the gas constant of air and c_p is the specific heat capacity at a constant pressure (for air $R/c_p = 0.286$). For thermal stratification a *static stability* criterion can be adopted:

$$\text{unstable: } \frac{\partial \Theta}{\partial z} < 0 \quad (39)$$

$$\text{neutral: } \frac{\partial \Theta}{\partial z} = 0 \quad (40)$$

$$\text{stable: } \frac{\partial \Theta}{\partial z} > 0 \quad (41)$$

In a nutshell, air parcels tend (i) to oscillate around a given height in stable atmosphere, (ii) to go far from the initial height in an unstable atmosphere and (iii) to remain in the same point in neutral atmosphere.

The static stability does not depend on wind. Since statically stable wind shear can generate turbulence, a comparison between the relative magnitudes of the shear production and buoyant consumption terms of the Turbulent Kinetic Equation (TKE) equation can be used to estimate when the flow might become *dynamically unstable*. An indicator is given by the dimensionless flux Richardson number, defined as the ratio between the buoyant and the mechanical production terms of the TKE budget equation²⁵:

$$R_f = \frac{\left(\frac{g}{\Theta_V}\right) \overline{(w' \Theta'_v)}}{\overline{(u'_i u'_j)} \frac{\partial \bar{U}_i}{\partial x_j}} \quad (42)$$

where Θ_v is the virtual potential temperature, that is the potential temperature that dry air must have to equal the density of moist air at the same pressure. The Richardson number can be expressed as a function of the gradients of mean velocity and temperature. The gradient Richardson number is then derived by the Richardson flux number by assuming horizontal homogeneity and neglecting the vertical component. This is defined by:

$$Rg = \frac{\frac{g}{\Theta_V} \frac{\partial \bar{\Theta}_V}{\partial z}}{\left[\left(\frac{\partial \bar{U}}{\partial z} \right)^2 + \left(\frac{\partial \bar{V}}{\partial z} \right)^2 \right]} \quad (43)$$

Based on the Richardson number, the following classification is usually given:

$$R_f < 0 \quad \text{for unstable stratification} \quad (44)$$

$$R_f > 0 \quad \text{for stable stratification} \quad (45)$$

$$R_f = 0 \quad \text{for neutral stratification} \quad (46)$$

The value $R_f = 1$ is a theoretical limit beyond which atmospheric turbulence is suppressed. $R_f = 1$ is the value at which the turbulent energy production by shear stress is consumed by buoyancy forces, and $R_f << 1$ indicates that the heat flux is negligible in the TKE balance. In stable conditions, a critical value of R_f can be defined and empirically estimated (0.20 - 0.25), below which stationary turbulence is possible. Above this value, intermittent or decaying turbulence can occur. This is the case of stably-stratified turbulent flows [256].

Stability in the PBL can be measured by a scaling parameter, defined as follows. Following the Monin-Obukhov Similarity Theory (MOST), it is assumed that the PBL dynamics is driven by the surface turbulent fluxes [165], assumed to be constant with the height.

A velocity scale u_* , called friction velocity, is defined as:

$$u_*^2 = \left[\overline{u' w'_s}^2 + \overline{v' w'_s}^2 \right]^{1/2} \quad (47)$$

²⁵ By convention: $U_1 = U$ and $U_2 = V$ are horizontal component of mean velocity, while $U_3 = W$ is the vertical one. Similarly for the velocity fluctuations: $u'_1 = u'$ and $u'_2 = v'$ and $u'_3 = w'$.

and a length scale L , called Oboukhov length, is defined as:

$$L = -\frac{\overline{\Theta_v} u_*^3}{\kappa g (\overline{w' \Theta'_v})_s} \quad (48)$$

where κ is a universal constant (the von Karman constant).

The Oboukhov length can be interpreted as a measure of stability. The sign of L is determined by the sign of the heat flux, and it is the same of R_f :

$$L < 0 \quad \text{for unstable flow} \quad (49)$$

$$L > 0 \quad \text{for stable flow} \quad (50)$$

$$L \rightarrow \infty \quad \text{for neutral flow} \quad (51)$$

L is proportional to the height above the surface at which buoyant factors first dominate over mechanical production of turbulence, and it is used to define the surface layer scaling parameter:

$$\zeta = \frac{z}{L} \quad (52)$$

where z is the height above the surface. As ζ decrease from ideal value 0 (neutral condition, $L \rightarrow \infty$) to -1 (slightly unstable) the buoyancy effects become more important.

Evolution of the PBL: The evolution of the PBL over land, at mid-latitude, has a well-defined structure, related to the diurnal cycle. The major components are the mixed layer (ML), the residual layer (RL), and the stable boundary layer (SBL).

In cloud free situation, the growth of the mixed layer starts about a half hour after sunrise, due to solar heating of the ground. The depth of the convective boundary layer (CBL) increases during the day by entraining the less turbulent air from above and reaches its maximum value in late afternoon. Although a nearly ML can form also in region of strong winds, the turbulence is usually convective, i.e., buoyancy-driven. Thermals of warm air (updraft) rise from the ground, their growth is limited by a stable layer at the top of ML, called inversion layer. With the passing of thermals ramp-cliff structures are observed in the temperature time series. Thermals of cool air (downdrafts) are related to the entrainment process at the top of the ML.

Turbulence is dominated by these large-scale coherent structures that extend vertically over the whole CBL, and the turbulent mixing is very strong. During cloudy days the growth of ML is slow, the intensity of thermals is reduced, and for high overcast, the ML may become non turbulent or neutrally-stratified. In the ML, mechanical turbulence is generated by wind shear across the top of the layer, with consequent formation and breakdown of so-called Kelvin-Helmholtz waves. In late afternoon, about half an hour before sunset, the surface buoyancy flux decreases and changes sign. As a consequence, turbulence decays in near-adiabatic remnant of the daytime boundary layer. This layer is sometimes called residual layer (RL). After sunset, turbulence in the upper part of the layer continues to decay, whilst at low levels both a surface inversion and shallower and stable nocturnal boundary layer (SBL) develops [90].

During the night the bottom portion of the RL is transformed into a stable boundary layer and the thickness of the nocturnal stable boundary layer gradually increases. The RL is entrained into the new ML in the next morning. In the

SBL the turbulence has low intensity and sporadic behaviour. A low-level wind maximum, called nocturnal jet or Low Level Jet (LLJ), generally forms at the top of surface layer and enhance wind shears that tend to generate turbulence. The buoyancy force, instead, acts to suppress turbulence. As a result, turbulence sometimes occurs in sporadic bursts.

Stratified Atmospheric Boundary Layer: The PBL with weak stratification is well described by the similarity theory [165] and by numerical models that assume stationary and homogeneous conditions. As stability increases, the structure and the description of the PBL becomes more complex as the balance between mechanical and buoyancy force varies from case to case. The process at the top of the PBL can become more important than the surface forces in driving the PBL turbulence, and the SL is very shallow, if any. The interaction between small-scale turbulence structures, non-turbulent motion and mean flow leads to several different scenarios where turbulence is often intermittent [149]. Following Mahrt [149] it would be useful to adopt a simple scheme to distinguish the stable boundary layer in two regimes:

1. Weakly stable regime, that refers to a boundary layer where SL, outer layer and entrainment zone can be defined. In this regime, turbulence decreases with height and is nearly continuous in time and space. This regime occurs with either cloud cover or strong wind and generally follows the similarity theory (“excluding nonstationarity and heterogeneity”).
2. Very stable regime, that occurs with strong stratification and weak wind. In this regime the boundary layer is thinner than the weakly stable boundary layer (typically of an order of magnitude), similarity theory is not satisfied and several vertical structures (usually non stationary) are possible. For example, turbulence can increases with height, and the maximum value can be reached in a layer intermittently coupled to the surface.

As already highlighted, a critical flux Richardson number can be used to separate between the two regimes: the turbulence decreases with increasing Richardson number, after which it varies slowly or remains stationary.

Some peculiar features of turbulence in the very stable regime [146,148,149] are given in the following:

- The range of turbulent scales decreases with increasing stability. In strong stability case, the turbulent eddies can be confined to small scale not directly interacting with the ground.
- The main source of turbulence can be at the top of the surface inversion.
- Submeso motions are always present, with scales ranging from the main turbulent eddies scale ($\sim O(100m)$) to the smallest meso-gamma scale ($\sim 2km$).
- A separation between turbulence and waves is not possible. There are intermediate ranges of scales having characteristics between those of turbulent and non turbulent motion (hybrid motion). Furthermore, a temporal overlap of turbulent and non turbulent is possible.
- The turbulence is typically not in equilibrium with the non-turbulent motion. The non-stationarity contributes to intermittent behavior of the turbulence.
- Small scales characterize vertical mixing, which is weak, and the impact of individual roughness elements may be important.
- Small correlations are present between vertical velocity fluctuations and scalars.

Intermittency: According to Mahrt (1999) [146] all turbulence can be considered intermittent to the degree that the fine scale structure occurs intermittently within larger eddies, and a definition of intermittency in the PBL depends on the considered scale [149]. In any case, intermittency can be seen as a strong variability of the turbulence in space and time. Tsinober (2009) [262], refers definitions of intermittency in the PBL:

- “*At any instant the production of small scales is ... occurring vigorously in some places and only weakly in the others*” (Tritton (1988) [261])
- “*Typical distribution of scalar and vector fields is one in which there appear characteristic structures accompanied by high peaks or spikes with large intensity and small duration of spatial extent. The intervals between the spikes are characterized by small intensity and large extent*” (Zeldovich et al. (1988) [285])
- “*Intermittency is a phenomenon where Nature spends little time, but acts vigorously*”

The intermittency in the PBL is traditionally divided into three different kinds depending on the causes from which it originates:

- *Internal or small-scale intermittency*
- *External or large-scale intermittency*
- *Global intermittency*

Internal Intermittency

As already said above in Section 3.1, small-scale, i.e., internal intermittency has been extensively studied since first experiments performed by Batchelor and Townsend (1949) [36]. Small-scale intermittency, also called microscale or fine-scale intermittency, affects small subregions of main/large-scale eddies. It arises from overall modulation of turbulence by the main eddies or in connection with sharp edges of the main eddies themselves, where dynamical flow instabilities occur [145]. For thermals in the CBL, small-scale turbulence is more intense inside than outside the eddies and is concentrated in small sub-regions of the eddies. The regions of concentrated shear at the edge of the main eddies are called microfronts, gust fronts, pulses. In a very stable boundary layer, where the turbulence is non-stationary for the external forcing by submeso motions, it is difficult to isolate internal intermittency. However, internal intermittency has been identified in such stability conditions both experimentally [124], than with numerical simulations [207,230].

External Intermittency

External intermittency is associated with the coexistence and the alternation of laminar and turbulent flow regions, in particular with the random movements of the boundary between turbulent and non-turbulent regimes, and to the continuous transition of laminar flow into turbulent via the boundary [24,262]. Significant regions of the outer layer of a boundary layer characterized by external intermittency may be non-turbulent [23].

Global Intermittency

When a laminar patch of fluid extends down to the surface, the external intermittency may become global. The global intermittency occurs on scale larger than

the scale of the main turbulent eddies. Global intermittency is often observed in the very stable regime, as extensively discussed in Mahrt (1999) [146], who also used the term global intermittency to indicate the turbulence intermittency at high levels of a weakly stable boundary layer. Direct numerical simulations of the turbulent Ekman layer performed by Ansorge and Mellado (2014) [23] reproduce global intermittency. Using as initial condition a neutrally stratified flow, they found that, beyond a certain stability, global intermittency is intrinsic to the stable stratified boundary layer.

Interestingly, the Manneville-Pomeau map introduced in Section 2 could resemble some of the features of both external and global intermittency, in particular the alternance of turbulent and “laminar” periods.

Wind gusts: During clear night, wind gusts are the main responsible for turbulent exchange between the surface and the upper boundary layer, thus contributing to mixing processes of scalar quantities. According to Acevedo et al. (2003) [1], “weak wind gusts below a threshold (approximately 1.5 m/s) mix the air down to the colder ground, cooling the surface layer” and “wind gusts above this threshold promote mixing with upper levels, warming the surface”.

In order to identify wind gusts, Cheng et al. [67] divide the turbulent fluctuations s' into two parts: the high frequency part, defined as turbulence in a narrow sense, and another that is traditionally defined as low-frequency turbulence. The frequency of turbulence fluctuations is larger than 0.017 Hz (time scales less than one minute), while the period of low-frequency turbulence is in the range [1 to 10 minutes]. The large-scale flow is calculated as a time average over 10 minutes. Then, the low-frequency turbulence identifies the so-called gusty wind disturbance. This definition is in agreement with that given by *World Meteorological Organization (WMO)* (1983), that defines gusty wind as a fluid flow fluctuation at time scales between 1 and 10 minutes. During strong wind, turbulence and wind gusts have different features. As highlighted by Cheng et al. [66], in such situations the turbulence is nearly isotropic, with weak and random coherent structures, while gusts are always anisotropic, and strongly correlated coherent structures are present.

5 Self-organized structures and crucial events in turbulence

An interesting general observation about coherent structures in turbulence is given in Robinson (1991) [227]:

- “it can be said that a **coherent motion** is defined as a three-dimensional region of the flow over which at least one fundamental flow variable (velocity components, density, temperature, humidity, vorticity, other scalars or vector fields) exhibits significant correlation with itself or with another variable over a range of space and/or time that is significantly larger than the smallest local scales of the flow.”

Further, according to Tsinober [262] :

- “The nature and characterization of the structure(s) of turbulent flows are among the most controversial issues in turbulence research”;

- “*intermittency [...] is intimately related to some aspect of the structure(s) of turbulence*”;
- “*the difficulties of defining what the structure(s) of turbulence are (mean) are of the same nature as the question about what is turbulence itself*”.

The following sentence is of particular interest:

- “*Fluid dynamical turbulence (even homogeneous and isotropic) has structure(s), i.e. contains a variety of strongly localized events, which are believed to influence significantly the properties of the turbulent flows*”.

The above sentences clearly show that the central role of coherent structures in turbulence and the intimate link between coherent structures and “strongly localized events” is widely recognized in the scientific community. However, the last sentence shows that the term *event* in the turbulence community is sometimes used to denote the coherent structure itself and, in general, they seem to refer to large-scale coherent structures. Then, considering also the discussion given in Section 2, it seems that there could be some slightly different terminology used in the turbulence and statistical physics communities. To avoid ambiguities, herein we will assume the conventions described in the following.

Self-organized structures

The term “coherent” is associated with “self-organized” or “self-organizing”. In other fields, such as neuroscience, a similar term is “synchronization”. However, the term *self-organization* will be here used as an abstract concept that could be seen as a general condition characterizing a class of cooperative multidimensional systems (infinite-dimensional in the fluid dynamics case). Coherence or synchronization belong to this general class and they involve some more specific mathematical definition of self-organization, e.g., phase coherence among different degrees of freedom.

Thus, in agreement with the jargon often used in the turbulence community, the term “coherent structure” will be used to denote large-scale eddies or large-scale vortex motions, which are examples of *self-organized turbulent structures*, a more generic term used hereafter.

We can then exploit the sentence by Robinson (1991) [227] to give the following

Definition (self-organized turbulent structures)

A self-organized turbulent structure is an emerging metastable state of the turbulent flow. It is defined as a three-dimensional region of the flow characterized by strong memory (time coherence) and a spatially coherent motion between different fluid particles over a range of space and/or time that is significantly larger than the smallest local scales of the flow, i.e., the Kolmogorov microscale of viscous dissipation.

The emerging self-organization of these structures is triggered by the strong interactions among different fluid particles and, in particular, by competition between inertia and viscosity and by the nonlinear mechanism of momentum transport. The non-linearities trigger the emergence of self-organized metastable states with coherence lengths that are much larger than the Kolmogorov microscale, that is, even if the interactions are local in space, i.e., between nearby fluid particles, self-organization emerges, a condition that was often found in complex systems (see, e.g., [268]).

Depending on the considered range of space/time scales, this terminology can

include not only large-scale structures, such as energy-containing eddies, but also smaller structures, such as the small-scale eddy motions generated by the instabilities at the sharp edges of the large-scale energy-containing eddies. Conversely, this definition includes also other structures that are not interpreted inside the concept of Kolmogorov-Oboukhov-Richardson energy cascade and that could also be non-turbulent in the strict sense and acting on time/space scales larger than the energy-containing turbulent eddies.

The term “episode” could be sometimes used to denote the overall occurrence of a self-organized structure; this terminology also includes the time duration (life-time) of the self-organized structure.

Turbulent events

According to the paradigm of TC/IDC systems introduced in Section 2, the terms “event”, “crucial/critical event” or “transition event” will denote a dynamical condition corresponding to a strong variation in some flow variables occurring on a time interval shorter than both external/driving and internal dynamical time scales of the turbulent flow, i.e., the Kolmogorov microscale.

Similarly to TC/IDC systems, the event occurrence is associated with a fast memory drop corresponding to a fast decay of the spatial coherence of the flow metastable structure. This is a somewhat different concept with respect to events that are defined on the basis of the crossing through a threshold. This kind of events will be named Threshold Crossing Events (TCEs), of which a particularly interesting case is given by Zero Crossing Events (ZCEs).

Going back to the RTE concept, this includes transitions given by a fast sequence of very short-time large excursion events, resulting in a *bursting* behavior. This is likely to be recognized as a short-time transition event, but it could be also considered as a self-organized structure when the total duration time of the bursting behavior is comparable or longer of the shortest time scale of the fluid flow. In the turbulent boundary layer, bursts are separated in two categories [227]: single-event (or isolated) burst and multiple event bursts. The first is associated with a local instability, while in the latter a more persistent ejection of near-wall fluid is due to the passage of a large-scale vortex structure. The main difference is in the degree of temporal intermittency and in the time period between two subsequent events. It is important to underline that the main difference between self-organized structures and events lies in the time duration of these two different dynamical conditions: relatively long duration time, also named “life-time”, for the self-organized structures and time duration shorter than all time scales of the system for crucial events.

and structure detection algorithms (see next Sections).

After the detection of events in the signals, there are many features that can be used to characterize both each single self-organized structure and each single event. Limiting to consider a single fluctuating variable (e.g., velocity, temperature or other), the main interesting features are:

- maximum and minimum values and related maximum excursion of the variable inside a turbulent structure;
- time instants in which the self-organized structure is born (arising/emergence, birth RTE occurrence time) and dies (decay/fallout, death RTE occurrence time). In some complex systems, the death time of a self-organized structure could practically coincide with the birth time of the successive one. In this

case, there is simply a sequence of crucial events marking the passage between two successive structures²⁶

Associated to the birth and death times we can derive different kind of Inter-Event Times (IETs):

- time duration of the structure (life-time), i.e., difference between the death and birth times of the same self-organized structure;
- time interval between birth times of two successive structures;
- time interval between death times of two successive structures;
- time interval between successive events, without distinguishing if birth or death events;
- others: time interval between peak values of two successive structures, time interval between minimum and maximum value inside the same turbulent structure, steepness of the signal at the event occurrence time.

Since they depend on each other, only a subset of these IETs is usually analyzed, depending on the feature we are interested in and/or that characterizes better the sequence of events and of self-organized structures.

Coherent turbulent structures

In atmospheric boundary layer, large-scales self-organized, i.e., coherent turbulent structures are usually described involving the following elements [227]:

- *vortex*, that is any rotating fluid region, with horizontal orientation (both stream-wise direction or curved and tilted) or vertical z direction;
- *sweep* (wallward motion of high momentum fluid) and *ejection* (upward motion of low momentum fluid);
- *low-speed* and *high-speed* perturbations from the mean value at any z -location.

According to the quadrant-splitting classification scheme [272], the instantaneous product signal $u'w'$ is used to define four different contributions to the Reynolds stress $\langle u'w' \rangle$, each one corresponding to one of the above elements:

1. Q1: $u' > 0$ and $w' > 0 \Rightarrow$ high-speed fluid reflected outwards from the wall;
2. Q2: $u' < 0$ and $w' > 0 \Rightarrow$ Ejection;
3. Q3: $u' < 0$, $w' < 0 \Rightarrow$ Low-speed fluid deflected towards the wall;
4. Q4: $u' > 0$, $w' < 0 \Rightarrow$ sweep.

In the boundary layer, local shear-layer instabilities near the boundaries can be responsible for the birth of vortexes. Low speed streaks between patterns of streamwise vortexes are often formed. This is an important mechanism of turbulent kinetic energy production [227,240].

Outer-layer structures with large streamwise length scales can modulate near-wall structures. These amplitude modulation effects become progressively stronger as the Reynolds number increases, as demonstrated in laboratory experiments and in atmospheric surface layer measurements [157]. In a mixing-layer flow spanwise vortexes develop at a plane of high shear [133,228].

Coherent structures have been extensively studied under different stability conditions, both experimentally and by numerical simulations. Khanna and Brasser

²⁶ Another equivalent view is that the disordered state is included or coincide with the RTE and, in any case, their overall time duration (transition event+disordered state) is so short that it can be represented as a point process [77].

(1997) [123] explored the relative roles of buoyancy and shear in the formation of coherent structures in the PBL. A wide range of atmospheric stability conditions was analyzed using a LES model with different values of the scaling parameter $\zeta = z/L$ (Eq. 52). In particular, Watanabe et al. (2019) [274] used direct numerical simulation (DNS) to investigate the flow structures in a stably stratified shear layer. They found structures similar to those of wall-bounded shear flows, as hairpin-shaped vortexes. Laima et al. (2020) [131] found a change in the form of the dominant turbulent eddy at the change of stability: small scale structures are present in strong stable conditions, large scale structure in neutral conditions and then thermal plumes in strongly unstable conditions.

According to Robinson (1991) [227], the main classes of coherent motions in wall-bounded shear flow are: ejection of low-speed fluid outward from the wall, sweeps of high-speed fluid inward toward the wall, low-speed streaks, hairpin-shaped vortex structures, sloping near-wall shear layers, near-wall pockets. Large vortex turbulent structures are observed below three-dimensional “bulges” that form in the outer region at the interface between turbulent and non-turbulent portions of the fluid flow.

6 Event detection techniques in turbulent signals

As previously said, the identification, analysis and modeling of self-organized structures and of associated transition events are the fundamental elements in the physical description of the flow in terms of self-organized motions, i.e., in the event-based approach.

For example, in convective turbulence, two self-organized states are naturally given by updrafts and downdrafts that alternate each other; similarly, in wall turbulence at high Reynolds number, ejections and sweeps are characterized by RTEs marking the rapid momentum exchanges between inner and outer layer. Regardless of the scales of motion involved and the causes leading to the alternance “self-organized \rightarrow self-organized” or “self-organized \leftrightarrow disorder/laminar”, intermittency is related to both amplitude variability (MI) and space/time ordering of events, RTEs or TCEs (CI).

The presence of self-organized states can be revealed and globally characterized by means of power-law decaying long-range time/space correlations. In fact, let us assume to have a set of Eulerian measures of the fluid flow (e.g., velocity, temperature and other scalars) and that crucial events emerge in the flow field. Given the availability of a single realization of the fluid flow random field, memory (time coherence) and spatial coherence can be globally evaluated by means of time/space two-time two-point correlations, computed as time or space averages. Let us assume a stationary condition, so that we can limit to consider time averages. Then, time averaged space/time correlations depend only on time lag and can be computed by a time moving average over the Eulerian data. For sufficiently long time lags, this surely includes time scales much larger than those of the rapid transition events. Given a generic zero mean signal $s'(t)$, the calculation of the time average is carried out as follows:

$$C_{s'}(\Delta t) = \langle s'(t)s'(t + \Delta t) \rangle = \lim_{T \rightarrow \infty} \frac{1}{T} \int_0^T s'(t)s'(t + \Delta t) dt \quad (53)$$

Let us limit to the case where self-organization death and birth events coincide. Then, considering that memory drops out passing through an event, the correla-

tion in Eq. (53) receives contributions from all those windows remaining inside the same turbulent structure, i.e., between two successive events. On the contrary, the contribution from time windows including at least one transition event is zero when carrying out the time average. For this reason, the time averaged correlation functions can give some statistical global information about the self-organizing ability of the system, thus characterizing the presence of self-organized structures.

Conversely, it is important to underline that the long-range correlation functions cannot be exploited to detect events. In fact, the correlation functions are global statistical features, defined by means of time averaging, that depend on a time lag and not on the actual time in which events occur. Conversely, memory is a dynamical feature, affecting the local dynamics of the system and, thus, also the evolution and occurrence of RTEs. We could try to see if the availability of a statistical ensemble of flow realizations allows to derive a correlation function that is sensitive to single event occurrences. In other words, could events be identified by looking for abrupt falls and climbs of the ensemble averaged correlation function? Actually, the answer is again negative. As in the case of time average, ensemble, or space, averaged correlation functions are statistical features over the ensemble of flow realizations, each one having its own sequence of RTEs that are averaged out in the correlation functions themselves.

The above reasoning proved that correlation functions can give a global picture of the self-organized structures in the turbulent flow, but lose the detailed flow structure, which is averaged out, and cannot be used to detect single events and recognize self-organized structures. The episodic description of turbulence is therefore based on characterizing self-organized structures in terms of local geometrical properties of the measured signals (e.g., velocity steepness). This approach includes the techniques to detect the short-time transition events and their occurrence times.

The detection of events is a delicate task that require proper algorithms. Different algorithms refer to slightly different operational definitions of transition event. Event detection algorithms could be divided into two main classes: the algorithms based on the crossing of one or two thresholds by the analyzed variable and the algorithms based on evaluating the local steepness of the signal. In the second case, some care has to be taken in the evaluation of the signal derivative, which is usually affected by noise much more than the original signal.

Limiting to the case of temporal signals, after the event detection algorithm has been applied we get a sequence of event, each one labelled by an integer number and associated with a *event occurrence time*, so that the following sequence of times is derived:

$$\mathcal{E} = \{t_k\}_{k \in A} , \quad (54)$$

where A is the set of the first integer numbers: $A = \{0, 1, 2, \dots, L\}$ and $t_0 = 0$ by convention. For an infinite duration, it results $L = \infty$. This event sequence can then be exploited to derive different complexity exponents.

Among the most used algorithms there are the threshold-crossing schemes such as U -level [141], modified U -level [140], Variable Interval Time Averaging (VITA) technique [46], the quadrant analysis technique [272]. The effectiveness of several detection algorithms was discussed in Bogard (1986) [48]. The dependence on the operational parameters, i.e. threshold levels and averaging or window times, is

minimized comparing the number of detected events with those identified by flow visualization.

U-level method and modified U-level method

The *U-level* and modified *U-level* methods use the measurements of the fluctuating streamwise velocity component (u'). Tubergen and Tiederman (1993) [263] affirm that among single-component burst detection scheme, the modified *U-level* method is to be preferred for its threshold independence. Metzger et al. (2010) [159] apply the *U-level* algorithm to wind-tunnel measurements. They identify a burst event by the occurrence of an ejection, here identified as a strong negative value of u' . The crossing through a lower threshold identify the leading edge of the burst event, while the trailing edge of the burst is detected by the crossing of an upper threshold. Bogard (1986) [48] recommends to set the lower threshold at one standard deviation of the signal ($-\sigma_u$), while the upper threshold at $-0.25\sigma_u$. With the modified U-level threshold algorithm two time scales can be examined:

1. the time period between events, T_e , defined as the time between the leading edges of successive events. Histograms of T_e at each fixed wall-normal location in the boundary layer for different Reynolds number data sets, follows a Poisson-like distribution;
2. the event duration, ΔT , calculated as the time between the trailing and leading edges of a single event. The general shape of the histograms of ΔT_m are also well-modelled by a Poisson distribution.

The Telegraph Approximation (TA)

The TA belongs to a class of thresholding techniques, such as the first passage time, often used in dynamical systems and stochastic processes theories. TA is defined through the Zero-Crossing Events (ZCEs) of the signal fluctuation [42]:

$$TA_s(t) = \frac{1}{2} \left(\frac{s'(t)}{|s'(t)|} + 1 \right) \quad (55)$$

where $s'(t) = s(t) - \langle s \rangle(t)$. The method finds the passages of the entire signal through the mean value, and it assumes value $TA_S = 1$ when s' is positive and $TA_S = 0$ when s' is negative. Thus, $TA_s(t)$ is made on sequences of 0 and 1 and the transitions $0 \rightarrow 1$ and $1 \rightarrow 0$ corresponds to the ZCEs, which are the same as the original signal. The mean value $\langle s \rangle(t)$ used to evaluate the ZCEs is evaluated in different ways: if the signal is stationary, the average can be computed over the entire time series, while in the general case it is computed as a local average over a sliding time windows of proper length T :

$$\langle s \rangle(t) = \int_{t-T/2}^{t+T/2} s(t') dt' . \quad (56)$$

Another often used alternative definition of mean value is given by carrying out a local trend over time intervals $[t, t + T]$, which is derived by means of the minimum square method, usually with a linear fitting function.

This method was firstly applied to turbulent thermal convection by Sreenivasan and co-workers [42,251]. This event definition is simply related to a threshold passage that could also include transitions with low signal steepness. The independence from the threshold in a given range was sometimes used as a quite

reasonable signature that ZCEs are genuine transition events. Authors exploiting TA claim that it allows to isolate the clustering from amplitude variability. However, this is only true for that part of clustering related to zero-crossing events (ZCEs). Thus, the usefulness and significance of this event detection algorithm is related to the presence and the leading role of updraft/downdraft or ejection/sweep alternance.

VITA method

The bandpass filter VITA method can be applied to either u' [159] or $u'w'$ [175]. This method was developed to detect large-scale self-organized, i.e., coherent structures, which were identified as turbulent bursts. As usual, the beginning and ending time of the structure defines the crucial transition events²⁷.

Thus, for any zero mean fluctuating turbulent signal $s'(t)$, the short-term variance D is defined as:

$$D(s'; t, t_{av}) \equiv \frac{1}{t_{av}} \int_{t-t_{av}/2}^{t+t_{av}/2} |s'(t')|^2 dt' - \frac{1}{t_{av}} \left(\int_{t-t_{av}/2}^{t+t_{av}/2} s'(t) dt \right)^2 \quad (57)$$

where t_{av} is the averaging time interval. The burst is identified when a peak in D exceeds a discriminatory level $k\sigma_s^2$, where k is the prescribed threshold and σ_s^2 is the mean square value of $s'(t)$, defined as:

$$\sigma_s^2 = \langle (s')^2 \rangle = \lim_{t_{av} \rightarrow \infty} D(s'; t, t_{av}) \quad (58)$$

According to the terminology of these authors, in addition to *ordinary bursts*, it is possible to detect a *super-burst* when a number of bursts coalesce into one single burst at longer t_{av} . At shorter t_{av} we have a cluster of bursts, each of which is called *sub-burst*.

A flux bursting structure is detected if s' is the turbulent flux $u'w'$. The method can be applied to detect an atmospheric burst, that occurs in the times when the calculated instantaneous flux have larger value than at others, as defined by Kline et al. (1967) [126]. These authors also studied the time interval between two bursts as the time from the centre of two successive bursts. This clearly is a different feature with respect to the inter-event time, but these two definitions could be equivalent. Narasimha and Kailas (1990) [175] found that, in a nearly-neutral atmospheric boundary layer, the probability distribution of the time intervals between bursts reveals two distinct types of bursts: lone (isolated) bursts and bunched bursts. This aspect was highlighted by Bogard (1986) [48] in a flow-visualization study. Successive ejections are spatially close if they come from the same streak, while they are separated when coming from different streaks. A burst is then a self-organized structure formed by a organized cycle of ejections. A burst is evidenced by VITA at longer averaging time.

The duration of a burst of intensity k is defined as the time during which $D(u'w')$ is greater than the threshold k .

Geometric shape method

Starting from the evidence that visual inspection of atmospheric boundary layer time series reveals common shapes, despite the different timescale and physics

²⁷ As already observed, here the authors use the term “event” to denote the motion that is here conventionally named “self-organized structure”. Regarding VITA method, we will use the term “burst” to denote the structure.

phenomena involved, an attempt to recognize the geometric shape from time series has been done by Belušić and L. Mahrt, 2012 [39]. The authors try to ask themselves the question: “*is geometry more universal than physics in atmospheric boundary layer?*” The method is then based on the recognition of the geometry of the structure more than on its amplitude, that varies across different scales. The main steps are the following:

- (i) A predefined shape function is moved through the time series. At each time point the linear correlation coefficient r is calculated. The procedure is repeated over several shape functions.
- (ii) The properties (length, location, etc) of the structure are saved and the corresponding part of the series is removed.
- (iii) After selecting the shape function with the next largest r , the previous step is repeated until all shape functions with $r > 0.9$ are selected.
- (iv) The procedure is repeated for different scales.

The threshold value $r = 0.9$ allows to distinguish between the different shapes. The shapes chosen are: a simple sine function, a step function, a ramp-cliff function, and a cliff-ramp function (or a reversed ramp-cliff). These shapes correspond to physical features of the boundary layer: a wave (sine), a (micro)front (step) [147], and differently oriented turbulent ramp-cliff patterns [25].

Since some definitions of self-organized structure are based on the existence of spectral phase correlation [69,221], the method was tested on a portion of the original series where self-organized structures were removed by phase randomization. Then, the method detects only events not based on the existence of phase correlation. The number of detected events in the surrogate time series was about 90% less compared to the original data. Furthermore, a visual inspection of the captured structures was performed. The analysis was applied to two boundary layer stability regimes: unstable and stable. Results highlighted that the geometry of the structures is nearly independent from the time scale, although the physical process generating the shape changes with the considered scale.

Noise test method

Kang et al. (2014) [118] proposed a method to extract and classify self-organized structures²⁸ from time series of turbulence data, without an *a priori* knowledge of the dynamics and of the generating mechanisms. The method was applied both to artificial and to atmospheric data and is based on determining the characteristics (i.e., colors) of background noise, which were assumed to be known *a priori*.

Two different noise models were considered: white noise and red noise, used to represent the background noise of atmospheric turbulence. In a white noise process, the elements of the time series at different times are not correlated. The Ljung-Box test [50] is applied to check if the data points are independently distributed. The null hypothesis H_0 (i.e. the data are independently distributed) is rejected when the p value is less than the significance level 0.05. In this case the data points do not resemble a white noise.

The red noise is modeled as a first-order autoregressive process AR(1), where the

²⁸ The authors use the term “coherent structure” to indicate fluid elements with given features, and the term “event” to indicate the trace of this same coherent structure in the time series. In order to avoid confusion, here we will use our convention, which was introduced above, thus denoting the Kang “event” as “self-organized turbulent structure”.

error term is given by a white noise. A time series $s'(t)$ is then represented as:

$$s'(t) = \Phi s'(t-1) + \epsilon(t) \quad (59)$$

being Φ ($0 < \Phi < 1$) the first-order autocorrelation coefficient and $\epsilon(t)$ a white noise process. Only stationary processes can be modeled as an AR(1) process, then a stationary test is first applied to $s'(t)$ ²⁹. If $s'(t)$ is found non-stationary, then the time series is different from a red noise. If $s'(t)$ is stationary, the time series is fitted with the AR(1) model $\tilde{s}(t) = \Phi \tilde{s}(t-1)$. The white noise test is performed on the residuals $\epsilon(t) = s'(t) - \tilde{s}(t)$. Finally, the given time series is a red noise if the residuals behave according to a white noise. Being AR(1) a stationary linear process that does not support oscillations, the events detected as non-AR(1) processes are non-stationary and/or oscillatory and/or nonlinear processes. The method consists of two steps:

(i) *First step: self-organized structure detection*

Given a sampled signal $s'(t)$ of total length m , sub-sequences of given length $l < m$ are considered. The q th sub-sequence $s_q(t)$ is defined as:

$$s'_q(t) = [s'(t_q), \dots, s'(t_{q+l-1})] \quad (60)$$

with $1 \leq q \leq m - l + 1$. Sub-sequences that are significantly different from noise identifies a potential “local structure”. A structure is defined only if a sequence of consecutive potential local structures is long enough. A real self-organized structure starting at time t_0 , with time scale Δ_t , is defined when the noise test identifies consecutive potential local structures in the time interval $(t_0 - \Delta_{t_1}, t_0 + \Delta_{t_2})$, with $\Delta_{t_{1,2}} \leq \Delta_t$.

The basic assumption of this method is that individual structures or trains of structures are separated by noise regions. It follows that the initial and final times of the period where the structure is identified corresponds to the crucial transition events introduced above.

(ii) *Second step: structure clusterization*

Self-organized structures with similar features are grouped together: each structure is described using a feature vector, then the Euclidean distance among vectors is used to cluster them. This allows shapes with similar features but different lengths, or time lags, to be cluster together.

Being n_e the number of structures extracted in the first step, and d the number of features of every group of structures, the second step groups together the n_e structures in $k < n_e$ clusters, in a d -dimensional space.

The method was tested on a subsequence of the original series where self-organized structures were removed by phase randomization. The number of detected structures in the surrogate time series was smaller than that in the original one. The authors use four basic shapes to generate artificial data: box, ramp-cliff, cliff-ramp and a sine function. In atmospheric real data, since some of the chosen features used for clusterization are correlated, a principal component analysis (PCA) is applied to the feature vector to reduce both correlation and dimension. An application to the method in stable atmospheric boundary is described in [119].

Velocity increments method

The method is based on the following steps [197,198,199,200]:

²⁹ The authors use the so-called Philips-Perron (PP) unit root test [30,212].

- (i) Given the non-zero mean signal $s(t)$, the local average $\bar{s}(t) = \langle s \rangle_T(t)$ is computed by applying a moving average over sliding windows $[t - T/2, t + T/2]$ or a linear detrending over disjoint time intervals $[nT, (n + 1)T]$. In atmospheric turbulence, the duration T is usually between 15 and 30 minutes in order to minimize the non-stationarities modulating the local turbulence and due to large- and meso-scale meteorological dynamics.
- (ii) The corresponding variance $\sigma^2 = \langle (s(t) - \bar{s}(t))^2 \rangle_T$ is computed. This is constant inside the time window and changes only passing from one window to the next one.
- (iii) The turbulent fluctuations $s(t)$ are then transformed into a sequence of normalized fluctuations:

$$s'(t) = \frac{s(t) - \bar{s}(t)}{\sigma} \quad (61)$$

- (iv) The crucial event is defined as passage of the signal increment through a threshold D_0 :

$$|\Delta s'(t)| = |s'(t + \Delta t) - s'(t)| > D_0. \quad (62)$$

In this formulation, positive and negative increments are not distinguished, but clearly the method can be generalized by removing the absolute value, thus introducing two kind of events: $+\rightarrow-$ and $- \rightarrow +$. The threshold D_0 is chosen according to the n -th percentile of the $|\Delta s'|$ distribution. Alternatively, a comparison between different thresholds is carried out.

PDF analysis method

In applying this method, events are defined as signal extremes caused by a physical mechanism different from background turbulence and noise. Thus, this method belongs to the class of TCEs.

To extract the extreme fluctuations of the signal, a threshold is defined based on the behavior of the PDF tails. Chosen a mathematical distribution as a reference PDF, the position where the PDF of the signal deviates from the reference PDF identifies the threshold value.

The method was proposed by Katul. et al. (1994) [122] and applied to sensible heat flux measurements $w'T'$. The procedure adopted in [122] is described by the following steps:

- (i) To obtain a time series with zero mean and unit variance, the measurements were normalized by removing the mean turbulent flux $\langle w'T' \rangle$ and dividing by the standard deviation σ_{wT} of the flux measurements.
- (ii) The PDF of the normalized time series was compared to a gaussian PDF with zero mean and unit variance.
- (iii) The threshold value H_c was defined as $H_c = \sigma_{wT}(H_n) + \langle w'T' \rangle$, where H_n is the most distant point at which the normalized $w'T'$ PDF intersects the reference PDF.

Liu et al., 2014 [139] used a Lévy stable distribution [134] as reference PDF of the vertical velocity in the unstable PBL. This choice is justified by the study of Liu et al., 2011 [138], that found that the PDF of vertical velocity in the unstable boundary layer can be fitted by a truncated Lévy stable distribution. The difference between the truncated stable and the stable PDF is only in the tails of the PDF. The truncated stable and the stable distributions have three common parameters: a characteristic exponent, a skewness parameter and a scale

parameter. The two distributions differ for a cut-off parameter and the truncated stable distribution becomes the stable distribution when the cut-off parameter equals zero.

The main steps to find the threshold value are the following:

- (i) A range $G = [s_{max} - D/2, s_{max} + D/2]$ is defined, where s_{max} is the maximum point defined by:

$$f(s_{max}) = \max f(s) \quad (63)$$

$f(x)$ is the PDF (original stable truncated PDF or the stable one).

- (ii) In this range, the normalized PDF f_G is defined as

$$f_G(s) = \frac{1}{c} f(s + s_{max}) ; \quad c = \int_G f(s) ds \quad (64)$$

where c is the normalization coefficient.

- (iii) The absolute value of relative deviation RD between maxima of the normalized truncated stable and of stable PDF is computed by:

$$RD = \frac{|\max f_G - \max \hat{f}_G|}{\max f_G} \cdot 100\% \quad (65)$$

where f_G and \hat{f}_G are normalized truncated stable and stable PDFs.

- (iv) The dependence on D of RD has a linear regime and the threshold is defined as the end point of the linear regime of RD :

$$T_{\pm} = s_{max} \pm D/2 . \quad (66)$$

Then, $s > T_+$ and $s < T_-$ represents extreme fluctuations and the passages through this threshold are used to select the transition events.

7 Event-based complexity measures: intermittency, clustering and friends

In the following we give a sample of some event-based measures that are extensively used, and sometimes also introduced *ex novo*, in the analysis of turbulent flow in the PBL [57,58,110,121,197,198,199,200,215].

Non-Gaussianity measures and imbalance

In general, the non-Gaussianity of a distribution $p(s')$ of a zero mean signal $s'(t)$ with variance $\sigma^2 = \langle (s')^2 \rangle$ is evaluated by means of normalized moments of order higher than 2:

$$\text{Skewness : } Sk = \frac{\langle (s')^3 \rangle}{\sigma^3} ; \quad \text{Kurtosis : } Ku = \frac{\langle (s')^4 \rangle}{\sigma^4} . \quad (67)$$

The Gaussian value of the kurtosis, $Ku = 3$ is a reference value to define non-Gaussianity. Clearly, the Gaussian skewness is zero.

The imbalance of $TA_s(t)$ is the same as the original zero mean signal $s'(t)$ and it can be evaluated by considering the relative time duration of the two states 0 and 1 [110]:

$$\Delta\Gamma = \Gamma_+ - \Gamma_- ; \quad \Gamma_+ = Pr \{TA_s(t) = 1\} ; \quad \Gamma_- = Pr \{TA_s(t) = 0\} \quad (68)$$

The imbalance of a distribution is related to the skewness of the distribution by the following formula [110]:

$$\Delta\Gamma = -\frac{1}{6}\sqrt{\frac{2}{\pi}} Sk \quad (69)$$

Spectral Exponents β_{TA} and β_s

The PSD of a zero mean signal $s'(t)$ is given by:

$$E(f) = 2 \lim_{T \rightarrow \infty} \frac{1}{T} |\hat{s}_T(f)|^2$$

being s_T the signal up to the time T , $\hat{s}(f)$ the Fourier transform of the signal $s'(t)$ and f the frequency³⁰. As known, the interest in the PSD lies in the Parseval's theorem stating:

$$\int_0^\infty E(f) df = \int_0^\infty |s'(t)|^2 dt ,$$

where the integral on the right-hand side represents the total energy of the signal. Thus, the PSD is interpreted as the distribution of the signal energy over the frequencies, i.e., on the time scale $\tau_f = 1/f$. The same reasoning can be done for the spatial Fourier transform, wave numbers and spatial scales.

In turbulence, PSDs display some typical power-law, such as the Kolmogorov-Oboukhov $-5/3$ law: $E(k) \sim k^{-5/3}$. In event-based approaches, the power-law behavior of the TA-PSD is of particular interest:

$$E_{TA}(f) \sim f^{-\beta_{TA}} , \quad (70)$$

where β_{TA} is the spectral exponent of the TA dichotomous signal. This was firstly investigated by Sreenivasan and co-workers [42], who also found a relationship with the scaling of the original signal:

$$E_s(f) \sim f^{-\beta_s} , \quad (71)$$

in both experimental data and some simple stochastic models [251]. This relationship is given by:

$$\beta_{TA} = \frac{\beta_s + 1}{2} \quad (72)$$

Thus, according to this formula³¹, when $\beta_s = 5/3$, it should result $\beta_{TA} = 4/3$.

Clustering Exponent α_c

The clustering exponent is based on the computation of the *event density* $\rho_\tau(t)$. As we deal with experimental sampled signals with sampling time Δt , we can rewrite for simplicity: $\rho_m(n)$ with $\tau = \tau_m = m\Delta t$ and $t = t_n = n\tau_m = nm\Delta t$.

Let us now consider the sequence of events given in Eq. (54): $\mathcal{E} = \{t_k\}_{k \in A}$, $A = \{0, \dots, L\}$ that is derived by the application of some event detection algorithm to the turbulent signal. Let us define $N = t_L/\Delta t$ as the total number of sampling times in the original time signal. Then, the algorithm works as follows³²:

³⁰ Clearly, experimental time series have a finite duration time T , so that the limit is not carried out. Further, the data are sampled in time and the Fourier transform becomes the time-discrete Fourier transform. The factor 2 follows from considering that the Fourier spectrum is symmetric for real-valued signals.

³¹ Here we have the $-5/3$ law because the temporal signals represent Eulerian velocities or other turbulent quantities. Then, under proper conditions, the Taylor's frozen hypothesis holds and the frequency spectrum is actually a wave number spectrum.

³² The clustering exponent seems to have been introduced at the community of atmospheric turbulence in Ref. [251]. The algorithm here presented is a guess taken from Refs. [250,57,110].

(i) A statistical ensemble is derived by dividing the event sequence $\{t_k\}$ into M subsequences of total duration $\tau_m = m\Delta t$, so that:

$$\mathcal{E}_n = \{k : n\tau_m \leq t_k < (n+1)\tau_m\} ; \quad 0 \leq n < M ; \quad M = [N/m] , \quad (73)$$

being $[a]$ the integer part of a . Each subsequence is a sample in the statistical ensemble and $m \ll N$ is chosen in such a way to get enough statistical samples in the ensemble ($M \gg 1$). Notice that: $\mathcal{E}_n \subset \mathcal{E}$ and, when $[N/m] = N/m$, $\mathcal{E} = \cup_n \mathcal{E}_n$.

(ii) Compute the event density by simply counting the size of \mathcal{E}_n , i.e., the number of events in the n -th time interval, and dividing by the number of sampling time inside the subsequence, which is given by m :

$$\rho_m(n) = \frac{\#\mathcal{E}_n}{m}$$

(iii) Compute the mean and variance of $\rho_m(n)$ by averaging over the statistical ensemble:

$$\langle \rho_m \rangle = \frac{1}{M} \sum_{n=0}^M \rho_m(n) \quad (74)$$

(75)

$$\sigma_\rho^2(m) = \langle (\rho_m(n) - \langle \rho_m(n) \rangle)^2 \rangle = \frac{1}{M} \sum_{n=0}^M (\rho_m(n) - \langle \rho_m(n) \rangle)^2 \quad (76)$$

Then, the *clustering exponent* α_c is defined by the following power-law scaling:

$$\sigma_\rho^2(m) \sim m^{-2\alpha_c} \quad \text{or, equivalently,} \quad \sigma_\rho^2(\tau_m) \sim \tau_m^{-2\alpha_c} \quad (77)$$

In general, higher clustering corresponds to lower α_c and *vice versa*. Regarding TA and, thus, a sequence of ZCEs, a white noise has clearly no clustering, because two successive jumps are completely independent from each other. The clustering exponent of the white noise is given by $\alpha_c = 0.5$, which is a reference value to which compare the experimental α_c value.

Oboukhov intermittency Exponents γ_q

This is probably the first measure of intermittency in turbulence and it was firstly proposed by Oboukhov in 1962 [181]. Turbulent intermittency found by Batchelor and Townsend [36] referred to the dissipation rate $\epsilon \sim |du/dx|^2$, thus it is possible to introduce the analogous temporal dissipation rate of a generic zero mean turbulent signal $s'(t)$:

$$\epsilon(t) = \left| \frac{ds'(t)}{dt} \right|^2 . \quad (78)$$

In the case of Eulerian measures, this can be related to the real dissipation rate when Taylor's frozen turbulence hypothesis can be assumed. In analogy with the Oboukhov's spatial local average, Eq. (29), a time average can be defined as:

$$\epsilon_\tau = \frac{1}{\tau} \int_t^{t+\tau} \epsilon(t') dt' \quad (79)$$

The Oboukhov intermittency exponents are then defined by the following relationships:

$$\frac{\langle \epsilon_\tau^q \rangle}{\langle \epsilon_\tau \rangle^q} \sim \tau^{-\gamma_q} \quad (80)$$

In general, if $\gamma_q = 0 \forall q$, there is no Oboukhov intermittency, i.e., intermittency related to the signal dissipation rate. The Oboukhov intermittency was applied to both the original signal and the associated sequence of crucial events, in particular to the TA signal. Given a sequence of events $\{t_k\}$, TCEs, RTEs o TA, a sequence of pulses can be build exploiting the Dirac δ functions:

$$e(t) = \sum_{k \in A} \delta(t - t_k) .$$

Then, when Oboukhov intermittency is applied to a sequence of pulses, it results:

$$\gamma_q \neq 0 \Rightarrow \text{clusterization of pulses} \quad (81)$$

$$\gamma_q = 0 \Rightarrow \text{no clusterization} \quad (82)$$

Then, also the Oboukhov intermittency exponent applied to a sequence of pulses is an estimate of clusterization related to crucial events. Of particular interest are the 2nd-order exponents of both original and TA signals: $\gamma_{2,s}$ and $\gamma_{2,TA}$. To simplify the notation, these 2nd-order exponents will be denoted as γ_s and γ_{TA} . The inter-comparison of these two exponents gives an estimate of the relative complexity of the clustering features encoded in the event sequence, often given by the TA signal, with respect to the amplitude variability.

It is worth noting that higher intermittency is given by a higher Oboukhov intermittency exponent γ_s and the same applies when considering the Oboukhov exponent γ_{TA} . Conversely, higher clustering is associated with a lower clustering exponent α_c .

TC/IDC exponent μ

We here refer to the already introduced temporal or intermittency-driven complexity (TC or IDC), following the convention introduced by Grigolini and co-workers [38,96,193,268]³³.

Given the usual event sequence $\mathcal{E} = \{t_k\}$ and the associated IETs $\{\tau_k\}$, the TC or IDC exponent is defined by the power-law decay in the IET-PDF:

$$\psi(\tau) \sim \tau^{-\mu} \quad (83)$$

Notice that t_0 has to be the occurrence time of the first detected event and not the start time of the signal³⁴. We recall that a power-law decay in the IET-PDF with $1 < \mu \leq 3$ is the signature of metastable self-organized structures and define an intermittent complex system in the sense explained above in Section 2.

Interestingly, in the turbulent trasport of scalars, the power-law scaling in the IET-PDF, Eq. (83), also denoted as inter-pulse period PDF, is claimed to be a signature of “active turbulence” (e.g., temperature in unstable convective turbulence), while a log-normal PDF is associated with “passive” scalars [57,251]:

$$\psi(\tau) \sim e^{-|a|\theta^2 + b\theta + c} ; \quad \theta = \log(\tau) ,$$

³³ This is named as persistence exponent and indicated with the γ greek letter in some of the cited papers devoted to intermittency in turbulent flows [57,58,60,110].

³⁴ By convention, a time shift is usually applied to get $t_0 = 0$.

being a , b and c proper constants depending on mean and variance of θ .

Diffusion exponents H and δ_*

A widely used approach to evaluate self-similarity exploits the properties of diffusion laws. As diffusion is originated by the sum of many random contributions, this method has a robust theoretical foundation in the limit theorems of probability theory, i.e., the Gaussian central limit theorem and the Lévy generalized limit theorem [91,134].

In general, the diffusion method works as follows:

- (i) Let us consider an experimental time series $\xi(t)$, which can be a turbulent velocity fluctuation or other zero mean turbulent signal.
- (ii) The diffusion variable is computed as:

$$X(t) = \int_0^t \xi(t') dt' \Rightarrow X_N = \sum_{n=0}^N \xi_n , \quad (84)$$

being $\xi_n = \xi(n\Delta t)$, $X_N = X(N\Delta t)$ and Δt the experimental sampling time.

- (iii) Different statistical indices can be computed on the diffusion variable $X(t)$. The averages are carried out as time averages and, thus, similarly to clustering and Oboukhov exponents, sliding windows are used to define a set of sub-trajectories.

In particular, two complexity exponents related to diffusion are of wide interest:

1. Second moment exponent H (Detrended Fluctuation Analysis)

In analogy with Eq. (73), let us consider signals sampled at $t_k = k\Delta t$ and a window lenght $\tau_m = m\Delta t$. Thus, we have the following sub-trajectories:

$$\tilde{X}_k^n = \tilde{X}_{k'}^n = X(k'\Delta t) ; \quad k' = k - mn , \quad k \in \mathcal{Q}_n(\tau_m) ; \quad (85)$$

$$\mathcal{Q}_n(\tau_m) = \{k : n\tau_m \leq t_k < (n+1)\tau_m\} , \quad 0 \leq n \leq M , \quad M = [N/m] ,$$

being N the total number of sampling times in the data. When not ambiguous, in the following we will use the simplified notation \mathcal{Q}_n in place of $\mathcal{Q}_n(\tau_m)$.

Notice that it always results: $0 \leq k' < m$ and that the set

$$\left\{ \tilde{X}_k^n ; k' = 0, \dots, m \right\} = \left\{ \tilde{X}_{k'}^n ; k \in \mathcal{Q}_n \right\}$$

is a statistical ensemble of stochastic trajectories that are assumed to be approximately independent and over which statistical features, and the associated scaling exponents, can be computed.

The second moment scaling H is computed by applying the Detrended Fluctuation Analysis (DFA) [209,210] (see also [200] for details). Given the time lag τ_m , the DFA firstly compute the variance over each single trajectory in the above statistical ensemble (average over k' or, equivalently, over k). At this stage, an important step is the estimation of the trend inside each time window $[n\tau_m, (n+1)\tau_m]$, usually by means of linear or

quadratic regression methods. After that, an average over the ensemble is carried out (average over n). In formulas:

$$\sigma_X^2(\tau_m) = \langle \langle X_k^n - \bar{X}_k^n \rangle_{\mathcal{Q}_n} \rangle_{\mathcal{Q}} \quad (86)$$

The averages $\langle \cdot \rangle_{\mathcal{Q}_n}$ and $\langle \cdot \rangle_{\mathcal{Q}}$ are carried out over the single trajectory and over the entire ensemble, respectively. The mean trend $\bar{X}_k^n = \langle \tilde{X} \rangle_k^{\tau_m, n}$ is evaluated over the n th trajectory (\mathcal{Q}_n) for the window length τ_m . This calculation is carried out for several τ_m and, for self-similar processes, we expect to get:

$$F(\tau_m) \sim \tau_m^H ; \quad F(\tau_m) = \sqrt{\sigma_X^2(\tau_m)} . \quad (87)$$

The exponent H is essentially the Hurst exponent of rescaling analysis [111]. The case of normal (Gaussian) diffusion is given by $H = 1/2$ and is a consequence of the central limit theorem.

Then, the range $H > 1/2$ is denoted as *fast diffusion* or *super-diffusion*, while $H < 1/2$ is named *slow diffusion* or *sub-diffusion*.

2. PDF self-similarity exponent (Diffusion Entropy analysis)

For a given time lag $\tau_m = m\Delta t$, let us consider a statistical sample with the trajectory increments:

$$\Delta X^m(k) = X_{k+m} - X_k = X(t_k + \tau_m) - X(t_k); \quad k \in \mathcal{P}_m$$

$$\mathcal{P}_m = \{k : 0 \leq k \leq N - m\} , \quad (88)$$

being, as said above, N the total length of the sampled diffusion variable $X_n = X(n\Delta t)$. Then, the PDF of this statistical sample of increments can be evaluated for several τ_m : $p(x, \tau_m)$. In the self-similar case, we have:

$$p(x, \tau_m) = \frac{1}{\tau_m^{\delta_*}} f\left(\frac{x}{\tau_m^{\delta_*}}\right) . \quad (89)$$

The variable $z = x/\tau_m^{\delta_*}$ is named “self-similarity variable” and it comes from a self-similarity transformation (see, e.g., [191]) that leaves the probability of interval unchanged. When Eq. (89) comes into action, the diffusion is said to be self-similar and, in particular, monoscaling. An efficient way to detect the scaling exponent δ was found to be the Diffusion Entropy (DE) analysis developed and widely applied by Grigolini and co-workers [11,100,99,235]. The main idea of DE is to evaluate the Shannon entropy of the diffusion process $X(t)$:

$$S(t) = - \int p(x, \tau_m) \log(p(x, \tau_m)) dx , \quad (90)$$

which, under the self-similarity condition given in Eq. (89), has the following behavior:

$$S(t) = A + \delta_* \log t ; \quad A = - \int f(y) \log f(y) dy . \quad (91)$$

8 Some relations between complexity exponents: SOC and EDDiS method

The relationship between the spectral exponents of the original signal and of the TA signal, which is given by the sequence of zero-crossing events, is already given in Eq. (72). As we will see in the next Section 9, this relation is far from being verified in atmospheric turbulence. Actually, Sreenivasan and Bershadskii (2006) [251] derived this formula in a heuristic way and verified it on some turbulence datasets, but they did not claim a wide validity of the formula itself. In this sense, the studies of Katul and co-workers was and is still relevant in understanding the limits of Eq. (72) and of its variants.

Self-Organized Criticality

An interesting aspect that has recently begun to attract the interest of some authors is the relationship between Self-Organized Criticality (SOC) [28,29,114] and turbulence intermittency in the sense of Oboukhov. A classical SOC formula relates the spectral exponents of the TA signal β_{TA} with the TC exponent μ , related to IET-PDF. For “nonintermittent” cases (in the Oboukhov sense), the relation between the exponents β_{TA} and μ is given by [114]:

$$\beta_{TA} = 3 - \mu \quad (92)$$

Discrepancy from this relation, since there are no amplitudes involved, should be entirely related to clustering, that is considered to be a part of intermittency by many authors and that we would rather say that it is an aspect of intermittency directly linked to crucial events rather than to large variability in the signal increments³⁵. Bershadskii et al. (2004) [42] found that the above relationship between the TA spectral and TC exponents must be modified to take into account the Oboukhov intermittency related to the signal dissipation rate:

$$\beta_{TA} = \left(3 - \frac{\gamma_{TA}}{2}\right) - \mu \quad (93)$$

where, as said in Section 7, γ_{TA} is the TA-based Oboukhov intermittency 2nd-order exponent and it is related to clustering features. We will discuss the application of this relationship to atmospheric turbulence in Section 9.

The EDDiS method

The Event-Driven Diffusion Scaling (EDDiS) approach is based on two main ingredients:

- (i) the sequence of crucial events $\{t_k\}$;
- (ii) the CTRW model.

According to the view of temporal complexity [38,96,144,205,193,280], a working hypothesis of EDDiS is given by the renewal condition for the crucial events. The renewal aging analysis gives some effort in evaluating the renewal condition and, conversely, an estimate of the memory content of a event sequence referred to the presence of random or deterministic modulation. However, being based on the

³⁵ This seems to be related to the previously introduced magnitude intermittency (MI) [137], that some authors also denote as amplitude variability [57,110], while the aspects related to TA and crucial events in general are associated with clustering intermittency (CI).

brand-new and aged IET-PDFs, this analysis can be affected by noise, so that, when renewal condition is not verified, this could be due to both modulation or noise [15]. Conversely, some theoretical studies on artificial data showed that, even without noise, the amount of memory, i.e., the departure from the renewal condition, can be linked to different underlying dynamics. In other words, renewal aging does not always unambiguously identify the correct dynamical model.

In order to overcome this limitation and to get a robust estimation of the TC/IDC exponent μ , Allegrini et al. (2009) [14] applied a tool, later named EDDiS by Paradisi and Allegrini (2015,2017) [192,193], that puts together a set of analyses based on three different CTRWs, on DFA and on DE, combining and comparing different results already known in literature about the relationship between μ , Hurst exponent H and PDF self-similarity δ_* (for a review, see [14,193,275] and references therein). The main aspect is that the above results are derived under the renewal condition. Thus, the working hypothesis of the EDDiS method is that the event sequence is a renewal process.

Thus, the most general version of the EDDiS algorithm works as follows (for a review, see [14,192,199,200]):

- (i) Let us consider the event sequence $\{t_k\}_{k \in A}$ of Eq. (54), with $A = \{0, 1, 2, \dots, L\}$, and the following three walking rules:
 - (a) *Asymmetric Jump (AJ) rule* The walker makes a jump ahead in correspondence of each event occurrence time t_k (sequence of pulses):

$$\begin{cases} \xi(t) = 0 & \text{if } t \neq t_k \ \forall k \\ \xi(t_k) = 1 \end{cases} \quad (94)$$

- (b) *Symmetric Jump (SJ) rule*

Given the random dichotomous variable $u \in \{-1, +1\}$ (coin tossing prescription) and a sample of u , $\{u_k\}_{k \in A}$, that is, a sequence of $+1$ and -1 , the SJ rule is:

$$\begin{cases} \xi(t) = 0 & \text{if } t \neq t_k \ \forall k \\ \xi(t_k) = u_k \end{cases} \quad (95)$$

The walker makes a unitary jump in a random direction in correspondence of an event: $\xi(t_k) = \pm 1$.

- (c) *Symmetric Velocity (SV) rule*

The walker moves with constant unitary velocity $V = 1$ and has the possibility of changing directions in correspondence of a crucial event. Taking the same sequence $\{u_k\}$ as in the SJ rule:

$$\xi(t_k) = u_k ; \quad t_k \leq t < t_{k+1} ; \quad k \in A \setminus \{L\} \quad (96)$$

This is actually the walking rule of the so-called *Lévy walk* [245,283].

- (ii) From the three walking rules three different CTRWs are built by simply applying Eq. (84), thus getting $X_{AJ}(t)$, $X_{SJ}(t)$ and $X_{SV}(t)$.
- (iii) The second moment and PDF self-similarity exponents H and δ_* are evaluated by applying DFA and DE to the three random walks. Under the working hypothesis of TC/IDC, i.e., a renewal process without any noise and with power-law decay in the IET-PDF: $\psi(\tau) \sim 1/\tau^\mu$, the following relationships were found in the literature [100,125,167,170,235,244,264,266] (for a review see also [161,193,275,283]):

(AJ)

$$\delta_{AJ}(\mu) = \begin{cases} \mu - 1 ; & 1 < \mu < 2 \\ 1/(\mu - 1) ; & 2 \leq \mu < 3 \\ 1/2 ; & \mu \geq 3 \end{cases} \quad H_{AJ}(\mu) = \begin{cases} \mu/2 ; & 1 < \mu < 2 \\ 2 - \mu/2 ; & 2 \leq \mu < 3 \\ 1/2 ; & \mu \geq 3 \end{cases} \quad (97)$$

(SJ)

$$\delta_{SJ}(\mu) = H_{SJ}(\mu) = \begin{cases} (\mu - 1)/2 ; & 1 < \mu < 2 \\ 1/2 ; & \mu \geq 2 \end{cases} \quad (98)$$

(SV)

$$\delta_{SV}(\mu) = \begin{cases} 1 ; & 1 < \mu < 2 \\ 1/(\mu - 1) ; & 2 \leq \mu < 3 \\ 1/2 ; & \mu \geq 3 \end{cases} \quad H_{SV}(\mu) = \begin{cases} 2 - \mu/2 ; & 1 < \mu < 3 \\ 1/2 ; & \mu \geq 3 \end{cases} \quad (99)$$

These renewal-based relationships between diffusion exponents and the TC exponent are summarized in Fig. 4.

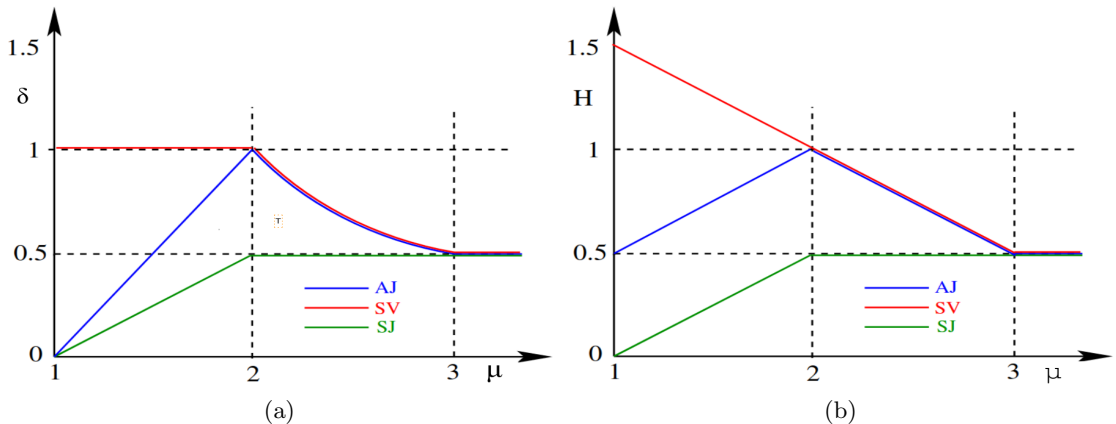


Fig. 4. Scaling δ_* (panel (a)) and H (panel (b)) vs. complexity index μ for the three walking rules: AJ (intermediate blue line), SJ (bottom green line) and SV (top blue line).

The three rules give a normal scaling $\delta_* = H = 1/2$ for $\mu \geq 3$, thus giving normal (Gaussian) diffusion, in agreement with the Lévy generalized limit theorem [134]. According to Eq. (87), AJ and SV rules are super-diffusive ($H > 1/2$) for $\mu < 3$, while SJ rule is subdiffusive for $\mu < 2$. All walking rules give a normal scaling $H = 1/2$ for $\mu > 3$ ³⁶. Interestingly, for $1 < \mu < 2$ the AJ rule, even if super-diffusive, displays a scaling δ_* less than $1/2$ for $\mu < 3/2$.

Regarding both theoretical findings and experimental applications of the EDDiS method, some observations are in order:

(1) Check of renewal condition:

By inverting the above relationships, it is possible to have more indirect estimations of μ . Being the AJ the most robust rule, we can invert H_{AJ} and δ_{AJ}

³⁶ For a Poisson process, i.e., an exponential IET-PDF $\psi(\tau) \sim \exp(-\tau/\bar{\tau})$, the asymptotic diffusion for $t \gg \bar{\tau}$ is normal: $\delta_* = H = 1/2$. This is not surprising as the Poisson process corresponds to the limit $\mu \rightarrow \infty$ of the IET-PDF given in Eq. (14).

to get [14,199]:

$$\delta_{AJ} = \begin{cases} 2H_{AJ} - 1 ; & 1 < \mu < 2 \\ 1/(3 - 2H_{AJ}) ; & 2 \leq \mu < 3 \\ H_{AJ} = 1/2 ; & \mu \geq 3 \end{cases} \quad (100)$$

When this condition is fulfilled within a given statistical significance, the renewal hypothesis can be accepted.

- (2) AJ rule can split the contribution of noisy events, acting in the short-time regime, from that of genuine complex events, i.e., displaying fractal intermittency³⁷ and triggering fast diffusion in the long-time limit. This was seen in many experimental datasets [14,15,17,18,19] and theoretical analyses [15,192].
- (3) Robust estimation of μ :
A direct estimation of μ can be carried out by a best fit on the IET-PDF. However, even in the presence of a small, but not negligible, percentage of noisy events, the slope of the IET-PDF can be drastically blurred and it can even display an apparent power-law that is different by the underlying true one [15]. This problem is cured by the diffusion scaling. In fact, when renewal condition is verified, the value of μ can be estimated by the three walking rules. For $\mu > 2$, SJ rule gives normal diffusion $H = \delta_* = 1/2$ and only two rules are available and four diffusion exponent, two for each rule.
- (4) The SV rule gives a counter-intuitive normal diffusion at long times when complex and noisy events are superposed. Allegrini et al. (2010) [15] and Paradisi and Allegrini (2015) [192] proposed a modeling approach and a data analysis method, later named Poisson Added Noise DiffusiOn Rescaling Analysis (PANDoRA) [193], that are based on the superposition of genuine complex events (fractal intermittency) and Poisson events and that gives an explanation of the above behavior.
- (5) The EDDiS method does not necessarily need the estimation of μ . In fact, in most datasets the SJ rule gives a normal diffusion, a signature of $\mu > 2$ ³⁸. Further, the best fit on the SV rule has often a low statistical significance due to the presence of noise. Conversely, the AJ rule is usually reliable and, as said above, robust under the presence of noisy events. Thus, the H or δ_* exponents can be used also beyond the validation of the renewal hypothesis and, thus, in a somewhat extended framework with respect to the more restricted assumptions of TC/IDC framework³⁹. For example, in Allegrini et al. (2010) [17] only the DE analysis was used, while other works of Allegrini, Paradisi and co-workers [18,19,200,196,197] reported only on the DFA results⁴⁰.

³⁷ We recall that, in the TC/IDC framework, fractal intermittency is associated with both inverse power-law IET-PDF and renewal condition.

³⁸ Paradisi et al. (2012) [200] confirmed this finding in a turbulence dataset by also applying a fractal dimension analysis by box counting method.

³⁹ In our opinion, in complex self-organized systems the presence of renewal crucial events is probably ubiquitous, even if there are often some difficulties in validating the renewal assumption and in getting a robust estimation of μ . However, the investigation of system's complexity by the diffusion exponent is still possible, especially by means of the AJ rule and DFA exponent H , due to the above cited ability of separating the contributions of noisy and complex events.

⁴⁰ By definition, the statistical ensemble of DFA is often much larger than that of DE analysis, even considering superposed realizations in the DE ensemble, that can also introduce some spurious effects in the averaging procedure. Conversely, the DFA, even in the multiscaling DFA version, is referred to the moments of the distribution and not to some information measure such as entropy, which could include some effect not retained in the moment analysis.

9 Intermittency, clustering and complexity in the PBL

Intermittency models of ideal homogeneous and isotropic turbulence, while remaining a benchmark, appear to be not applicable in a straightforward way to atmospheric turbulence. This is the case not only for the classical models, K41 monoscaling or K62 log-normal multiscaling models [129,181], but also for more recent findings about intermittency and multiscaling in turbulence modeling [242,243]. For this reason, in the last two decades or so, a wide literature was devoted to the complexity analysis of high time-resolution wind data, the goal being the investigation of a general formulation for turbulent flows over complex terrain in terms of a few complexity measures, related to both MI and CI [110,137].

In fact, complexity features become particularly relevant, as they are related to turbulent structures and events triggered by a particular mixture of internal, external and global intermittency that simultaneously affect clustering and rapid large excursions [23,24,146,149,254]. The studies in PBL turbulence over complex terrain from the viewpoint of event-based complexity investigated many different exponents and the general picture is still not clear. In the following we will discuss some of the open issues.

At the beginning of event-based complexity in PBL turbulence

Milestone papers in this research field are the studies of Bershadskii et al. (2004) and Sreenivasan and Bershadskii (2006) [42,43,251], where fundamental results were found in experimental data both from laboratory experiments and field experimental campaign in the atmospheric surface layer⁴¹. To our knowledge, these authors firstly applied the TA to turbulence data. In particular, they evaluated the TA spectral exponent jointly with the classical one and proposed the relation (72) [251] between spectral exponents, whose validity was found to be true for the analyzed datasets. Further, Bershadskii et al. (2004) [42] investigated both clustering and TC-IDC and Oboukhov intermittency exponents μ and γ_{TA} derived from the TA signal. They firstly proposed the formula given in Eq. (93), extending the SOC relationship, Eq. (92), to include the effect of Oboukhov intermittency associated with the signal dissipation rate. Sreenivasan et al. (2006) [251] proposed and investigated by means of both numerical models and experimental data, the relationship given in Eq. (72) between the spectral exponents β_{TA} and β_s . They also applied the clustering exponent α_c to different experimental datasets.

The main experimental findings of the above studies were the following:

- For temperature in laboratory turbulent convection, an experimental value $\beta_{TA} \simeq 1.38$ was found to be not compatible with the SOC prediction:

$$\beta_{TA}(SOC) = 3 - \mu_{exp} \simeq 1.63,$$
being $\mu_{exp} \simeq 1.37$ [42]. The reduction given by the difference $\beta_{TA}(exp) - \beta_{TA}(SOC) = -0.25$ was claimed to be associated with (Oboukhov) intermittency.
- The solution to the previous result was given by the same authors [42], who derived, and validated on experimental data, the formula given in Eq. (93),

⁴¹ In [251] the authors use the atmospheric surface layer data given in Ref. [252] and the wind tunnel data from [208]. In Ref. [42] laboratory data of thermal convection taken from [179] were analyzed. Notice that collecting the data inside the surface layer (about 35 m over the ground) means that the observed velocity fluctuations around the mean logarithmic profile should display a behavior quite near to the ideal homogeneous and isotropic energy cascade [128,182,225].

which generalizes the SOC relationship (92). In particular, they found the experimental value $\gamma_{TA} = 0.47 \pm 0.03$, which is compatible with the difference between the experimental exponent β_{TA} and that predicted by SOC.

- Sreenivasan et al. (2006) [251] derived an asymptotic expansion of α_c for $Re_T \rightarrow \infty$, being $Re_T = \lambda_T U / \nu$ the Taylor microscale Reynolds number⁴², and found an asymptotic minimum value:

$$\alpha_c \rightarrow 0.1 \text{ for } Re_T \rightarrow \infty$$

- Conversely, for $200 < Re_T < 20000$, α_c range is from 0.25 to 0.4 for scales between the dissipative and inertial ranges, while $\alpha_c \simeq 0.5$ (white-noise) for scales larger than the integral scale L of energy-containing eddies. Then, there is a pronounced clustering at short times, but no clustering at long times.

Is there universal complexity in the PBL ?

Following the approach firstly introduced in Refs. [43,42,251], several authors carried out similar TA-based analyses on turbulence fluctuations, e.g, streamwise and spanwise velocity, temperature, over complex terrain such as vegetated canopies [57,58,59,110,137]. It is worth noting that the common jargon is that of “separating”, “distinguish” or “isolating” the role of CI from the MI and that MI is found to “mitigate” or “amplify” intermittency⁴³, referring to the comparison between γ_{TA} and γ_s (see above, Section 7). Other similar sentences are of the kind “amplitude intermittency [here MI] might mitigate clustering” [42], which seems to refer to the clustering exponent α_c , but it could also refer generically to intermittency. In particular, some authors claim that, when $\gamma_{TA} \simeq \gamma_s$, the “observed (Oboukhov) intermittency may be due to clusterization not amplitude variations” [57]⁴⁴.

The overall picture is that of the emergence of a event-driven dynamical process where crucial events play a crucial role. However, the underlying mechanisms of event triggering and associated birth/decay of self-organized turbulent structures is still unclear.

The above cited studies about PBL turbulence over complex terrain apply the TA technique firstly proposed in Bershadskii et al. (2004) [42] in order to compare some complexity exponents of the original signals with those of the TA. In particular, they compare spectral exponents (β_s and β_{TA}) and Oboukhov intermittency exponents (γ_s and γ_{TA}) for both signal and its Telegraph Approximation (TA), and, by definition only for TA, the clustering exponent α_c and the temporal complexity, or persistence, exponent μ .

⁴² The Taylor microscale λ_T is the smallest size of the large eddies, i.e., the size at which viscous dissipation is no more negligible. We recall that the Kolmogorov microscale λ_K is the scale at which the TKE is entirely dissipated into heat due to viscosity. Clearly, $\lambda_K \ll \lambda_T \ll L$.

⁴³ MI is sometimes named “amplitude variability” or “amplitude intermittency”. This concept seems to be associated with the Oboukhov intermittency of the original signal and, thus, related to the “dissipation rate” of the signal itself, actually to the derivative of the energy signal [57,110].

⁴⁴ In our opinion, this kind of terminology could sound slightly ambiguous. In fact, the Oboukhov intermittency exponent, and also the other exponents, give some indications of how (how much) the analyzed signal is self-organizing (self-organized) over different temporal or spatial scales and if there is some kind of self-similarity, whatever monoscaling or multiscaling. All these exponents refer to the single analyzed signal, thus comparing event-based complexity measures with those of the original signal is surely interesting, but it should be treated carefully and conclusions derived from these comparisons will surely deserve further attention.

Over flat terrain quite far from the ground and above vegetated canopies, the evaluation of the spectral exponents β_{TA} and β_s was found to be in quite good agreement with Eq. (72). In fact, the analyses estimate the small-scale usual values $\beta_s = 5/3$ and $\beta_{TA} = 4/3$, which are also typical of the already discussed internal intermittency. However, some authors [57] found a net failure of the relationship (72) inside the canopy. Statistically significant linear regressions with coefficient different from $1/2$ were found, but different datasets gave different linear regression coefficients. Further, the spectral relationship (72) was found to be no more valid in the region very near to the ground ($< 1\text{m}$) [110] and in the quiescent layer developed in a nocturnal high stable boundary layer [60].

Regarding clustering behaviour isolated from amplitude variations, this has rarely been considered in PBL turbulence except in a few studies [57,58,60,70,137,215]. Interestingly, different values of the clustering exponent α_c were found at small and large scales, thus giving a double-regime for clustering. In particular, we have:

- For horizontal velocity, there is essentially no significant clustering at large scales, i.e., $\alpha_c \simeq 0.5$ (compatible with white noise).
- However, at large scale $\alpha_c \approx 1$ at different height, after the development of a low-level jet (LLJ) in a nocturnal stable boundary layer.
- Clustering is higher (lower α_c) at small scales than large scales: $\alpha_c \sim 0.24 - 0.30$. This is in agreement with laboratory experiments at $Re_T \sim 200 - 20000^{45}$, where it was found: $\alpha_c \sim 0.25 - 0.40$ [251].
- α_c is less scattered at small than large scales (signature of a quasi-universal behavior at small scales)
- Inside the canopy, the temperature clustering α_c was the most vertically heterogeneous.
- At the canopy bottom, for temperature it results $\alpha_c \simeq 0.1$ in the stable case, which corresponds to the minimum limit value found in Ref. [251], but for velocity⁴⁶.

Regarding the Oboukhov intermittency exponent, a comparison between γ_s of the original signal and γ_{TA} of its TA counterpart is carried out in recent papers [57,58,60,110,136]. Streamwise/spanwise velocity fluctuations and temperature fluctuations were the main investigated signals. In summary, a universal relationship between the clustering exponent α_c and the Oboukhov intermittency exponents γ_s and γ_{TA} was not found within vegetated canopies [57,58] and in a high stable boundary layer [60].

Over flat terrain, but very near to the ground ($< 1\text{m}$), Huang et al. (2021) [110] investigated the difference between small and large scale, finding that:

- At small scale, γ_{TA}/γ_s is homogeneous across heights and stability conditions both for T and u.
- Both velocity and temperature Oboukhov intermittency exponents are more sensitive at large than small scales when considering the height of about 1 m.

Regarding the TC exponent μ , Cava and Katul (2009) [57] found the following results:

⁴⁵ We recall that Re_T is the Reynolds number based on the Taylor microscale, i.e., the shortest size of the large scale eddies.

⁴⁶ In fact, for temperature, the limit value was found to be $\alpha_c \simeq 0.07$.

- Above the canopy, the IET-PDFs are well approximated by a log-normal distribution for all turbulent signals and all stability conditions. This is in agreement with Ref. [251].
- Very near to the ground there are no significant best fit neither power-law nor log-normal.
- In the stable case, the IET-PDF is well described by a power-law distribution mainly in the short-time regime. A quite good linear regression is found between measured β_{TA} and calculated β_{TA} by Eqs. 92 and 93. The best fits show similar linear coefficient and correlation coefficient.

In summary, a universal behavior of TA-based complexity exponents was not found and a general parameterization, e.g., dependence on site geometrical parameters, has not yet been derived. Some kind of universal behavior was found in the region just above the canopy, where exponents, and relations between exponents, similar to those of Refs. [42,250], were found. On the contrary, no clear and universal scaling and multiscaling seems to emerge in the PBL both inside vegetated canopies and over flat terrain at a distance less than one meter from the ground, thus pointing out a possible, not negligible, dependence on the particular site. For example, inside vegetated canopies, the presence of energy short-circuiting and wake production in the crown and in the trunk space affects the PSD and a clear power-law decaying slope is not always evident [57,58]. When a power-law is seen, the PSD has a lower decay with respect to the theoretical prediction of Sreenivasan and Bershadskii (2006) [251].

Neutral, unstable, stable

Different stability conditions are expected to display different complexity exponents, as they are associated with different kinds of self-organizing mechanisms of the turbulent flow and, thus, to the different topologies of the associated turbulent structures. As an example, both laboratory experiments and field campaigns found that hairpin vortices dominate the vertical fluxes in the neutral PBL, while thermal plumes play the major role in unstable conditions [135].

The investigation of the stable and very stable boundary layers is becoming a particular interesting challenge. The stable and strongly stable conditions is the one that, more than the others, presents a intricate superposition or alternance of different types of intermittency, which can also act at similar time and space scales [146,254]. As mentioned previously, a feature of the stable boundary layer is the emergence of turbulence patches at different temporal and spatial scales (external or global intermittency), which then play a crucial role in the dynamics of self-organized turbulent structures [23,149]. In addition, turbulence variability can modify the shape of various sized eddies, or their small subregions (internal, or small-scale, intermittency)⁴⁷. Although the nature of the observed intermittent turbulence is still not well understood, it seems triggered by the various non-turbulent submeso motions (whose characteristic scale range between the largest turbulence eddy scale ($\sim O(100m)$) and the smallest meso-gamma scale ($\sim 2km$)) [151,150]. Submeso motions include a multitude of processes, such as meandering and gravity waves, and can have different shapes, such as steps, ramps, pulses, waves. Conversely, in neutral and unstable conditions, the self-organized struc-

⁴⁷ We recall that internal intermittency is associated with the inertial subrange and, by definition, expected to consistent with the Kolmogorov-Oboukhov similarity modeling approach, modified to include intermittency effects, such as in the She-Leveque model [242].

tures come from the sharp edge instabilities of the main energy-containing eddies. In neutral conditions, the main eddies are triggered by the mean wind at the top of the PBL, which is driven by the mesoscale pressure gradients. In unstable conditions, the large-scale energy-containing eddies are given by thermal plumes energized by the buoyancy, i.e., the overall temperature gradient between the top of the boundary layer and the ground.

Katul and co-workers mainly investigated the dependence of complexity exponent on stability conditions, again finding a number of empirical observations that are not really conclusive and difficult to put in a theoretical framework [57,58,110]. Cava et al. (2019) [60] analyzed the evolution of a nocturnal boundary layer from a weakly stable to a very stable boundary layer, highlighting the role of submeso motions. Three phases were considered: a first weakly stratified state at the beginning of the period, characterized by Richardson number $Ri \sim 0.1$, a transition period characterized by the development of a low-level jet (LLJ) where the PBL is highly stable ($Ri \gg 0.25$), a third period after the complete development of the LLJ, where the SBL present vertical layer, that is: (i) a shallow layer close to the ground with fully-developed turbulence ($Ri \sim 0.1$); (ii) a quiescent layer under the LLJ nose with weak or intermittent turbulence ($0.2 < Ri < 0.5$), dominated by submeso motion; (iii) a turbulent layer above. The analysis was performed in the inertial subrange (ISR) and in the low-frequency range (LFR). In general:

- Temperature appears more intermittent with respect to streamwise velocity in the stable case, thus suggesting that small (inertial) scales could be affected by large-scale structures.
- Atmospheric stability has minor effects on clustering above the canopy.
- Over flat terrain, < 1 m from the ground, there are only slight differences among velocity and temperature and for different stability conditions.
- In the nocturnal stable boundary layer, large scales were found to be more heterogeneous than small scales along the height.

Regarding clustering features, different values of α_c were found at small and large scales. In particular, we have:

- Large scales of temperature are more dependent on stability, whereas velocity is less heterogeneous with respect to stability condition.
- Inside the canopy both velocity components and scalars have higher clustering for strongly stable atmosphere. Typically, we have: $\alpha_c \sim 0.2 - 0.3$ for all variables.
- Clustering increases (α_c decreases) with increasing stability for all turbulent signals.
- Temperature displays higher (lower) clustering than velocity for stable (unstable) conditions.
- At small scale, after the development of the LLJ, the clustering exponent α_c did not change in the layer closer to the ground and in the upper layer. A decrease was observed in the quiescent layer, where was $\alpha_c < 0.2$ especially for velocity components. At low frequency range (large scale) α_c dropped for all the variables at all levels, assuming value $\alpha_c \approx 0.1$. We recall that the role of submeso motions is strictly related to external and global intermittency, which play a major role in triggering crucial events when PBL is stable [21,255].

Regarding the Oboukhov intermittency exponents of temperature and of related TA, the following results were found in Refs. [57,58,60,110]:

- For temperature inside the canopy and in unstable/convective atmosphere: $\gamma_{TA}/\gamma_s < 1$, a result somewhat opposite to that found in Ref. [42].
- Always for temperature inside the canopy, but for near-neutral and stable conditions: $\gamma_{TA}/\gamma_s \simeq 1$.
- For horizontal velocity over flat terrain ($< 1\text{m}$), $\gamma_{TA}/\gamma_s > 1$ across all stability regimes.

Regarding the TC exponent μ , a double-regime often emerges in the IET-PDF with different shapes at small (inertial) and large scales. The shapes, and also the emergence of double-regime, depends on the stability condition, on the height and on the experimental site. It results that the IET-PDFs are not always well fitted by a power-law decay and, further, there is no general consensus about the temporal complexity exponent μ in the PBL. In particular, we have [57,58,60,64,70,110]:

- Within the crown region of vegetated canopies, the emerging double-regime was more evident for velocity and in unstable conditions: a inverse power-law decay in the short IET range and a log-normal distribution in the large IET range.
- In the trunk region, no double-regime was seen and the log-normal distribution gave good fittings for both temperature and velocity and for all stability conditions.
- There was no clear fitting shape of the IET-PDF for temperature in strongly stable conditions inside the canopy and near the ground.
- Analyzing temperature in a dataset from the surface layer of an unstable boundary layer, Chowduri et al. (2020) [71] found power-law decay at small scales and a stretched exponential cut-off at large scales.
- In the nocturnal boundary layer [60] the IET-PDF is well described by a power-law distribution mainly in the short-time range.

The challenge of dissimilarity

The transport properties of velocity and scalars, including heat transport related to temperature, are found to display substantial different behaviors depending on the stability condition of the PBL. In particular, scalar transport increases, while momentum transport decreases, in passing from neutral to unstable conditions. This was found to be strictly related to the topological change of large-scale turbulent (coherent) structures, that are substantially modified by buoyancy [135]. In fact, as said above, the neutral condition is associated with hairpin vortices and hairpin packets dominating the vertical transport fluxes, while the unstable condition display the typical convective thermal plumes that extend vertically over all the PBL [274,123]. In general, scalar intermittency is usually found to be higher than velocity intermittency [63,120,250,273]. Being transition events related to the birth-death of self-organized turbulent structures, it is clear that these different topologies of turbulent structures among velocity and scalar transport are reflected in a dissimilarity of their event-based complexity features.

Regarding clustering, temperature is often found to display more clustering at large scales with respect to the velocity counterpart [57,110]. In fact, the asymptotic regime $\alpha = 0.5$ (no clustering) is reached at much larger scales for temperature. This behavior becomes more evident going deeper into the canopy. This

is related to the ramp-cliff patterns of temperature, which are known to increase intermittency and, inside canopies, are usually associated with sources and sinks (e.g., heat sources/sinks for temperature), which play a major role in the deepest layer of the canopy [55,56,59,57,58]. In fact, these ramp-like temporal patterns are associated with metastable self-organized structures emerging from the direct dynamical interaction, at relatively large scales, between the degrees of freedom of the fluid flow and the surrounding boundaries. The boundaries affect the flow through both the geometrical constraints and the source/sink distribution, these last one especially affecting scalar dynamics and, thus, diffusion/transport properties of the turbulent flow, a regime known as near-field approximation [57]. For this reason, in the large scale regime, clustering and intermittency of temperature and other scalars such as humidity, are much more enhanced with respect to the velocity field inside the canopy. Due to ramp-like patterns, this enhancement is even more evident in stable conditions.

Regarding the clustering exponent at small scales, we have [57,58,60,110]:

- Inside the canopy and for all stability conditions, at small scales clustering was found to be higher (lower α_c) for temperature than for velocity. This finding is more evident for stable condition and is in agreement with Ref. [251]. A similar, but weaker, effect was also found over flat terrain very near to the ground [110].
- Temperature assumes values of α_c much lower than 0.5 (no clustering) for a more extended range of small scales with respect to velocity, till the value $\alpha_c \simeq 0.1$ for stable conditions and in the lowest levels of the canopy.
- Temperature clustering has the highest dependence on the height from the ground.
- Similarly to large scales, clustering is higher (lower α_c) for temperature than for velocity for all stability conditions and for all heights.

The limit value $\alpha_c = 0.1$ is in agreement with the theoretical prediction of Sreenivasan and Bershanskii (2006) [251] for fully developed turbulence far from boundaries ($Re_T \rightarrow \infty$), even if the above prediction regards the clustering of velocity turbulent fluctuations. On the contrary, a maximum value $\alpha = 0.07$ for temperature clustering was predicted.

Regarding the dissimilarity of Oboukhov intermittency, the following results were found:

- Inside the canopy, γ_{TA} for both streamwise and spanwise velocities was found to be higher than for scalars, e.g., temperature, for all stability conditions.
- Inside the canopy, the values of γ_{TA} for temperature were found to decrease with height, while the dependence of velocity on height is weak.
- For both velocity components inside canopy, $\gamma_{TA}/\gamma_s > 1$.
- For temperature $\gamma_{TA}/\gamma_s \sim 1$ at small scale at ground (< 1 m) and inside the canopy in strongly stable conditions.
- For streamwise velocity at small scales and near the ground (< 1 m), it results⁴⁸ $\gamma_{TA}/\gamma_s \sim 1.5$.

⁴⁸ Similarly to previous papers, also these authors claim that, for velocity fluctuations, “amplitude variations lower intermittency”, i.e., MI mitigate Oboukhov intermittency of the original signal. Conversely, for temperature, MI does not have a role in the Oboukhov intermittency, which is then claimed to be associated with clustering.

- In the stable boundary layer, before the development of a LLJ: $\gamma_{TA}/\gamma_s > 1$ for u, w and $\gamma_{TA}/\gamma_s \approx 1$ for T at small scales; $\gamma_{TA}/\gamma_s > 1$ for u and $\gamma_{TA}/\gamma_s \approx 1$ for w and T at large scales.
- In the nocturnal stable boundary layer, after the development of the LLJ, γ_{TA}/γ_s increases for all signals at large scales and at all vertical levels.
- Temperature at large scales has a stronger dependence on atmospheric stability with respect to velocity.

To be SOC or not to be SOC ?

The link with SOC [28,29,114,172] and turbulence, which is discussed since Ref. [42], is an interesting perspective in the studies about intermittency in atmospheric turbulence [57,58,60,110]. The interesting aspect to be studied is given by the range of validity of Eq. (93) and by the existence of possible variations to this formula.

Bershanskii et al. (2004) [42] verified this relationship in both laboratory experiments and field measurements, but it was more recently found that it is not always valid in turbulence inside a canopy sublayer or very near to the ground [57,58,60,110]. This seems to occur, in particular, under stable conditions, where the temperature fluctuations T' does not obey Eq. (93). Interestingly, Huang et al. (2021) [110] found a statistically significant statistical regression with coefficients that are not the same as in Eq. (93), also finding different behaviors at large and small (inertial) scale regimes. However, these same authors claim that even the improvement of the relation (93) is not appropriate to describe the temperature in the stable case⁴⁹.

Cava et al. (2019) [60] estimated the linear regression between measured β_{TA} and calculated β_{TA} , using both Eqs. 92 and 93. They found higher correlation coefficients after the development of the LLJ, but with similar coefficients and statistical significance for both comparisons. The authors deduce that clustering and external intermittency have a role greater than the internal intermittency, and that the SOC relation (Eq. 92) is a reasonable model.

Interestingly, stable PBL turbulence is the most intricate case. There is a lack in understanding what kind of self-organized structures emerge, if they are waving motion, turbulence, laminar or at the transition between laminar and turbulent conditions. Further, there could be some ambiguities arising in the dynamical origin of self-organized structures revealed by event detection methods, in particular the telegraph approximation (TA). In fact, the crucial events could be associated to internal, external or global intermittency. This is in agreement with a claim by Huang et al. (2021) [110]: “the modified SOC relation ... displays signatures of excess intermittency in [temperature] beyond the [Oboukhov] intermittency exponent” (γ_{TA} in our notation).

Renewal theory and diffusion scaling in atmospheric turbulence

Paradisi and co-workers investigated the existence of crucial events in turbulent flows near the ground over flat terrain by applying the velocity increment method [198,200,199,197] and the EDDiS approach. The main results of this analysis are the following:

⁴⁹ We recall that the relationship (93) is already a modification of the classical SOC relation given by Eq. (92) to include Oboukhov intermittency.

- (i) The Renewal Aging analysis applied to both vertical velocity and PM2.5 aerosol concentration signals gave a slightly aging reduction in the Experimental Aging with respect to the Renewal Aging for aging times of 2000 sec., thus proving the presence of a small memory in the time series, which could be interpreted as a residual effect of slow modulation [8,9,45,204,201] from large scale meteorological persistent motions, being most of the effect encoded in the local mean and variance used to normalize the signal in Eq. (61). The TC exponent seems slightly smaller for PM2.5 than for vertical velocity. This could be related to the presence of local source and/or to internal degrees of freedom, e.g., nucleation and coagulation processes. However, statistically significant results about the TC exponents were not found and this low robustness could be related to the use of the IET distributions, which were more recently found to be highly affected by noisy events, also including false positives related to the threshold choice.
- (ii) The EDDiS method was applied to the three velocity components, limiting the analysis to the AJ and SJ rules and the DFA exponent H [200]. The detected values of H were found to be very robust with respect to changes in the threshold D_0 . For streamwise and spanwise velocity fluctuations u/v : $H \simeq 0.93 - 0.96$ and for vertical velocity fluctuations w : $H \simeq 0.95 - 0.98$.
- (iii) The renewal assumption was further verified on the vertical component by applying Eq. (100) [199], i.e., by looking at the combination of H and δ_* estimated from the AJ rule⁵⁰. Thus, on the basis of the renewal assumption, the estimation of the TC/IDC exponents are given by $\mu = 2.08 - 2.14$ for horizontal velocity fluctuations u/v and $\mu = 2.04 - 2.1$ for vertical velocity fluctuations [200]. This also follows from the constrain $\mu \geq 2$ given by the finding $H_{AJ} = \delta_{AJ} = 0.5$. This constrain was also confirmed in Paradisi et al. (2012) by means of a fractal analysis of the event sequence [200].
- (iv) Even if not explicitly stated, the previous analyses were carried out in neutral conditions. A comparison between neutral and stable conditions was carried out on the three velocity components and showed a decrease in the temporal complexity, i.e., an increase in the TC/IDC exponent going from the neutral ($\mu = 2.02 - 2.06$) to the stable condition ($\mu = 2.24 - 2.28$) [197].

The comparison between this EDDiS approach and the velocity increment events and other studied based on other complexity measures and on the TA signal is not clear and should need further investigation.

Wind gusts as crucial events

Cheng et al. (2014) [65] applied the approach proposed in Paradisi et al. (2012) [200] to wind gusts. According to these authors, wind gusts can be interpreted as self-organized flow structures given by strong winds after a cold front with downward vertical velocity associated with a peak in the horizontal velocity and *vice versa* [67,66]. Their findings about the exponent H seem not definitive and have a large variability depending on height: $H \sim 0.54 - 0.8$ for horizontal velocity and $H \sim 0.67 - 0.87$. Interestingly, the short-term noise emerged at time scales up to 5 – 10 sec., whereas in Paradisi et al. (2012) [200] noise appeared up to about 1 sec.

⁵⁰ The renewal assumption is also in agreement with so-called *surface renewal* models proposed by Higbie and, later, by Perlmutter [103,211] (see also [142,232]) and exploited in the atmospheric turbulence framework by Katul et al. (2006) [121] as a possible model for external intermittency.

Babić et al. (2016)[27] use the VITA method to detect coherent structures during strong wind events (bora wind occurring in a topographically complex site near the eastern coast of the Adriatic Sea) and relate them to the features of measured heat and momentum flux. In particular, they found that for wind speed greater than $12m/s$ observed during nearly neutral conditions, the vertical momentum flux at a height of $22m$ was greater than that at the adjacent levels. The authors conclude that the sweep part of the sweep-ejection cycle could potentially cause the observed momentum flux divergence.

10 Concluding remarks

The goal of this review was to put a first bridge between turbulence studies exploiting event-based complexity approaches, such as the clustering and Oboukhov intermittency exponents, and studies about intermittent complex systems, where concepts and ideas developed in the fields of non-equilibrium statistical physics, probability theory and dynamical system theory are jointly exploited. Fluid turbulence is not only one of the most important unsolved problems of classical mechanics and a challenge for mathematical physicists, but, outside topics involving biological systems and living matter, it is also a basic example of a non-living self-organized complex system displaying non-trivial intermittency at several time and space scales.

These studies can have also some impact on applications, in particular on the modeling of turbulent transport. For example, spatial and temporal clustering is directly related to an increase in the interaction among different “fluid elements or particles”. This enhancement is crucial in the transport properties of the turbulent flow and, thus, in the (advection) diffusion and transport of several quantities: humidity and water droplets, temperature, inert gases; chemicals and pollen plumes; aerosol or inertial particles, e.g., sand storms, being “inertial” here referred to particles that, at variance with passive scalars, have a finite mass⁵¹. As an example, it is known that there is a strict interplay between clustering features of turbulence at small scales and the inertia of particles that affect the tendency to agglomerate of inertial/aerosol particles themselves. Further, intense events associated with ejections, sweeps or other self-organized turbulent structures, determine very rapid movements of self-organized portion of fluid with high vorticity from one region to another one. This clearly affects the transport properties of the turbulent flow.

As far as we understand, the application of the event-based complexity paradigm to turbulence is still in its early stages, and future investigations should probably seek to contextualize the event-based approaches to turbulence in the framework of intermittent complex systems and look at them from the “metastable self-organization” viewpoint (see Section 2).

An interesting research topic is the complexity of turbulent flows over complex terrain or very near to the ground, that was briefly discussed in Section 9. The temporal complexity features were investigated in different studies and a high variability in the complexity exponent was found, in particular about the shape

⁵¹ We recall that a passive scalar is a particle that is ideally “docked” to a fluid particle, thus following exactly its same motion dynamics in the turbulent flow. Inertial, or aerosol, particles have a finite mass that determine, at each time instant, a small, but crucial, separation from the fluid particle trajectory due to inertia. Thus, inertial particles move across different fluid particles.

and the double-regime of the IET-PDF. In Ref. [57] the authors derived well fitted shapes that, depending on height and stability condition, could display double-regime (power-law at small and log-normal at large scales) or single-regime (log-normal), while in Ref. [58] they found a power-law decay with exponential cut-off for unstable conditions. The authors of Ref. [64] found a result similar to that of Ref. [58], but on cornfield canopies instead of tree canopies. More recently, in Ref. [70] a net power-law decay with a stretched exponential cut-off was found in the unstable surface layer. At variance with these studies, where the TA signal was used to investigate the event-based complexity features, Paradisi et al. [200,199,197] proposed an approach based on renewal theory [76]. In this approach, by one hand, the detected RTEs could be compatible with surface renewal models [103,211,121] and, on the other hand, on EDDiS method, i.e., a method that can treat noisy events in a proper way and give a robust estimation of both diffusion exponents and TC/IDC exponents, often referred to as *persistence* in atmospheric turbulence studies. This allowed to find some interesting results but the link to TA-based complexity analyses need to be further investigated.

In summary, there is the lack of a general theoretical framework giving a correct interpretation of the experimental analyses, which does not give universal behaviors in the complexity exponents. In particular, parameterizations, i.e., dependence on site geometry, synoptic and mesoscale meteorological variables and atmospheric stability, are still not understood.

Among the open questions, we recall the ones that, in our opinion, are most interesting:

- The interplay between crucial transition events and the concepts of internal, external and global intermittency in atmospheric turbulence is still not clear. This is a crucial open question in the case of strongly stable PBL. Thus, have the RTEs the same geometrical features at the small inertial scales of internal intermittency and at the large scale of global intermittency? In other words, is there a unified picture for self-organized turbulent structures? Until now, the answer seems to be negative, but this needs a deeper understanding.
- It is still not clear if the lack of a net scaling/multiscaling could be also related to the superposition/alternance of different mechanisms working at the same scales (internal, external, global).

Thus, by one hand, it should be necessary to understand the reliability of event detection algorithms by a comparison between different methods. The correct relationship with the underlining self-organized metastable structures should also deserve some more attention. On the other hand, it would be suitable to investigate the inter-relationship between the different event-based complexity exponents by means of methodological/theoretical studies involving stochastic models mimicking the dynamics of turbulent structures or through numerical simulations of fluid dynamics basic equations.

10.1 A personal memento by Paolo Paradisi

I went to know Paolo Grigolini in Pisa during the summer of 2002, during my first year as a researcher in the Lecce branch of the Institute of Atmospheric Sciences and Climate, National Research Council (Consiglio Nazionale delle Ricerche, CNR), where I used to work on stochastic models for turbulent diffusion of pollutants in the atmosphere.

I met him to discuss about a possible scientific collaboration and I remember a walk from the Department of Physics in Largo Bruno Pontecorvo to the Pisa Research Area in Giuseppe Moruzzi street, where the CNR Research Area of Pisa is still located today. I was going to give a seminar on anomalous diffusion, Continuous Time Random Walks and fractional diffusion equations.

During the walk we were immersed in this beautiful sunny atmosphere alongside the panorama given to us by the aqueduct, known as “Acquedotto Mediceo dei Condotti”, which runs along the path, and Paolo Grigolini introduced me, or tried to introduce me, to an extensive philosophical picture that involved what, according to him, could be the true deep meaning of the crucial events in natural phenomena. At the time, I didn’t fully understand his speech, but today I know that we were talking about the role of intermittency in complexity, that is to say, the role of transition events between self-organized metastable states in the cooperative dynamics of a complex system.

Today my understanding about the role of crucial, or critical, events is much improved, even if the speech that Paolo Grigolini gave me in that walk is largely forgotten and what little I have left in my memory I must probably understand still today. In fact, when I gave my seminar, which aroused interest and a good discussion with Paolo Grigolini and other colleagues, Paolo Grigolini himself clarified the role of events in the problem in the consequent solution that I had presented, underlining that the role of events was central in my solution, but that this aspect was not still clear to me. In fact, as a good mathematical physicist, I used to interpret events as a theoretical simplification that is, an approximated assumption of a real behavior. This is actually not a wrong interpretation, but it represents a somewhat partial and reductive vision.

Regarding the topic of this chapter, the event-based approach to turbulence, me and Paolo Grigolini had also an interesting discussion on how to concretize our collaboration and, having specified my interest in turbulent diffusion, in an instant Paolo Grigolini found the connection with the well-known Manneville-Pomeau map [155,216], a nonlinear model which, despite its simplification, captures the essence of turbulent bursting.

Our collaboration, which mainly concerned physical problems other than turbulence, then began in 2004 and continued until 2009. In those years I used to make frequent research visits at both Center of Nonlinear Sciences in Denton (Texas) and Department of Physics in Pisa (Italy). This is a period of my life that I remember with pleasure from the point of view of both scientific research and personal acquaintances, not only with Paolo Grigolini but also with many of his and other students, partly experiencing the typical lifestyle of an American university. In 2009, during the famous Grigolini’s Friday afternoon meetings in Pisa, we started some discussions with some researchers working in the fascinating world of neurosciences. As a consequence, the work on brain events begun, a research line we were immediately enthusiastic about, and that is nowadays still inspiring me.

I am therefore delighted to have this opportunity to thank Paolo Grigolini for the contribution he made to my personal research path on anomalous diffusion and complex systems, which, thanks to him, I believe to be also the route of many others. This joined, in some sense, the other important contribution to my personal research view that comes from the collaboration with Prof. Francesco Mainardi of the Physics Department in Bologna (see [191]), collaboration that

began with the degree thesis and continued for a few years later. A path whose deep contents I was still partly unaware of and which today I am able to delineate more clearly, also thanks to the collaboration with Paolo Grigolini.

References

1. O.C. Acevedo and D.R. Fitzjarrald. In the core of the night - effects of intermittent mixing on a horizontally heterogeneous surface. *Boundary-Layer Meteorology*, 106(1):1–33, 2003.
2. V.S. Afraimovich, V.P. Zhigulin, and M.I. Rabinovich. On the origin of reproducible sequential activity in neural circuits. *Chaos*, 14(4):1123–1129, 2004. DOI: 10.1063/1.1819625.
3. O.C. Akin, P. Paradisi, and P. Grigolini. Periodic trend and fluctuations: The case of strong correlation. *Phys. A*, 371:157–170, 2006.
4. O.C. Akin, P. Paradisi, and P. Grigolini. Perturbation-induced emergence of Poisson-like behavior in non-Poisson systems. *J. Stat. Mech.: Theory Exp.*, page P01013, 2009.
5. G. Alfonsi. Coherent structures of turbulence: Methods of eduction and results. *Appl. Mech. Rev.*, 59(1-6):307–323, 2006. DOI: 10.1115/1.2345370.
6. P. Allegrini, G. Aquino, P. Grigolini, L. Palatella, and A. Rosa. Generalized master equation via aging continuous-time random walks. *Phys. Rev. E*, 68(5 2):561231–5612311, 2003. DOI: 10.1103/physreve.68.056123.
7. P. Allegrini, G. Aquino, P. Grigolini, L. Palatella, A. Rosa, and B.J. West. Correlation function and generalized master equation of arbitrary age. *Phys. Rev. E*, 71(6), 2005. DOI: 10.1103/PhysRevE.71.066109.
8. P. Allegrini, F. Barbi, P. Grigolini, and P. Paradisi. Renewal, modulation, and superstatistics in times series. *Phys. Rev. E*, 73(4), 2006. DOI: 10.1103/PhysRevE.73.046136.
9. P. Allegrini, F. Barbi, P. Grigolini, and P. Paradisi. Aging and renewal events in sporadically modulated systems. *Chaos Solitons Fract*, 34:11–18, 2007.
10. P. Allegrini, V. Benci, P. Grigolini, P. Hamilton, M. Ignaccolo, G. Menconi, L. Palatella, G. Rafaelli, N. Scafetta, M. Virgilio, and J. Yang. Compression and diffusion: A joint approach to detect complexity. *Chaos Solitons Fractals*, 15(3):517–535, 2003. DOI: 10.1016/S0960-0779(02)00136-4.
11. P. Allegrini, V. Benci, P. Grigolini, P. Hamilton, M. Ignaccolo, G. Menconi, L. Palatella, G. Rafaelli, N. Scafetta, M. Virgilio, and J. Yang. Compression and diffusion: A joint approach to detect complexity. *Chaos Sol. Fract.*, 15(3):517–535, 2003. DOI: 10.1016/S0960-0779(02)00136-4.
12. P. Allegrini, M. Bologna, P. Grigolini, and B.J. West. Fluctuation-dissipation theorem for event-dominated processes. *Phys. Rev. Lett.*, 99(1), 2007. DOI: 10.1103/PhysRevLett.99.010603.
13. P. Allegrini, P. Grigolini, and B.J. West. Dynamical approach to lévy processes. *Phys. Rev. E*, 54(5):4760–4767, 1996. DOI: 10.1103/PhysRevE.54.4760.
14. P. Allegrini, D. Menicucci, R. Bedini, L. Fronzoni, A. Gemignani, P. Grigolini, B.J. West, and P. Paradisi. Spontaneous brain activity as a source of ideal 1/f noise. *Phys. Rev. E*, 80(6), 2009. DOI: 10.1103/PhysRevE.80.061914.
15. P. Allegrini, D. Menicucci, R. Bedini, A. Gemignani, and P. Paradisi. Complex intermittency blurred by noise: theory and application to neural dynamics. *Phys. Rev. E*, 82(1 Pt 2):015103, 2010.
16. P. Allegrini, P. Paradisi, D. Menicucci, R. Bedini, A. Gemignani, and L. Fronzoni. Noisy cooperative intermittent processes: from blinking quantum dots to human consciousness. *J. Phys. Conf. Ser.*, 306(1):012027, 2011.
17. P. Allegrini, P. Paradisi, D. Menicucci, and A. Gemignani. Fractal complexity in spontaneous eeg metastable-state transitions: New vistas on integrated neural dynamics. *Front. Physio.*, 1, 2010. DOI: 10.3389/fphys.2010.000128.
18. P. Allegrini, P. Paradisi, D. Menicucci, M. Laurino, R. Bedini, A. Piarulli, and A. Gemignani. Sleep unconsciousness and breakdown of serial critical intermittency: New vistas on the global workspace. *Chaos Solitons Fract.*, 55:32–43, 2013.
19. P. Allegrini, P. Paradisi, D. Menicucci, M. Laurino, A. Piarulli, and A. Gemignani. Self-organized dynamical complexity in human wakefulness and sleep: Different critical brain-activity feedback for conscious and unconscious states. *Phys. Rev. E Stat. Nonlin. Soft Matter Phys*, 92(3), 2015.
20. K.H. Andersen, P. Castiglione, A. Mazzino, and A. Vulpiani. Simple stochastic models showing strong anomalous diffusion. *Eur. Phys. J. B*, 18(3):447–452, 2000. DOI: 10.1007/s100510070032.
21. D. Anfossi, D. Oettl, G. Degrazia, and A. Goulart. An analysis of sonic anemometer observations in low wind speed conditions. *Boundary-Layer Meteorology*, 114(1):179–203, 2005.
22. F. Anselmet, Y. Gagne, and E.J. Hopfinger. High-order velocity structure functions in turbulent shear flows. *J. Fluid Mech.*, 140:63–89, 1984.
23. C. Ansorge and J.P. Mellado. Global intermittency and collapsing turbulence in the stratified planetary boundary layer. *Bound.-Layer Meteorol.*, 153(1):89–116, 2014.
24. C. Ansorge and J.P. Mellado. Analyses of external and global intermittency in the logarithmic layer of ekman flow. *J. Fluid Mech.*, 805:611–635, 2016.

25. R.A. Antonia, A.J. Chambers, and E.F. Bradley. Relationships between structure functions and temperature ramps in the atmospheric surface layer. *Bound.-Layer Meteorol.*, 23(4):395–403, 1982.
26. G. Aquino, P. Grigolini, and B.J. West. Linear response and fluctuation-dissipation theorem for non-poissonian renewal processes. *EPL*, 80(1), 2007. DOI: 10.1209/0295-5075/80/10002.
27. N. Babić, Ž. Večenaj, H. Kozmar, K. Horvath, S.F.J. De Wekker, and B. Grisogono. On turbulent fluxes during strong winter bora wind events. *Boundary-Layer Meteorology*, 158(2):331–350, 2016.
28. P. Bak, C. Tang, and K. Wiesenfeld. Self-organized criticality: An explanation of the 1/f noise. *Phys. Rev. Lett.*, 59(4):381–384, 1987. DOI: 10.1103/PhysRevLett.59.381.
29. P. Bak, C. Tang, and K. Wiesenfeld. Self-organized criticality. *Phys. Rev. A*, 38(1):364–374, 1988. DOI: 10.1103/PhysRevA.38.364.
30. A. Banerjee, J.J. Dolado, J.W. Galbraith, and D. Hendry. *Co-Integration, Error-Correction, and the Econometric Analysis of Non-Stationary Data*. Oxford University Press, 1993.
31. A.-L. Barabási and Z.N. Oltvai. Network biology: Understanding the cell’s functional organization. *Nat. Rev. Genet.*, 5(2):101–113, 2004. DOI: 10.1038/nrg1272.
32. M. Barati Moghaddam, M. Mazaheri, and J. Mohammad Vali Samani. Inverse modeling of contaminant transport for pollution source identification in surface and groundwaters: a review. *Groundwater Sustainable Dev.*, 15, 2021.
33. F. Barbi, M. Bologna, and P. Grigolini. Linear response to perturbation of nonexponential renewal processes. *Phys. Rev. Lett.*, 95(22), 2005. DOI: 10.1103/PhysRevLett.95.220601.
34. E. Barkai. Ctrw pathways to the fractional diffusion equation. *Chem. Phys.*, 284(1-2):13–27, 2002. DOI: 10.1016/S0301-0104(02)00533-5.
35. G.K. Batchelor and Cambridge University Press. *The Theory of Homogeneous Turbulence*. Cambridge Science Classics. Cambridge University Press, 1953.
36. G.K. Batchelor and A.A. Townsend. The nature of turbulent motion at large wave-numbers. *Proc. R. Soc. Lond. A*, 199:238–255, 1949. DOI: 10.1098/rspa.1949.0136.
37. G. Bateson. *Steps to an ecology of mind*. Chandler Publishing Company, New York, 1972. ISBN: 0-345-27370-2.
38. M. T. Beig, A. Svenkeson, M. Bologna, B. J. B. J. West, and P. Grigolini. Critical slowing down in networks generating temporal complexity. *Phys. Rev. E*, 91:012907, 2015.
39. D. Belušić and L. Mahrt. Is geometry more universal than physics in atmospheric boundary layer flow? *J Geophys Res Atmos*, 117(9), 2012.
40. R. Benzi and U. Frish. Turbulence. *Scholarpedia*, 5(3):3439, 2010. URL: <http://www.scholarpedia.org/article/Turbulence>.
41. R. Benzi, G. Paladin, G. Parisi, and A. Vulpiani. On the multifractal nature of fully developed turbulence and chaotic systems. *J. Phys. A: Gen. Phys.*, 17(18):3521–3531, 1984. DOI: 10.1088/0305-4470/17/18/021.
42. A. Bershadskii, J.J. Niemela, A. Praskovsky, and K.R. Sreenivasan. “clusterization” and intermittency of temperature fluctuations in turbulent convection. *Phys. Rev. E*, 69(5):5, 2004.
43. A. Bershadskii, J.J. Niemela, and K.R. Sreenivasan. Solar flares and thermal wind reversals: Critical metastable states. *Phys. Lett. A*, 331(1-2):15–19, 2004. DOI: 10.1016/j.physleta.2004.08.053.
44. S. Bianco, P. Grigolini, and P. Paradisi. Fluorescence intermittency in blinking quantum dots: renewal or slow modulation ? *J. Chem. Phys.*, 123(17):174704, 2005.
45. S. Bianco, P. Grigolini, and P. Paradisi. A fluctuating environment as a source of periodic modulation. *Chem. Phys. Lett.*, 438(4-6):336–340, 2007.
46. R.F. Blackwelder and R.E. Kaplan. On the wall structure of the turbulent boundary layer. *J. Fluid Mech.*, 76(1):89–112, 1976.
47. S. Boccaletti, V. Latora, Y. Moreno, M. Chavez, and D.-U. Hwang. Complex networks: Structure and dynamics. *Phys. Rep.*, 424(4-5):175–308, 2006. DOI: 10.1016/j.physrep.2005.10.009.
48. D.G. Bogard. Burst detection with single-point velocity measurements. *J. Fluid Mech.*, 162:389–413, 1986. DOI: 10.1017/S0022112086002094.
49. G. Bohara, B.J. West, and P. Grigolini. Bridging waves and crucial events in the dynamics of the brain. *Front. Physiol.*, 9, 2018. DOI: 10.3389/fphys.2018.01174.
50. G.E.P. Box and D.A. Pierce. Distribution of residual autocorrelations in autoregressive-integrated moving average time series models. *J. Am. Stat. Assoc*, 65(332):1509–1526, 1970.
51. P.C. Bressloff and J.M. Newby. Stochastic models of intracellular transport. *Rev. Mod. Phys.*, 85(1):135–196, 2013. DOI: 10.1103/RevModPhys.85.135.
52. E. Bullmore and O. Sporns. Complex brain networks: Graph theoretical analysis of structural and functional systems. *Nat. Rev. Neurosci.*, 10(3):186–198, 2009. DOI: 10.1038/nrn2575.
53. G. Buzsáki. *Rhythms of the Brain*. Oxford University Press, 2009. ISBN: 978-0-19-530106-9, DOI: 10.1093/acprof:oso/9780195301069.001.0001.
54. P. Castiglione, A. Mazzino, P. Muratore-Ginanneschi, and A. Vulpiani. On strong anomalous diffusion. *Physica D*, 134(1):75–93, 1999. DOI: 10.1016/S0167-2789(99)00031-7.
55. D. Cava, U. Giostra, M. Siqueira, and G. Katul. Organised motion and radiative perturbations in the nocturnal canopy sublayer above an even-aged pine forest. *Bound.-Lay. Met.*, 112(1):129–157, 2004. DOI: 10.1023/B:BOUN.0000020160.28184.a0.

56. D. Cava and G.G. Katul. Spectral short-circuiting and wake production within the canopy trunk space of an alpine hardwood forest. *Bound.-Layer Meteorol.*, 126(3):415–431, 2008. DOI: 10.1007/s10546-007-9246-x.
57. D. Cava and G.G. Katul. The effects of thermal stratification on clustering properties of canopy turbulence. *Bound. Lay. Met.*, 130(3):307–325, 2009.
58. D. Cava, G.G. Katul, A. Molini, and C. Elefante. The role of surface characteristics on intermittency and zero-crossing properties of atmospheric turbulence. *J Geophys Res Atmos*, 117(1), 2012.
59. D. Cava, G.G. Katul, A.M. Sempreviva, U. Giostra, and A. Scrimieri. On the anomalous behaviour of scalar flux-variance similarity functions within the canopy sub-layer of a dense alpine forest. *Bound.-Lay. Met.*, 128(1):33–57, 2008. DOI: 10.1007/s10546-008-9276-z.
60. D. Cava, L. Mortarini, U. Giostra, O. Acevedo, and G. Katul. Submeso motions and intermittent turbulence across a nocturnal low-level jet: A self-organized criticality analogy. *Bound.-Lay. Met.*, 2019. DOI: 10.1007/s10546-019-00441-8.
61. A. Celani, A. Lanotte, A. Mazzino, and M. Vergassola. Universality and saturation of intermittency in passive scalar turbulence. *Phys. Rev. Lett.*, 84(11):2385–2388, 2000. DOI: 10.1103/PhysRevLett.84.2385.
62. R. Cesari, P. Paradisi, and P. Allegrini. Source identification by a statistical analysis of backward trajectories based on peak pollution events. *Int. J. Environ. Pollut.*, 55(1-4):94–103, 2014.
63. A.J. Chambers and R.A. Antonia. Atmospheric estimates of power-law exponents M and M_θ . *Boundary-Layer Meteorology*, 28(3-4):343–352, 1984. DOI: 10.1007/BF00121313.
64. M. Chamecki. Persistence of velocity fluctuations in non-gaussian turbulence within and above plant canopies. *Phys. Fluids*, 25(11), 2013.
65. X. Cheng, F. Hu, and Q. Zeng. Stochastic method to determine the scale and anomalous diffusion of gusts in a windy atmospheric boundary layer. *Chin. Sci. Bull.*, 59(34):4890–4898, 2014.
66. X. Cheng, L. Wu, F. Hu, and Q.-C. Zeng. Parameterizations of some important characteristics of turbulent fluctuations and gusty wind disturbances in the atmospheric boundary layer. *J Geophys Res Atmos*, 117(8), 2012.
67. X. Cheng, Q.-C. Zeng, and F. Hu. Characteristics of gusty wind disturbances and turbulent fluctuations in windy atmospheric boundary layer behind cold fronts. *J Geophys Res Atmos*, 116(6), 2011.
68. D.R. Chialvo. Emergent complex neural dynamics. *Nat. Phys.*, 6(10):744–750, 2010. DOI: 10.1038/nphys1803.
69. A.C.-L. Chian, R.A. Miranda, D. Koga, M.J.A. Bolzan, F.M. Ramos, and E.L. Rempel. Analysis of phase coherence in fully developed atmospheric turbulence: Amazon forest canopy. *Nonlinear Processes Geophys.*, 15(4):567–573, 2008. DOI: 10.5194/npg-15-567-2008.
70. S. Chowdhuri, T. Kalmár-Nagy, and T. Banerjee. Persistence analysis of velocity and temperature fluctuations in convective surface layer turbulence. *Phys. Fluids*, 32:076601, 2020.
71. S. Chowdhuri, S. Kumar, and T. Banerjee. Revisiting the role of intermittent heat transport towards reynolds stress anisotropy in convective turbulence. *J. Fluid Mech.*, 2020. DOI: 10.1017/jfm.2020.471.
72. A. Compte. Stochastic foundations of fractional dynamics. *Phys. Rev. E*, 53(4):4191–4193, 1996. DOI: 10.1103/PhysRevE.53.4191.
73. Y. F. Contoyiannis, F. K. Diakonos, and A. Malakis. Intermittent dynamics of critical fluctuations. *Phys. Rev. Lett.*, 89:035701, 2002. DOI: 10.1103/PhysRevLett.89.035701.
74. Y.F. Contoyiannis and F.K. Diakonos. Criticality and intermittency in the order parameter space. *Phys. Lett. A*, 268(4):286–292, 2000. DOI: 10.1016/S0375-9601(00)00180-8.
75. E.R. Corino and R.S. Brodkey. A visual investigation of the wall region in turbulent flow. *J. Fluid Mech.*, 37(1):1–30, 1969. DOI: 10.1017/S0022112069000395.
76. D.R. Cox. *Renewal Processes*. Methuen & Co., London, 1970. ISBN: 0-412-20570-X; first edition 1962.
77. D.R. Cox and V. Isham. *Point Processes*. Chapman and Hall, 1 edition, 1980. ISBN: 9780412219108.
78. M. Dentz, P.K. Kang, A. Comolli, T. Le Borgne, and D.R. Lester. Continuous time random walks for the evolution of lagrangian velocities. *Phys. Rev. Fluids*, 1(7), 2016. DOI: 10.1103/PhysRevFluids.1.074004.
79. F. Di Tullio, P. Paradisi, R. Spigler, and G. Pagnini. Gaussian processes in complex media: New vistas on anomalous diffusion. *Front. Phys.*, 7, 2019. DOI: 10.3389/fphy.2019.00123.
80. M. D’Ovidio, S. Vitali, V. Sposini, O. Sliusarenko, P. Paradisi, G. Castellani, and G. Pagnini. Centre-of-mass like superposition of ornstein-uhlenbeck processes: A pathway to non-autonomous stochastic differential equations and to fractional diffusion. *Fract. Calc. Appl. An.*, 21(5):1420–1435, 2018. DOI: 10.1515/fca-2018-0074.
81. S. Duchek. Organizational resilience: a capability-based conceptualization. *Business Research*, 13(1):215–246, 2020. DOI: 10.1007/s40685-019-0085-7.
82. G. Falkovich and K.R. Sreenivasan. Lessons from hydrodynamic turbulence. *Phys. Today*, 59(4):43, 2006. DOI: 10.1063/1.2207037.

83. J. Finnigan. Turbulence in plant canopies. *Ann. Rev. Fluid Mech.*, 32:519–571, 2000. DOI: doi:10.1146/annurev.fluid.32.1.519.
84. S. Fortunato. Community detection in graphs. *Phys. Rep.*, 486(3-5):75–174, 2010. DOI: 10.1016/j.physrep.2009.11.002.
85. Z.R. Fox, E. Barkai, and D. Krapf. Aging power spectrum of membrane protein transport and other subordinated random walks. *Nat. Commun.*, 12(1), 2021. DOI: 10.1038/s41467-021-26465-8.
86. D. Fraiman, P. Balenzuela, J. Foss, and D. R. Chialvo. Ising-like dynamics in large-scale functional brain networks. *Phys. Rev. E*, 79:061922, 2009. DOI: 10.1103/PhysRevE.79.061922.
87. U. Frisch. *Turbulence, the Legacy of A.N. Kolmogorov*. Cambridge Univ. Press, Cambridge, 1995. ISBN: 0-521-45713-0.
88. U. Frisch, A. Mazzino, and M. Vergassola. Intermittency in passive scalar advection. *Phys. Rev. Lett.*, 80(25):5532–5535, 1998. DOI: 10.1103/PhysRevLett.80.5532.
89. U. Frisch, P.-L. Sulem, and M. Nelkin. A simple dynamical model of intermittent fully developed turbulence. *J. Fluid Mech.*, 87(4):719–736, 1978. DOI: 10.1017/S0022112078001846.
90. J.R. Garratt. *The Atmospheric Boundary Layer*. Cambridge University Press, 1994. ISBN: 0-521-46745-4.
91. B.V. Gnedenko and A.N. Kolmogorov. *Limit distributions for sums of independent random variables*. Addison-Wesley Publishing Co., Reading, 1968. Translated from Russian.
92. R. Gorenflo, F. Mainardi, D. Moretti, G. Pagnini, and P. Paradisi. Discrete random walk models for space-time fractional diffusion. *Chem. Phys.*, 284(1-2):521–541, 2002.
93. R. Gorenflo, F. Mainardi, D. Moretti, G. Pagnini, and P. Paradisi. Fractional diffusion: Probability distributions and random walk models. *Phys. A: Stat. Mech.*, 305(1-2):106–112, 2002.
94. R. Gorenflo, F. Mainardi, D. Moretti, and P. Paradisi. Time fractional diffusion: A discrete random walk approach. *Nonlin. Dynam.*, 29(1-4):129–143, 2002. DOI: 10.1023/A:1016547232119.
95. R. Gorenflo, F. Mainardi, and A. Vivoli. Continuous-time random walk and parametric subordination in fractional diffusion. *Chaos Sol. Fract.*, 34(1):87–103, 2007. DOI: 10.1016/j.chaos.2007.01.052.
96. P. Grigolini. Emergence of biological complexity: Criticality, renewal and memory. *Chaos Solit. Fractals*, 81(Part B):575–88, 2015.
97. P. Grigolini and D.R. Chialvo. Emergent critical brain dynamics - editorial. *Chaos Solit. Fract*, 55(1-2), 2013.
98. P. Grigolini and D.R. (Eds.) Chialvo, editors. *Emergent Critical Brain Dynamics*. Elsevier, Amsterdam, 2013. Special Issue - Chaos, Solitons & Fractals, Vol. 55, Pages 1-120.
99. P. Grigolini, D. Leddon, and N. Scafetta. Diffusion entropy and waiting time statistics of hard-x-ray solar flares. *Phys. Rev. E*, 65(4):046203/1–046203/12, 2002. DOI: 10.1103/PhysRevE.65.046203.
100. P. Grigolini, L. Palatella, and G. Raffaelli. Asymmetric anomalous diffusion: an efficient way to detect memory in time series. *Fractals*, 9(4):439–449, 2001. DOI: 10.1142/S0218348X01000865.
101. P. Grigolini, A. Rocco, and B.J. West. Fractional calculus as a macroscopic manifestation of randomness. *Phys. Rev. E*, 59(3):2603–2613, 1999. DOI: 10.1103/PhysRevE.59.2603.
102. L. Guo, Y. Chen, S. Shi, and B.J. West. Renormalization group and fractional calculus methods in a complex world: A review. *Fract. Calc. Appl. An.*, 24(1):5–53, 2021. DOI: 10.1515/fca-2021-0002.
103. R. Higbie. The rate of absorption of a pure gas into a still liquid during short periods of exposure. *Trans. Amer. Inst. Chem. Eng.*, 31:365–388, 1935.
104. R. Hilfer and L. Anton. Fractional master equations and fractal time random walks. *Phys. Rev. E*, 51(2):R848–R851, 1995. DOI: 10.1103/PhysRevE.51.R848.
105. T. Hoffmann, M.A. Porter, and R. Lambiotte. Generalized master equations for non-poisson dynamics on networks. *Phys. Rev. E*, 86(4), 2012. DOI: 10.1103/PhysRevE.86.046102.
106. T. Hoffmann, M.A. Porter, and R. Lambiotte. Random walks on stochastic temporal networks. *Understanding Complex Systems*, pages 295–313, 2013. DOI: 10.1007/978-3-642-36461-7_15.
107. P. Holme and J. Saramäki. Temporal networks. *Phys. Rep.*, 519(3):97–125, 2012. DOI: 10.1016/j.physrep.2012.03.001.
108. P. Holme and J. Saramäki. *Temporal network theory*. Springer Nature, Cham, Switzerland, 2019. ISBN: 978-3-030-23494-2; ISSN: 2509-9574; DOI: 10.1007/978-3-030-23495-9.
109. J. Huang, G. Katul, and J. Albertson. The role of coherent turbulent structures in explaining scalar dissimilarity within the canopy sublayer. *Environ. Fluid Mech.*, 13(6):571–599, 2013.
110. K.Y. Huang, G.G. Katul, and M. Hultmark. Velocity and temperature dissimilarity in the surface layer uncovered by the telegraph approximation. *Bound.-Layer Meteorol.*, 180(3):385–405, 2021. DOI: 10.1007/s10546-021-00632-2.
111. H.E. Hurst. Long-term storage capacity of reservoirs. *Trans. Am. Soc. Civil Eng.*, 116(1):770–799, 1951. DOI: 10.1061/TACEAT.0006518.
112. F. Höfling and T. Franosch. Anomalous transport in the crowded world of biological cells. *Rep. Prog. Phys.*, 76(4), 2013. DOI: 10.1088/0034-4885/76/4/046602.
113. H. Jeffreys. On the dynamics of geostrophic winds. *Q. J. R. met. Soc.*, 52:85–104, 1926.
114. H.J. Jensen. *Self-Organized Criticality: Emergent Complex Behavior in Physical and Biological Systems*. Cambridge University Press, 1998. ISBN: 9780511622717, DOI: 10.1017/CBO9780511622717.

115. H. Jeong, B. Tombor, R. Albert, Z.N. Oltval, and A.-L. Barabásl. The large-scale organization of metabolic networks. *Nature*, 407(6804):651–654, 2000. DOI: 10.1038/35036627.
116. S.V. Kailas and R. Narasimha. Similarity in vita-detected events in a nearly neutral atmospheric boundary layer. *Proc. Roy. Soc. London A*, 447(1930):211–222, 1994. DOI: 10.1098/rspa.1994.0136.
117. J. C. Kaimal and J. J. Finnigan. *Atmospheric boundary layer flows: their structure and measurement*. Oxford University Press, New York, 1994.
118. Y. Kang, D. Belušić, and K. Smith-Miles. Detecting and classifying events in noisy time series. *J Atmos Sci*, 71(3):1090–1104, 2014.
119. Y. Kang, D. Belušić, and K. Smith-Miles. Classes of structures in the stable atmospheric boundary layer. *Q. J. R. Meteorol. Soc.*, 141(691):2057–2069, 2015.
120. G. Katul, C.-I. Hsieh, and J. Sigmon. Energy-inertial scale interactions for velocity and temperature in the unstable atmospheric surface layer. *Boundary-Layer Meteorology*, 82(1):49–80, 1997.
121. G. Katul, A. Porporato, D. Cava, and M. Siqueira. An analysis of intermittency, scaling, and surface renewal in atmospheric surface layer turbulence. *Phys. D*, 215(2):117–126, 2006.
122. G.G. Katul, J. Albertson, M. Parlange, Chia-Ren Chu, and H. Stricker. Conditional sampling, bursting, and the intermittent structure of sensible heat flux. *J. Geophys. Res.*, 99(D11):22,869–22,876, 1994.
123. S. Khanna and J.G. Brasseur. Three-dimensional buoyancy- and shear-induced local structure of the atmospheric boundary layer. *Journal of the Atmospheric Sciences*, 55(5):710–743, 1998.
124. E. Kit, C.M. Hocut, D. Liberzon, and H.J.S. Fernando. Fine-scale turbulent bursts in stable atmospheric boundary layer in complex terrain. *J. Fluid Mech.*, 833:745–772, 2017.
125. J. Klafter, A. Blumen, and M.F. Shlesinger. Stochastic pathway to anomalous diffusion. *Phys. Rev. A*, 35(7):3081–3085, 1987. DOI: 10.1103/PhysRevA.35.3081.
126. S.J. Kline, W.C. Reynolds, F.A. Schraub, and P.W. Runstadler. The structure of turbulent boundary layers. *J. Fluid Mech.*, 30(4):741–773, 1967.
127. A.N. Kolmogorov. Dissipation of energy in the locally isotropic turbulence. *Dokl. Akad. Nauk SSSR*, 32:16–18, 1941.
128. A.N. Kolmogorov. The local structure of turbulence in incompressible viscous fluid for very large reynolds numbers. *Dokl. Akad. Nauk SSSR*, 30:301–305, 1941.
129. A.N. Kolmogorov. A refinement of previous hypotheses concerning the local structure of turbulence of a viscous incompressible fluid at high Reynolds number. *J. Fluid Mech.*, 13:82–85, 1962.
130. R. Kraichnan. Anomalous scaling of a randomly advected passive scalar. *Phys. Rev. Lett.*, 72(7):1016–1019, 1994.
131. S. Laima, H. Ren, H. Li, and J. Ou. Numerical simulation of coherent structures in the turbulent boundary layer under different stability conditions. *Energies*, 13(5), 2020.
132. L.D. Landau and E.M. Lifshitz. *Fluid Mechanics*. Pergamon Press, London, 1959. ISBN: 978-0-080-09104-4. [As far as we know, the first publication in Russian was in 1944, see [87], pag. 93].
133. J.C. Lasheras and H. Choi. Three-dimensional instability of a plane free shear layer: An experimental study of the formation and evolution of streamwise vortices. *J. Fluid Mech.*, 189(5):53–86, 1988.
134. P. Lévy. *Théorie de l'addition des variable aléatoires*. Gauthier-Villars, Paris, 2 edition, 1954. ISBN: 978-2-87647-207-5; First published 1937.
135. D. Li and E. Bou-Zeid. Coherent structures and the dissimilarity of turbulent transport of momentum and scalars in the unstable atmospheric surface layer. *Bound.-Layer Meteorol.*, 140(2):243–262, 2011.
136. Q. Li and Z. Fu. The effects of non-stationarity on the clustering properties of the boundary-layer vertical wind velocity. *Bound. Lay. Met.*, 149(2):219–230, 2013. DOI: 10.1007/s10546-013-9840-z.
137. L. Liu and F. Hu. Finescale clusterization intermittency of turbulence in the atmospheric boundary layer. *J Atmos Sci*, 77(7):2375–2392, 2020.
138. L. Liu, F. Hu, and X.-L. Cheng. Probability density functions of turbulent velocity and temperature fluctuations in the unstable atmospheric surface layer. *J Geophys Res Atmos*, 116(12), 2011.
139. L. Liu, F. Hu, and X.-L. Cheng. Extreme fluctuations of vertical velocity in the unstable atmospheric surface layer. *Nonlinear Processes Geophys.*, 21(2):463–475, 2014.
140. S.S. lu and W.W. Willmarth. Measurements of the structure of the reynolds stress in a turbulent boundary layer. *J. Fluid Mech.*, 60(3):481–511, 1973. DOI: 10.1017/S0022112073000315.
141. T.S. Luchik. Timescale and structure of ejections and bursts in turbulent channel flows. *J. Fluid Mech.*, 174:529–552, 1987.
142. X. Luo, M. Wang, J. Lee, and J. Hendry. Dynamic modelling based on surface renewal theory, model validation and process analysis of rotating packed bed absorber for carbon capture. *Applied Energy*, 301, 2021. DOI: 10.1016/j.apenergy.2021.117462.

143. K. Mahmoodi, B.J. West, and P. Grigolini. Self-organizing complex networks: Individual versus global rules. *Front. Physio.*, 8(JUL), 2017. DOI: 10.3389/fphys.2017.00478.
144. K. Mahmoodi, B.J. West, and P. Grigolini. Self-organized temporal criticality: Bottom-up resilience versus top-down vulnerability. *Complexity*, 2018, 2018. DOI: 10.1155/2018/8139058.
145. L. Mahrt. Intermittency of atmospheric turbulence. *J Atmos Sci.*, 46(1):79–95, 1989.
146. L. Mahrt. Stratified atmospheric boundary layers. *Bound.-Layer Meteorol.*, 90(3):375–396, 1999.
147. L. Mahrt. Common microfronts and other solitary events in the nocturnal boundary layer. *Q. J. R. Meteorol. Soc.*, 136(652):1712–1722, 2010.
148. L. Mahrt. Variability and maintenance of turbulence in the very stable boundary layer. *Bound.-Layer Meteorol.*, 135(1):1–18, 2010.
149. L. Mahrt. Stably stratified atmospheric boundary layers. *Annu. Rev. Fluid Mech.*, 46:23–45, 2014.
150. L. Mahrt, S. Richardson, N. Seaman, and D. Stauffer. Turbulence in the nocturnal boundary layer with light and variable winds. *Quarterly Journal of the Royal Meteorological Society*, 138(667):1430–1439, 2012.
151. L. Mahrt, C. Thomas, and J. Preuger. Space-time structure of mesoscale modes in the stable boundary layer. *Q. J. R. Meteorol. Soc.*, 135:67–75, 2009.
152. F. Mainardi. Fractional relaxation-oscillation and fractional diffusion-wave phenomena. *Chaos Sol. Fract.*, 7(9):1461–1477, 1996. DOI: 10.1016/0960-0779(95)00125-5.
153. F. Mainardi. *Fractional calculus and waves in linear viscoelasticity: An introduction to mathematical models*. Imperial College Press, 2010. ISBN: 978-184816330-0, DOI: 10.1142/P614.
154. F. Mainardi and G. Pagnini. The wright functions as solutions of the time-fractional diffusion equation. *Appl. Math. Comput.*, 141(1):51–62, 2003. DOI: 10.1016/S0096-3003(02)00320-X.
155. P. Manneville. Intermittency, self-similarity and 1/f spectrum in dissipative dynamical systems. *J. Phys. (Paris)*, 41(11):1235–1243, 1980. DOI: 10.1051/jphys:019800410110123500.
156. N. Masuda, M.A. Porter, and R. Lambiotte. Random walks and diffusion on networks. *Phys. Rep.*, 716–717:1–58, 2017. DOI: 10.1016/j.physrep.2017.07.007.
157. R. Mathis, N. Hutchins, and I. Marusic. Large-scale amplitude modulation of the small-scale structures in turbulent boundary layers. *J. Fluid Mech.*, 628:311–337, 2009.
158. H. R. Maturana and F. J. Varela. *Autopoiesis and Cognition: The Realization of the Living*. Reidel Publishing Company, London, 1980. ISBN: 90-277-1015-5 [originally published in Chile, Editorial Universitaria S.A., 1972].
159. M. Metzger, B. McKeon, and E. Arce-Larreta. Scaling the characteristic time of the bursting process in the turbulent boundary layer. *Phys. D: Nonlinear Phenom.*, 239(14):1296–1304, 2010.
160. R. Metzler, J.-H. Jeon, A.G. Cherstvy, and E. Barkai. Anomalous diffusion models and their properties: Non-stationarity, non-ergodicity, and ageing at the centenary of single particle tracking. *Phys. Chem. Chem. Phys.*, 16(44):24128–24164, 2014. DOI: 10.1039/c4cp03465a.
161. R. Metzler and J. Klafter. The random walk's guide to anomalous diffusion: A fractional dynamics approach. *Phys. Rep.*, 339(1):1–77, 2000. DOI: 10.1016/S0370-1573(00)00070-3.
162. R. Metzler and J. Klafter. The restaurant at the end of the random walk: recent developments in fractional dynamics descriptions of anomalous dynamical processes. *J. Phys. A*, 37(31):R161–R208, 2004. DOI: 10.1088/0305-4470/37/31/R01.
163. T. Misteli. The self-organizing genome: Principles of genome architecture and function. *Cell*, 183(1):28–45, 2020. DOI: 10.1016/j.cell.2020.09.014.
164. D. Molina-García, T.M. Pham, P. Paradisi, C. Manzo, and G. Pagnini. Fractional kinetics emerging from ergodicity breaking in random media. *Phys. Rev. E*, 94(5), 2016. DOI: 10.1103/PhysRevE.94.052147.
165. A.S. Monin and A.M. Yaglom. *Statistical Fluid Mechanics: Mechanics of turbulence*, volume 1. Dover Publications, New York, 1971.
166. A.S. Monin and A.M. Yaglom. *Statistical Fluid Mechanics: Mechanics of turbulence*, volume 2. Dover Publications, New York, 1975. ISBN: 978-0-486-45891-5. [First published in Russian by Nauka Press, Moscow, in 1965].
167. E.W. Montroll. Random walks on lattices. *Proc. Symp. Appl. Math.*, 16:193–220, 1964.
168. E.W. Montroll. Random walks on lattices. iii. calculation of first-passage times with application to exciton trapping on photosynthetic units. *J. Math. Phys.*, 10(4):753–765, 1969. DOI: 10.1063/1.1664902.
169. E.W. Montroll and H. Scher. Random walks on lattices. iv. continuous-time walks and influence of absorbing boundaries. *J. Stat. Phys.*, 9(2):101–135, 1973. DOI: 10.1007/BF01016843.
170. E.W. Montroll and G.H. Weiss. Random walks on lattices. ii. *J. Math. Phys.*, 6(2):167–181, 1965. DOI: 10.1063/1.1704269.
171. A. Mura and F. Mainardi. A class of self-similar stochastic processes with stationary increments to model anomalous diffusion in physics. *Integral Transforms Spec. Funct.*, 20(3-4):185–198, 2009. DOI: 10.1080/10652460802567517.
172. M.A. Muñoz. Colloquium: Criticality and dynamical scaling in living systems. *Rev. Mod. Phys.*, 90(3), 2018. DOI: 10.1103/RevModPhys.90.031001.
173. R. Narasimha. Turbulence: waves or events? *Curr. Sci.*, 68(1):33–38, 1995.

174. R. Narasimha and S. V. Kailas. Energy events in the atmospheric boundary layer. In H. U. Meier and P. Bradshaw, editors, *Perspectives in turbulence studies*, page 88–222. Springer., Berlin, 1987. DOI: 10.1007/978-3-642-82994-9_8, ISBN: 978-3-642-82996-3.
175. R. Narasimha and S.V. Kailas. Turbulent bursts in the atmosphere. *Atmos. Environ. A, Gen. Top.*, 24(7):1635–1645, 1990. DOI: 10.1016/0960-1686(90)90497-B.
176. R. Narasimha, S.R. Kumar, A. Prabhu, and S.V. Kailas. Turbulent flux events in a nearly neutral atmospheric boundary layer. *Phil. Trans. Roy. Soc. A*, 365(1852):841–858, 2007. DOI: 10.1098/rsta.2006.1949.
177. S.P. Neuman and D.M. Tartakovsky. Perspective on theories of non-fickian transport in heterogeneous media. *Adv. Water Resour.*, 32(5):670–680, 2009. DOI: 10.1016/j.advwatres.2008.08.005.
178. G. Nicolis and I. Prigogine. *Self-Organization in Nonequilibrium Systems. From Dissipative Structures to Order through Fluctuations*. J. Wiley & Sons, New York, 1977.
179. J.J. Niemela and K.R. Sreenivasan. Confined turbulent convection. *J. Fluid Mech.*, 481:355–384, 2003. DOI: 10.1017/S0022112003004087.
180. H. Niu, Y.Q. Chen, and B.J. West. Why do big data and machine learning entail the fractional dynamics ? *Entropy*, 23(3):1–32, 2021. DOI: 10.3390/e23030297.
181. A. Oboukhov. Some specific features of atmospheric turbulence. *J. Fluid Mech.*, 13(1):77–81, 1962. DOI: doi:10.1017/S0022112062000506.
182. A. M. Oboukhov. Energy distribution in the spectrum of turbulent flow. *Izv. Akad. Nauk. SSSR Ser. Geogr. Geofiz.*, 5:453–466, 1941.
183. E. Ott. *Chaos in Dynamical Systems*. Cambridge University Press, Cambridge, 2nd ed. edition, 2002. ISBN: 978-0-511-80326-0.
184. N.T. Ouellette. On the dynamical role of coherent structures in turbulence. *C.R. Phys.*, 13(9–10):866–877, 2012. DOI: 10.1016/j.crhy.2012.09.006.
185. G. Pagnini. Erdélyi-kober fractional diffusion. *Fractional Calculus and Applied Analysis*, 15(1):117–127, 2012. DOI: 10.2478/s13540-012-0008-1.
186. G. Pagnini. Fractional kinetics in random/complex media. In V.E. Tarasov, editor, *Applications in Physics, Part B*, pages 183–205. De Gruyter, 2019. ISBN: 9783110571721, DOI: 10.1515/9783110571721-008.
187. G. Pagnini, A. Mura, and F. Mainardi. Generalized fractional master equation for self-similar stochastic processes modelling anomalous diffusion. *Int. J. Stoch. Anal.*, 2012, 2012. DOI: 10.1155/2012/427383.
188. G. Pagnini and P. Paradisi. A stochastic solution with gaussian stationary increments of the symmetric space-time fractional diffusion equation. *Fract. Calc. Appl. Anal.*, 19(2):408–440, 2016. DOI: 10.1515/fca-2016-0022.
189. G. Palla, I. Derényi, I. Farkas, and T. Vicsek. Uncovering the overlapping community structure of complex networks in nature and society. *Nature*, 435(7043):814–818, 2005. DOI: 10.1038/nature03607.
190. P. Paradisi. *Analisi di fenomeni diffusivi mediante processi stocastici non-Markoviani (Analysis of diffusive phenomena by non-Markovian stochastic processes)*. Master Thesis, Bologna University, 1997.
191. P. Paradisi. Fractional calculus in statistical physics: The case of time fractional diffusion equation. *Commun. Appl. Ind. Math.*, 6(2):e–530, 2015. DOI: 10.1685/journal.caim.530.
192. P. Paradisi and P. Allegrini. Scaling law of diffusivity generated by a noisy telegraph signal with fractal intermittency. *Chaos Soliton Fract*, 81(Part B):451–62, 2015.
193. P. Paradisi and P. Allegrini. Intermittency-driven complexity in signal processing. In Riccardo Barbieri, Enzo Pasquale Scilingo, and Gaetano Valenza, editors, *Complexity and Nonlinearity in Cardiovascular Signals*, pages 161–195. Springer, Cham, 2017.
194. P. Paradisi, P. Allegrini, F. Barbi, S. Bianco, and P. Grigolini. Renewal, modulation and blinking quantum dots. *AIP Conf. Proc.*, 800(1):92–97, 2005.
195. P. Paradisi, P. Allegrini, and D. Chiarugi. A renewal model for the emergence of anomalous solute crowding in liposomes. *BMC Syst. Biol.*, 9(3), 2015.
196. P. Paradisi, P. Allegrini, A. Gemignani, M. Laurino, D. Menicucci, and A. Piarulli. Scaling and intermittency of brain events as a manifestation of consciousness. *AIP Conf. Proc.*, 1510:151–161, 2013. DOI: 10.1063/1.4776519.
197. P. Paradisi, R. Cesari, and P. Allegrini. Scaling laws of turbulence intermittency in the atmospheric boundary layer: The role of stability. *J. Phys.: Conf. Series*, 633(1), 2015.
198. P. Paradisi, R. Cesari, D. Contini, A. Donateo, and L. Palatella. Characterizing memory in atmospheric time series: an alternative approach based on renewal theory. *Eur. Phys. J. - Spec. Top.*, 174:207–218, 2009.
199. P. Paradisi, R. Cesari, A. Donateo, D. Contini, and P. Allegrini. Diffusion scaling in event-driven random walks: an application to turbulence. *Rep. Math. Phys.*, 70:205–220, 2012.
200. P. Paradisi, R. Cesari, A. Donateo, D. Contini, and P. Allegrini. Scaling laws of diffusion and time intermittency generated by coherent structures in atmospheric turbulence. *Nonlinear Proc. Geophys.*, 19:113–126, 2012. P. Paradisi et al., Corrigendum, *Nonlin. Processes Geophys.* **19**, 685 (2012).

201. P. Paradisi, R. Cesari, and P. Grigolini. Superstatistics and renewal critical events. *Cent. Eur. J. Phys.*, 7:421–431, 2009.
202. P. Paradisi, R. Cesari, F. Mainardi, A. Maurizi, and F. Tampieri. A generalized fick's law to describe non-local transport effects. *Phys. Chem. Earth*, 26(4):275–279, 2001. DOI: 10.1016/S1464-1909(01)00006-5.
203. P. Paradisi, R. Cesari, F. Mainardi, and F. Tampieri. The fractional fick's law for non-local transport processes. *Physica A*, 293(1-2):130–142, 2001. DOI: 10.1016/S0378-4371(00)00491-X.
204. P. Paradisi, P. Grigolini, S. Bianco, and O.C. Akin. Renewal aging in non-homogeneous poisson processes with periodic rate modulation. *Int. J. Bif. Chaos*, 18(9):2681—2691, 2008.
205. P. Paradisi, G. Kaniadakis, and A. M. Scarfone. The emergence of self-organization in complex systems - preface. *Chaos Soliton Fract*, 81(Part B):407–11, 2015.
206. P. Paradisi, M. Raglanti, and L. Sebastiani. Online communication and body language. *Front. Behav. Neurosci.*, 15, 2021. DOI: 10.3389/fnbeh.2021.709365.
207. E.R. Pardyjak, P. Monti, and H.J.S. Fernando. Flux richardson number measurements in stable atmospheric shear flows. *J. Fluid Mech.*, 459:307–316, 2002.
208. B.R. Pearson, P.-A. Krogstad, and W. van de Water. Measurements of the turbulent energy dissipation rate. *Phys. Fluids*, 14:1288, 2002.
209. C.-K. Peng, S.V. Buldyrev, A.L. Goldberger, S. Havlin, F. Sciortino, M. Simons, and H.E. Stanley. Long-range correlations in nucleotide sequences. *Nature*, 356(6365):168–170, 1992.
210. C.-K. Peng, S.V. Buldyrev, S. Havlin, M. Simons, H.E. Stanley, and A.L. Goldberger. Mosaic organization of dna nucleotides. *Phys. Rev. E*, 49(2):1685–1689, 1994.
211. D.D. Perlmutter. Surface-renewal models in mass transfer. *Chem. Eng. Sci.*, 16(3-4):287–296, 1961. DOI: 10.1016/0009-2509(61)80039-0.
212. P. Perron. Trends and random walks in macroeconomic time series. further evidence from a new approach. *Journal of Economic Dynamics and Control*, 12(2-3):297–332, 1988.
213. N. Piccinini, D. Lambert, B.J. West, M. Bologna, and P. Grigolini. Nonergodic complexity management. *Phys. Rev. E*, 93(6), 2016. DOI: 10.1103/PhysRevE.93.062301.
214. D. Poggi and G. Katul. The ejection-sweep cycle over bare and forested gentle hills: A laboratory experiment. *Bound.-Layer Meteorol.*, 122(3):493–515, 2007. DOI: 10.1007/s10546-006-9117-x.
215. D. Poggi and G. Katul. Flume experiments on intermittency and zero-crossing properties of canopy turbulence. *Phys. Fluids*, 21(6), 2009. DOI: 10.1063/1.3140032.
216. Y. Pomeau and P. Manneville. Intermittent transition to turbulence in dissipative dynamical systems. *Commun. Math. Phys.*, 74(2):189–197, 1980. DOI: 10.1007/BF01197757.
217. M.E. Porter. Clusters and the new economics of competition. *Harv. Bus. Rev.*, 76(6):77–90, 1998.
218. Ludwig Prandtl. Über flüssigkeitsbewegung bei sehr kleiner reibung. *Verhandl. III, Internat. Math.-Kong.*, Heidelberg, Teubner, Leipzig, 1904, pages 484–491, 1904.
219. I. Prigogine. *Introduction to Thermodynamics of Irreversible Processes*. Charles C. Thomas Publisher, Springfield, Illinois, 1955.
220. L. Primavera and G. Alfonsi. On identification of vortical structures in turbulent shear flow. *J. Flow Vis. Image Process.*, 15(3):201–216, 2008. DOI: 10.1615/JFlowVisImageProc.v15.i3.20.
221. A. Provenzale, L.A. Smith, R. Vio, and G. Murante. Distinguishing between low-dimensional dynamics and randomness in measured time series. *Phys. D: Nonlinear Phenom.*, 58(1-4):31–49, 1992. DOI: 10.1016/0167-2789(92)90100-2.
222. M.I. Rabinovich, V.S. Afraimovich, C. Bick, and P. Varona. Information flow dynamics in the brain. *Phys. Life Rev.*, 9(1):51–73, 2012.
223. M.I. Rabinovich, R. Huerta, and V. Afraimovich. Dynamics of sequential decision making. *Phys. Rev. Lett.*, 97(18), 2006.
224. M.I. Rabinovich, R. Huerta, P. Varona, and V.S. Afraimovich. Transient cognitive dynamics, metastability, and decision making. *PLoS Comput. Biol.*, 4(5), 2008.
225. L. F. Richardson. Some measurements of atmospheric turbulence. *Philos. Trans. Roy. Soc. London A*, 582:1–28, 1920.
226. L. F. Richardson. *Weather Prediction by Numerical Processes*. Cambridge University Press, Cambridge, 1922. ISBN: 9780511618291.
227. S.K. Robinson. Coherent motions in the turbulent boundary layer. *Ann. Rev. Fluid Mech.*, 23(1):601–639, 1991.
228. M.M. Rogers and R.D. Moser. The three-dimensional evolution of a plane mixing layer: The kelvin-helmholtz rollup. *J. Fluid Mech.*, 243:183–226, 1992.
229. Y. Roh, G. Heo, and S.E. Whang. A survey on data collection for machine learning: A big data-ai integration perspective. *IEEE Trans. Knowl. Data Eng*, 33(4):1328–1347, 2021. DOI: 10.1109/TKDE.2019.2946162.
230. C. Rorai, P.D. Mininni, and A. Pouquet. Turbulence comes in bursts in stably stratified flows. *Phys. Rev. E Stat. Nonlin. Soft Matter Phys*, 89(4), 2014.
231. M. Rosvall and C.T. Bergstrom. Maps of random walks on complex networks reveal community structure. *Proceedings of the National Academy of Sciences of the United States of America*, 105(4):1118–1123, 2008. DOI: 10.1073/pnas.0706851105.

232. E. Ruckenstein. Some remarks on renewal models. *Chem. Eng. Sci.*, 18(4):233–241, 1963. DOI: 10.1016/0009-2509(63)87004-9.

233. M. Sahimi. *Flow and Transport in Porous Media and Fractured Rock: From Classical Methods to Modern Approaches*. John Wiley & Sons, Ltd, 2 edition, 2011. ISBN: 9783527636693; DOI: 10.1002/9783527636693.

234. A.I. Saichev and G.M. Zaslavsky. Fractional kinetic equations: solutions and applications. *Chaos*, 7(4):753–764, 1997. DOI: 10.1063/1.166272.

235. N. Scafetta and P. Grigolini. Scaling detection in time series: diffusion entropy analysis. *Phys. Rev. E*, 66(3), 2002. DOI: 10.1103/PhysRevE.66.036130.

236. E. Scalas, R. Gorenflo, and F. Mainardi. Uncoupled continuous-time random walks: Solution and limiting behavior of the master equation. *Phys. Rev. E*, 69(1):8, 2004. DOI: 10.1103/PhysRevE.69.011107.

237. H. Scher and M. Lax. Stochastic transport in a disordered solid. i. theory. *Phys. Rev. B*, 7(10):4491–4502, 1973. DOI: 10.1103/PhysRevB.7.4491.

238. H. Scher and M. Lax. Stochastic transport in a disordered solid. ii. impurity conduction. *Phys. Rev. B*, 7(10):4502–4519, 1973. DOI: 10.1103/PhysRevB.7.4502.

239. H. Schlichting and K. Gersten. *Boundary-Layer Theory*. Springer-Verlag, Berlin Heidelberg, 9th edition, 2017. ISBN: 978-3-662-52917-1.

240. W. Schoppa and F. Hussain. Coherent structure generation in near-wall turbulence. *J. Fluid Mech.*, 453:57–108, 2002.

241. L. Seuront, H. Yamazaki, and F.G. Schmitt. Intermittency. In G.H.Z. Baumert, J. Simpson, and J. Sündermann, editors, *Marine Turbulence: Theories, Observations, and Models. Results of the CARTUM Project*, pages 66–78. Cambridge University Press, Cambridge, 2005. ISBN: 9780521153720.

242. Z.-S. She and E. Leveque. Universal scaling laws in fully developed turbulence. *Phys. Rev. Lett.*, 72(3):336–339, 1994. DOI: 10.1103/PhysRevLett.72.336.

243. Z.-S. She and Z.-X. Zhang. Universal hierarchical symmetry for turbulence and general multi-scale fluctuation systems. *Acta Mech. Sin./Lixue Xuebao*, 25(3):279–294, 2009. DOI: 10.1007/s10409-009-0257-3.

244. M.F. Shlesinger. Asymptotic solutions of continuous-time random walks. *J. Stat. Phys.*, 10(5):421–434, 1974. DOI: 10.1007/BF01008803.

245. M.F. Shlesinger, B.J. West, and J. Klafter. Lévy dynamics of enhanced diffusion: Application to turbulence. *Phys. Rev. Lett.*, 58(11):1100–1103, 1987. DOI: 10.1103/PhysRevLett.58.1100.

246. O.Y. Sliusarenko, S. Vitali, V. Sposini, P. Paradisi, A. Chechkin, G. Castellani, and G. Pagnini. Finite-energy lévy-type motion through heterogeneous ensemble of brownian particles. *J. Phys. A*, 52(9), 2019. DOI: 10.1088/1751-8121/aafe90.

247. C. Song, T. Koren, P. Wang, and A.-L. Barabási. Modelling the scaling properties of human mobility. *Nat. Phys.*, 6(10):818–823, 2010. DOI: 10.1038/nphys1760.

248. V. Sposini, A.V. Chechkin, F. Seno, G. Pagnini, and R. Metzler. Random diffusivity from stochastic equations: Comparison of two models for brownian yet non-gaussian diffusion. *New J. Phys.*, 20(4), 2018. DOI: 10.1088/1367-2630/aaeb96.

249. V. Sposini, S. Vitali, P. Paradisi, and G. Pagnini. Fractional diffusion and medium heterogeneity: The case of the continuous time random walk. In L. Beghin, F. Mainardi, and R. Garrappa, editors, *Nonlocal and Fractional Operators*, pages 275–286. Springer International Publishing, Cham, 2021. ISBN: 978-3-030-69236-0.

250. K.R. Sreenivasan and R.A. Antonia. The phenomenology of small-scale turbulence. *Ann. Rev. Fluid Mech.*, 29:435–472, 1997. DOI: 10.1146/annurev.fluid.29.1.435.

251. K.R. Sreenivasan and A. Bershadskii. Clustering properties in turbulent signals. *J. Stat. Phys.*, 125(5-6):1141–1153, 2006.

252. K.R. Sreenivasan and B. Dhruva. Is there scaling in high-reynolds-number turbulence? *Prog. Theor. Phys. Suppl.*, 130:103–120, 1998. DOI: 10.1143/PTPS.130.103.

253. Roland B. Stull. *An Introduction to Boundary Layer Meteorology*. Springer, Dordrecht, 1997.

254. J. Sun, L. Mahrt, R.M. Banta, and Y.L. Pichugina. Turbulence regimes and turbulence intermittency in the stable boundary layer: During cases-99. *J Atmos Sci*, 69(1):338–351, 2012.

255. J. Sun, C.J. Nappo, L. Mahrt, D. Belušić, B. Grisogono, D.R. Stauffer, M. Pulido, C. Staquet, Q. Jiang, A. Pouquet, C. Yagüe, B. Galperin, R.B. Smith, J.J. Finnigan, S.D. Mayor, G. Svensson, A.A. Grachev, and W.D. Neff. Review of wave-turbulence interactions in the stable atmospheric boundary layer. *Rev. Geophys.*, 53(3):956–993, 2015.

256. F. Tampieri. *Turbulence and Dispersion in the Planetary Boundary Layer*. Springer International Publishing Switzerland, 2017.

257. S. Tardu. *Transport and Coherent Structures in Wall Turbulence*. John Wiley & Sons, 2014. DOI: 10.1002/9781118576663.

258. G.I. Taylor. Diffusion by continuous movements. *Proc. London Math. Soc.*, s2-20(1):196–212, 1921. DOI: 10.1112/plms/s2-20.1.196.

259. B.T. Thomas Yeo, F.M. Krienen, J. Sepulcre, M.R. Sabuncu, D. Lashkari, M. Hollinshead, J.L. Roffman, J.W. Smoller, L. Zöllei, J.R. Polimeni, B. Fisch, H. Liu, and R.L. Buckner. The organization of the human cerebral cortex estimated by intrinsic functional connectivity. *J. Neurophysiol.*, 106(3):1125–1165, 2011. DOI: 10.1152/jn.00338.2011.

260. E.J. Topol. High-performance medicine: the convergence of human and artificial intelligence. *Nat. Med.*, 25(1):44–56, 2019. DOI: 10.1038/s41591-018-0300-7.

261. D.J. Tritton. *Physical fluid dynamics*. Clarendon press, Oxford, 1988.

262. A. Tsinober. *An Informal Conceptual Introduction to Turbulence: Second Edition of An Informal Introduction to Turbulence*. Fluid Mech. its Appl. Springer Netherlands, 2009.

263. R.G. Tubergen and W.G. Tiederman. Evaluation of ejection detection schemes in turbulent wall flows. *Exp. Fluids*, 15(4-5):255–262, 1993.

264. J.K.E. Tunaley. Asymptotic solutions of the continuous-time random walk model of diffusion. *J. Stat. Phys.*, 11(5):397–408, 1974. DOI: 10.1007/BF01026731.

265. J.K.E. Tunaley. Theory of ac conductivity based on random walks. *Phys. Rev. Lett.*, 33(17):1037–1039, 1974. DOI: 10.1103/PhysRevLett.33.1037.

266. J.K.E. Tunaley. Some properties of the asymptotic solutions of the montroll-weiss equation. *J. Stat. Phys.*, 12(1):1–10, 1975. DOI: 10.1007/BF01024180.

267. J.K.E. Tunaley. Moments of the montroll-weiss continuous-time random walk for arbitrary starting time. *J. Stat. Phys.*, 14(5):461–463, 1976. DOI: 10.1007/BF01040704.

268. M. Turalska, B. J. West, and P. Grigolini. Temporal complexity of the order parameter at the phase transition. *Phys. Rev. E*, 83:061142, 2011.

269. F. Vanni, M. Luković, and P. Grigolini. Criticality and transmission of information in a swarm of cooperative units. *Phys. Rev. Lett.*, 107(7), 2011. DOI: 10.1103/PhysRevLett.107.078103.

270. G.M. Viswanathan, M.G.E. Da Luz, E.P. Raposo, and H.E. Stanley. *The physics of foraging: An introduction to random searches and biological encounters*. Cambridge University Press, Cambridge, 2011. ISBN: 9781107006799; DOI: 10.1017/CBO9780511902680.

271. S. Vitali, V. Sposini, O. Sliusarenko, P. Paradisi, G. Castellani, and G. Pagnini. Langevin equation in complex media and anomalous diffusion. *J. R. Soc. Interface*, 15:20180282, 2018. DOI: 10.1098/rsif.2018.0282.

272. J.M. Wallace, H. Eckelmann, and R.S. Brodkey. The wall region in turbulent shear flow. *J. Fluid Mech.*, 54(1):39–48, 1972. DOI: 10.1017/S0022112072000515.

273. Z. Warhaft. Passive scalars in turbulent flows. *Ann. Rev. Fluid Mech.*, 32:203–240, 2000. DOI: 10.1146/annurev.fluid.32.1.203.

274. T. Watanabe, J.J. Riley, K. Nagata, K. Matsuda, and R. Onishi. Hairpin vortices and highly elongated flow structures in a stably stratified shear layer. *Journal of Fluid Mechanics*, 878:37–61, 2019.

275. G.H. Weiss and R.J. Rubin. Random walks: Theory and selected applications. In I. Prigogine and S.A. Rice, editors, *Advances in Chemical Physics*, volume 52, pages 363–506. John Wiley and Sons, New York, 1983. DOI: 10.1002/9780470142769.ch5.

276. B.J. West. Fractal physiology, complexity, and the fractional calculus. In W.T. Coffey S.A. Rice and Y.P. Kalmykov, editors, *Fractals, Diffusion and Relaxation in Disordered Complex Systems: Advances in Chemical Physics*, volume 133, pages 1–92. John Wiley and Sons, 2006. DOI: 10.1002/0470037148.ch6.

277. B.J. West. Fractal physiology and the fractional calculus: A perspective. *Front. Physio.*, 1 OCT, 2010. DOI: 10.3389/fphys.2010.00012.

278. B.J. West. Colloquium: Fractional calculus view of complexity: A tutorial. *Rev. Mod. Phys.*, 86(4), 2014. DOI: 10.1103/RevModPhys.86.1169.

279. B.J. West, M. Bologna, and P. Grigolini. *Physics of Fractal Operators*. Springer, New York, 2003. ISBN: 978-1-4419-3054-5, DOI: 10.1007/978-0-387-21746-8.

280. B.J. West, E.L. Geneston, and P. Grigolini. Maximizing information exchange between complex networks. *Phys. Rep.*, 468(1-3):1–99, 2008. DOI: 10.1016/j.physrep.2008.06.003.

281. B.J. West and P. Grigolini. *Crucial Events: why are catastrophes never expected?* Studies of Nonlinear Phenomena in Life Science, vol. 17. World Scientific, Hackensack, New Jersey, 2021. ISBN: 9789811234095.

282. B.J. West, M. Turalska, and P. Grigolini. Fractional calculus ties the microscopic and macroscopic scales of complex network dynamics. *New J. Phys.*, 17, 2015. DOI: 10.1088/1367-2630/17/4/045009.

283. V. Zaburdaev, S. Denisov, and J. Klafter. Lévy walks. *Rev. Mod. Phys.*, 87(2):483–530, 2015. DOI: 10.1103/RevModPhys.87.483.

284. M. Zanin, D. Papo, P.A. Sousa, E. Menasalvas, A. Nicchi, E. Kubik, and S. Boccaletti. Combining complex networks and data mining: Why and how. *Phys. Rep.*, 635:1–44, 2016. DOI: 10.1016/j.physrep.2016.04.005.

285. Ya.B. Zel'dovich, S.A. Molchanov, A.A. Ruzmaikin, and D.D. Sokoloff. Intermittency, diffusion and generation in a nonstationary random medium. *Sov. Sci. Rev.*, C7:1–110, 1988.

286. J. Zhong, T.S. Huang, and R.J. Adrian. Extracting 3d vortices in turbulent fluid flow. *IEEE Trans. Pattern Anal. Mach. Intell.*, 20(2):193–199, 1998. DOI: 10.1109/34.659938.

287. Y. Zhou. Turbulence theories and statistical closure approaches. *Phys. Rep.*, 935:1–117, 2021.
DOI: 10.1016/j.physrep.2021.07.001.